









# NAVAL POSTGRADUATE SCHOOL

Monterey, California



## THESIS

A MATHEMATICAL MODEL  
FOR THE  
LONGITUDINAL CONTROL SYSTEM  
OF THE  
SPACE SHUTTLE ORBITER

by

Cole J. Pierce

Thesis Advisor:

Daniel J. Collins

Approved for public release; distribution unlimited.

T178048



REPORT DOCUMENTATION PAGE		READ INSTRUCTIONS BEFORE COMPLETING FORM
1. REPORT NUMBER	2. GOVT ACCESSION NO.	3. RECIPIENT'S CATALOG NUMBER
4. TITLE (and Subtitle) A Mathematical Model for the Longitudinal Control System of the Space Shuttle Orbiter		5. TYPE OF REPORT & PERIOD COVERED Master's thesis; March 1977
7. AUTHOR(s) PIERCE, Cole J., LCDR, USN		6. PERFORMING ORG. REPORT NUMBER
9. PERFORMING ORGANIZATION NAME AND ADDRESS Naval Postgraduate School Monterey, California 93940		8. CONTRACT OR GRANT NUMBER(s)
11. CONTROLLING OFFICE NAME AND ADDRESS Naval Postgraduate School Monterey, California 93940		10. PROGRAM ELEMENT, PROJECT, TASK AREA & WORK UNIT NUMBERS
14. MONITORING AGENCY NAME & ADDRESS (if different from Controlling Office)		12. REPORT DATE 25 March 1977
		13. NUMBER OF PAGES 192
		15. SECURITY CLASS. (of this report) UNCLAS
		15a. DECLASSIFICATION/DOWNGRADING SCHEDULE
16. DISTRIBUTION STATEMENT (of this Report)  Approved for public release; distribution unlimited		
17. DISTRIBUTION STATEMENT (of the abstract entered in Block 20, if different from Report)		
18. SUPPLEMENTARY NOTES		
19. KEY WORDS (Continue on reverse side if necessary and identify by block number)  Model Control system Space Shuttle Orbiter		
20. ABSTRACT (Continue on reverse side if necessary and identify by block number)  The analysis of a fly-by-wire longitudinal control system, specifically that of the space shuttle orbiter, was undertaken in order to demonstrate the construction of a mathematical model depicting the relationships between forcing function and response. Each facet of modern control theory, including stability, was developed. Several computer programs were written, which should be of value to the Department of Aeronautics, for the HP9830 computer/plotter; these		





programs are basic to the study of control theory, demonstrate the importance of the transfer function, the characteristic equation, and the various forms of feedback, and will plot time and frequency (Bode) response graphs given the proper inputs. The Continuous System Modeling Program, version III, and the IBM360 were used to analyze the complex control system installed in the orbiter. The demonstration of the model and its interface with the CSMP program was given, and the efficiency of this procedure was made clear.



Approved for public release; distribution unlimited

A Mathematical Model  
for the  
Longitudinal Control System  
of the  
Space Shuttle Orbiter

by

Cole Jon Pierce  
Lieutenant Commander  
United States Navy

Submitted in partial fulfillment of the  
requirements for the degree of

MASTER OF SCIENCE IN AERONAUTICAL ENGINEERING

from the

NAVAL POSTGRADUATE SCHOOL  
March 1977

---



## ABSTRACT

The analysis of a fly-by-wire longitudinal control system, specifically that of the space shuttle orbiter, was undertaken in order to demonstrate the construction of a mathematical model depicting the relationships between forcing function and response. Each facet of modern control theory, including stability, was developed. Several computer programs were written, which should be of value to the Department of Aeronautics, for the HP9830 computer/plotter; these programs are basic to the study of control theory, demonstrate the importance of the transfer function, the characteristic equation, and the various forms of feedback, and will plot time and frequency (Bode) response graphs given the proper inputs. The Continuous System Modeling Program, version III, and the IBM360 were used to analyze the complex control system installed in the Orbiter. The demonstration of the model and its interface with the CSMP program was given, and the efficiency of this procedure was made clear.



## TABLE OF CONTENTS

I. PHYSICAL DESCRIPTION OF THE ORBITER -----	7
II. DEFINITIONS AND SYMBOLOGY -----	14
III. MATHEMATICAL MODELS OF LINEAR SYSTEM ELEMENTS -----	28
IV. STABILITY -----	37
V. EQUATIONS OF MOTION -----	50
VI. COMPUTER METHODS OF ANALYSIS -----	63
VII. LONGITUDINAL FEEDBACK -----	101
VIII. THE ORBITER -----	141
BIBLIOGRAPHY -----	190
INITIAL DISTRIBUTION LIST -----	192





## ACKNOWLEDGEMENTS

In appreciation of the help I have received while writing this paper, I would like to thank

Professor Schmidt  
Department of Aeronautics

Professor Strum  
Department of Electrical Engineering

especially

Professor Collins  
Department of Aeronautics

most especially

my wife, Jo Ann



## I. PHYSICAL DESCRIPTION OF THE ORBITER

The space shuttle orbiter is the vanguard of a new generation and new concept of spacecraft, having been designed to fly as an atmospheric vehicle as well as to operate as a spacecraft in near-earth orbit. In order to function in this dual role, it requires the performance, stability, and control systems of both types.

For orbital flight, attitude control is achieved by means of a reaction control system such as those used in earlier spacecraft. Whereas earlier vehicles followed an unguided re-entry and parachute let-down, the orbiter is to be flown to a runway landing and therefore requires the conventional aerodynamic roll, pitch, and yaw controls for atmospheric flight. The longitudinal system for maintaining the desired pitch angle, pitch rate, and stability about the pitch axis is the subject of this paper.

The space shuttle orbiter is of conventional design, incorporating a low-mounted, highly swept delta wing and a small vertical stabilizer on a thick, rather square body. Sea level weight of the vehicle, in re-entry configuration, is approximately 186,000 lbs. The wetted area of the wing



is 2690 square feet, yielding a wing loading of 69 psf. Overall length is 122.3 ft, and wing span is 78 ft.<sup>1</sup> The landing speed of the orbiter, necessarily high because of the wing loading, is 190 knots.

The primary aerodynamic control surfaces are split elevons at the trailing edge (to perform the functions of ailerons and elevators) and a combination rudder/speed-brake at the trailing edge of the vertical stabilizer. The rudder splits symmetrically along its vertical hinge to produce aerodynamic drag for speed control, hence its use as a speed brake. Body flaps are located at the trailing edge of the fuselage and, although they were originally intended to provide heat shielding for the main engines during re-entry, will be used as an active longitudinal trim device. Figure 1-1 is a three-view of the vehicle and shows the location of the primary control surfaces.

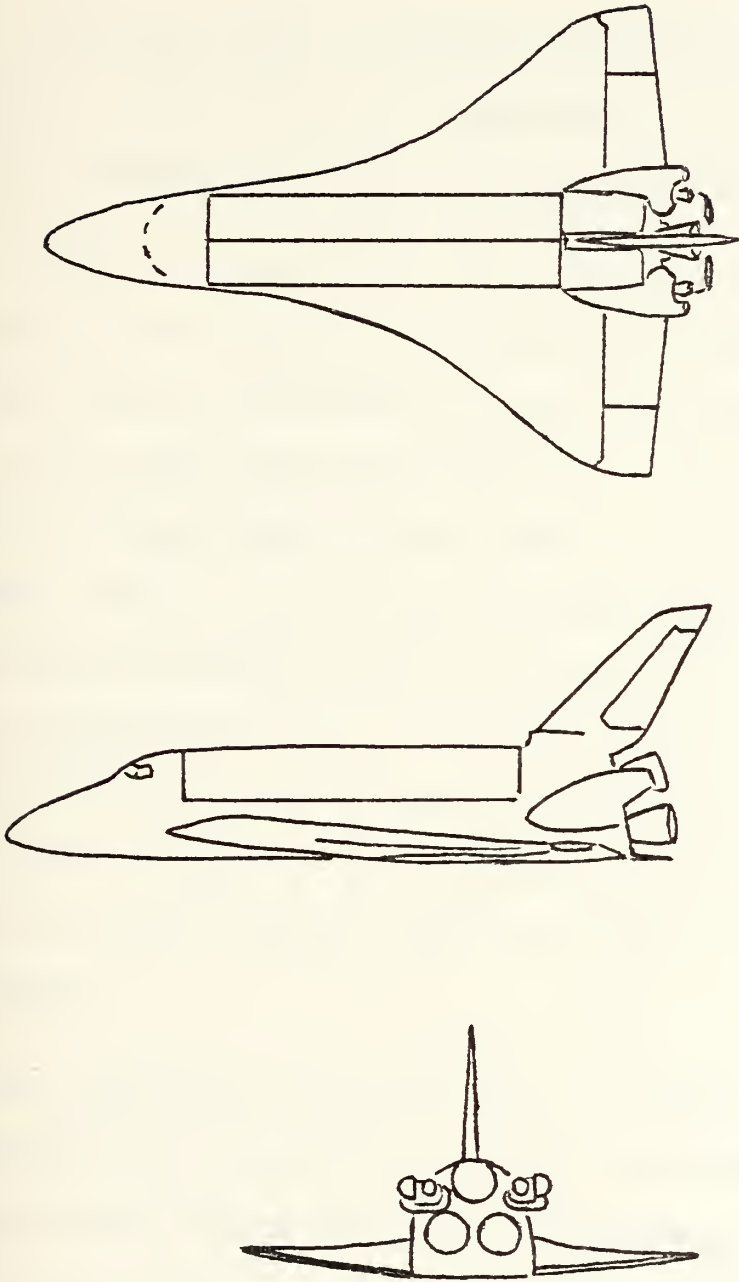
The elevons are split because of wing deflection and hinge moment considerations, and are quite large, comprising twenty per cent of the total wing area. Their maximum deflection is 35 degrees up and 20 down; maximum deflection

---

<sup>1</sup> By comparison, the commercial Douglas DC-9 measures 119.3 feet in length and has a span of 93.4 feet.



Figure 1-1



Three-view of the Orbiter





rate is twenty degrees per second.

The speed brake provides additional longitudinal control in some regimes by generating a pitching moment, but its primary use is for terminal area energy management.

The elevons are the primary pitch attitude control, but since their normal deflection is trailing edge down, the body flap is available to reduce the load on them. Use of the flap enables the elevons to trail as much as possible and minimizes their chances of overheating. The body flap is also an aid to longitudinal control at high angles of attack where the elevons lose much of their effectiveness. Due to rudder blanking, the orbiter is in fact directionally unstable in this regime (the early re-entry phase). The existence of a lightly damped dutch roll mode, however, provides dynamic stability for the vehicle.

The trajectory followed by the vehicle from orbit to touchdown is sensitive and complex as with former spacecraft and occurs as follows. Following de-orbit, the reaction control system engines orient the orbiter to a normal front-end-forward top-side-up attitude prior



to reaching re-entry interface at 400,000 feet. The angle of attack during re-entry varies between thirty and forty degrees. When the velocity decreases to 9000 feet per second, a slow pitch down maneuver commences which is completed by 70,000 feet; here, the angle of attack has been reduced to ten degrees and the velocity to 1500 feet per second. Terminal area energy management is then enabled to control airspeed and to position the orbiter to arrive on the final approach at 12,000 feet, six nautical miles from touchdown. Most of the phase prior to the final approach position will be flown at a large roll angle and at relatively high "g" in order to follow a steeper trajectory. This results in shortening the range and time to touchdown, which reduces the total heat load endured by the vehicle and extends the lifetime of the thermal protection system.

The flight control system itself has three modes: automatic, control stick steering, and direct. Each mode may be selected individually for longitudinal and/or lateral-directional control.

The automatic mode consists of hands-off coupling of guidance commands through the digital flight control system to the control surfaces. Control stick steering



is a pitch (roll) rate command system for the longitudinal (lateral-directional) channel with gain scheduled as a function of the dynamic pressure. This mode is further compensated for angle of bank and for the pitching moment created by the speed brake. The direct system relates controller deflections proportionally to the control surfaces; this mode will be hopefully unnecessary as the vehicle is marginally stable longitudinally, even with a forward center of gravity. "The aerodynamic characteristics of the orbiter, together with its total dependence on avionics for flight control, classify it as a digital fly-by-wire, control-configured vehicle."<sup>2</sup> The entire approach, from de-orbit to re-entry to touchdown, will normally be flown entirely in the automatic mode.

---

<sup>2</sup> LCOL C.G. Fullerton, USAF, "Space Shuttle Orbiter Approach and Landing Test Program," The Society of Experimental Test Pilots, 1975 Report, page 158



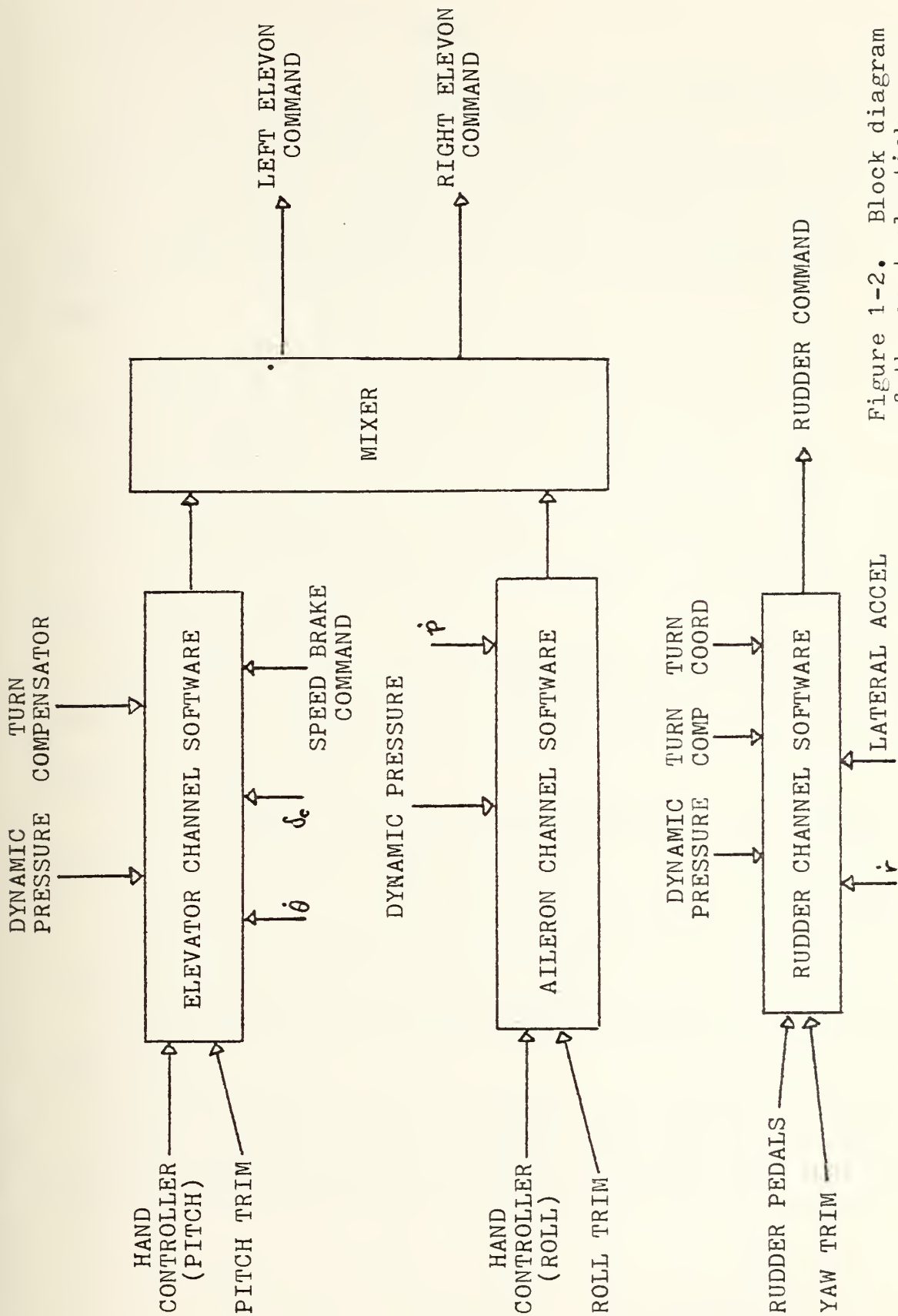


Figure 1-2. Block diagram of the control stick steering mode





## II. DEFINITIONS AND SYMBOLOGY

As in any field of study, that of automatic control has many terms which have a particular meaning when used in this context. So that further references to some of these terms is facilitated, the following definitions apply:

**Angle of attack:** the angle between the fuselage reference line and the flight path; denoted by  $\alpha$ .

**Block diagram:** a graphical representation, such as a schematic diagram, of the physical components of a system or a set of mathematical equations describing their input/output relationships.

**Bode plot:** a plot of the magnitude of response of a system to a sinusoidal input measured against the frequency of that input.

**Characteristic equation:** the denominator of a system's transfer function set equal to zero.

**Closed-loop:** a system in which the input is affected or modified by some stage of output.

**Control matrix:** describes how the control input affects the plant.

**Control system:** a set of physical components related in such a manner so as to control or regulate itself or



some other system.

**Damping:** frictional retardation of the magnitude of a deflection (displacement) or rate.

**Damping ratio:** the ratio of the amount of damping actually present in a system to the amount that would critically damp that system.

**Error signal:** the actual actuating signal of the system; it is generally the difference between the input and feedback signals.

**Feedback:** a signal, which is some form of the output signal, that is added to or subtracted from the original input in order to compare the desired output with that actually obtained.

**Forcing function:** see Input.

**Frequency response:** a measure of the output of the system as a function of input frequency.

**Gain:** the measure of magnitude of an input or feedback signal.

**Initial condition:** one of the two types of inputs to a system.

**Input:** a stimulus applied to a control system in order to produce a desired output.

**Linear differential equation:** one consisting of the sum of linear (first degree) terms; it has the property



that the response of a system due to several inputs acting at once is equal to the sum of the responses of each input acting alone. An equation may be linearized by making valid assumptions (approximations) about the system or by considering the system to operate in a restricted environment where the variations from linearity are small (piece-wise linearity).

Open-loop: a system in which the input is not affected or modified by any stage of output.

Output: the actual response of the system caused by the input reacting with the various components of the system; it is not necessarily the response implied by the input.

Plant: the object or system which is to be controlled.

Reaction control system: a control system which generates rolling, pitching, and/or yawing moments by venting jet, rocket, or compressor air exhaust about the axis desired.

Resolvent matrix: denoted by  $\bar{\Phi}(s)$ ; the matrix which, when multiplied by the control vector and the Laplace of the input, yields the Laplace of the output of the system.

Root locus: a method of graphing the roots of a characteristic equation as a function of gain; useful in stability analysis.



Stability, dynamic: the quality of a system that determines whether its response to any input will be bounded or unbounded.

Stability, static: the tendency of a system following displacement from a rest position, considered positive if the initial tendency is to return to the original position.

State variable: a variable which determines the state of the system; the state variables of a dynamic system are the smallest set of variables which completely determines the behavior of the system for any time  $t \geq 0$ .

Steady state response: that part of the total response which does not approach zero as time approaches infinity.

Terminal area energy management: a dynamic program using inputs of orbiter position and velocity to guide the vehicle to its final approach path, minimizing the heat load when possible.

Time constant: inverse of frequency.

Time-invariant differential equation: a differential equation in which none of the terms depends explicitly upon the independent variable,  $t$ .<sup>3</sup>

Time response: a measure of the output of the system as a function of time.

---

<sup>3</sup> Only linear, time-invariant differential equations will be considered in the development of the equations of motion in this study.





Transfer function: the ratio of the Laplace transform of the output (response) of a system to the Laplace transform of the input (forcing function) under the assumption that the initial conditions are zero.

Transfer matrix: the matrix of transfer functions for a multiple input/output system.

Transient response: that part of the total response which approaches zero as time approaches infinity.

Undamped natural frequency: the frequency at which a system would vibrate were it not damped.

Unit impulse: an input whose magnitude approaches infinity and whose duration approaches zero, but whose product of magnitude times duration equals one.

A glossary of symbols follows:

a lift curve slope,  $\frac{\partial C_L}{\partial \alpha}$

b wing span

$\bar{c}$  mean aerodynamic chord

$C_{L_\alpha}$   $\frac{\partial C_L}{\partial \alpha}$ , variation in lift with respect to angle of attack; generally linear at angles of attack below the stall region; coefficient of

$C_{M_\alpha}$   $\frac{\partial C_M}{\partial \alpha}$ , variation of pitching moment about the center of gravity with respect to angle of attack; must be negative for positive static stability; coefficient of



$C_{M_0}$  pitching moment that remains when lift forces equal zero, coefficient of  
 e span efficiency factor, relative to the elliptical wing and lift distribution  
 f any function, time domain, as  $f(t)$   
 F any function, Laplace domain, as  $F(s)$   
 g transfer function, time domain, as  $g(t)$   
 G transfer function, Laplace domain, as  $G(s)$   
 I moment of inertia, subscripted as to axis about which it is taken  
 K gain  
 $\mathcal{L}$  Laplace transform of, as  $\mathcal{L}[f(t)]$   
 $\mathcal{L}^{-1}$  inverse Laplace transform of, as  $\mathcal{L}^{-1}[F(s)]$   
 L,M,N moments about X-, Y-, and Z-axes, respectively  
 p,q,r perturbations in roll, pitch, and yaw rates  
 $\dot{p}, \dot{q}, \dot{r}$  perturbations in roll, pitch, and yaw accelerations  
 P,Q,R rates of roll, pitch, and yaw  
 S wing area  
 u,v,w perturbations in forward, side, and vertical velocities  
 $\dot{u}, \dot{v}, \dot{w}$  perturbations in forward, side, and vertical accelerations  
 U,V,W velocities in forward, side, and vertical directions  
 x,y,z distances along X-, Y-, and Z-axes



X,Y,Z axis system, right-handed; also force components  
in X, Y, and Z directions

$\alpha$  angle of attack

$\delta$  Dirac delta, unit impulse function  $\delta(t)$

$\delta_e$  deflection, elevon

$\zeta$  damping ratio

$\theta, \dot{\theta}$  pitch angle, rate perturbations

$\Theta$  pitch angle, relative to earth, positive nose up

$\rho$  air density

$\Phi$  roll angle, relative to earth, positive right wing  
down (see also resolvent matrix)

$\omega$  frequency

In order to derive the equations of motion of a system, a reference frame must be decided upon. The most natural of these would be a frame in which the axes were aligned with the physical structure of the vehicle, one which is called the body-fixed axis system. Such a system is depicted in Figure 2-1. Components of velocities, forces and moments, and distances relative to their respective axial motions are listed in Table 2-1.

In the development of the equations of motion for a vehicle, this reference frame has several advantages. The rotary inertial properties are constant (assuming



motion	velocity	applied forces and moments	distance
forward	U	X	x
side	V	Y	y
vertical	W	Z	z
roll	P	L	
pitch	Q	M	
yaw	R	N	

Table 2-1

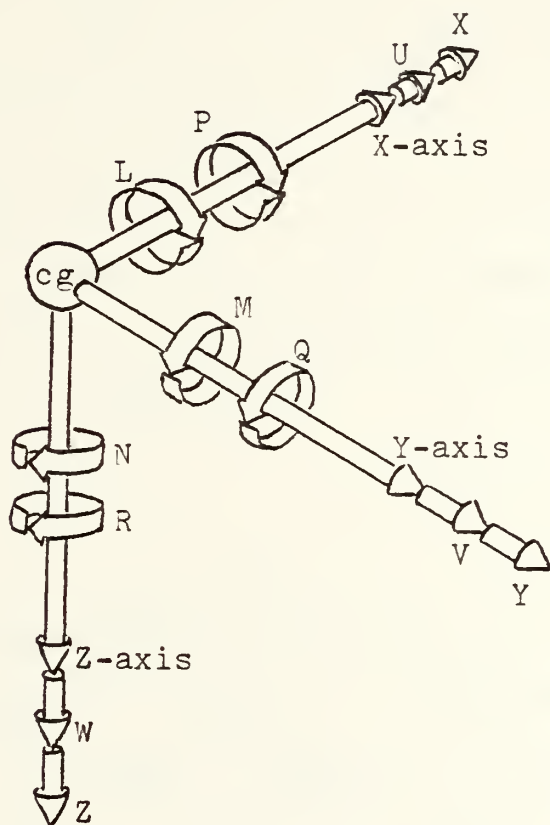


Figure 2-1<sup>4</sup>

<sup>4</sup> Adapted from McRuer, Ashkenas, and Graham, Aircraft Dynamics and Automatic Control, Princeton, 1973





constant mass) so that any derivatives with respect to time are zero. The pilot senses forces and moments with respect to the body-fixed frame, calculates his reactions to vehicular motion and to his changing external environment in terms of the body-fixed axes, and generally measures his position (attitude), velocities, and accelerations from a body-fixed system. This is especially true when he is dealing with primarily relative motion, as in air combat maneuvering.

An alternative to the body-fixed system is the space-fixed system where forces and moments are measured relative to an axis system oriented, for example, to a flat earth, as in Figure 2-2.

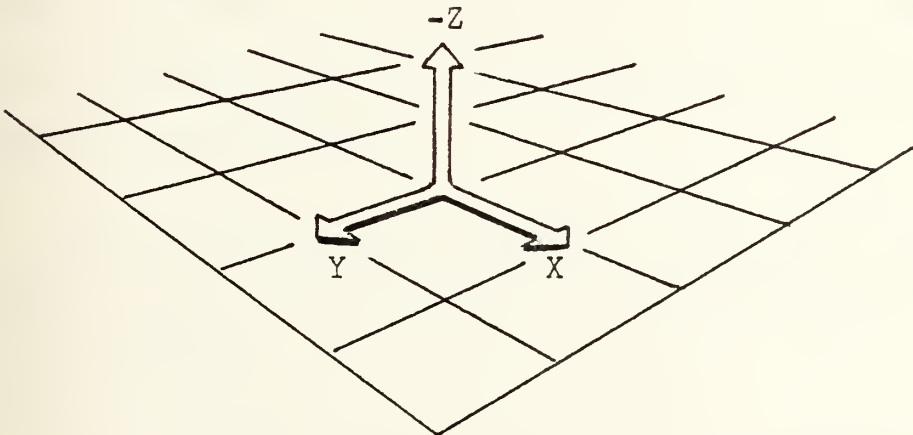


Figure 2-2



This system, however, has the very undesirable feature of requiring inclusion in the equations of motion the variations of moments of inertia of a vehicle as the vehicle changes its velocity vector and/or attitude. This system would be ideal for an aircraft which changed neither, but such is not the case in this study.

Corrections must also be made to the equations of motion in the body-fixed axis system, but these corrections are limited to inertial forces and accelerations and do not involve changing the apparent physical characteristics of the vehicle. Further simplifications are enabled by this choice of systems; one, the small angle assumption is made possible leading to the linearization of the equations of motion (see Chapter V); two, the symmetry of the aircraft across its X-Z plane eliminates several terms in the equations.

The body-fixed axis system is clearly the better selection for the development of the equations of motion of the vehicle.

A definition of "flight control" is necessary in



order to identify those parameters of the vehicle with which the study is concerned. The definition is borrowed from M<sup>C</sup>Ruer, Ashkenas, and Graham<sup>5</sup>:

- "Control: the development and application to a vehicle of appropriate forces and moments that
1. establish some equilibrium state of vehicle motion (operating point control)
  2. restore a disturbed vehicle to its equilibrium (operating point) state and/or regulate, within desired limits, its departure from operating point conditions (stabilization)."

This definition includes the concept of stability and effectively excludes the domain of guidance.

In light aircraft, all functions of control (turning, climbing, accelerating) are performed by the pilot using the control wheel (or stick), the throttle, and various other aerodynamic controls, usually the flap handle, which are directly connected to the device which they operate. For example, the pilot desires to pull up; he uses some degree of back stick, the elevator responds immediately and in proportion to the amount of stick travel, and a pitch rate is generated. The pilot's environment remains

---

<sup>5</sup> Ibid.



relatively constant throughout the flight envelope of the airplane; a ten pound pull on the stick will give, for example, 1.3 g's at a given airspeed in every case.

Even for higher performance aircraft operating in the dynamic environment of air-to-air combat, this is an entirely satisfactory system.<sup>6</sup> Even though a given elevator deflection will not create the same pitch rate at 20000 feet as it does at sea level, the pilot quickly compensates for this by modifying control stick position. However, maintaining a particular pitch angle can better be performed by an automatic control system. Using a set of accelerometers to sense minute deviations from an operating (trim) condition, an automatic control system can command the rapid and precise control deflections necessary to maintain the vehicle near the desired flight condition. A pilot attempting to maintain a given pitch angle will find his sensory threshold much higher than (and his response on the controls much less precise than) an automatic system. This type of system is installed on many aircraft as an auto-pilot, engaged by the pilot when desired, to maintain certain flight conditions such as

---

<sup>6</sup> Present-day fighters have flight control systems augmented by 2- or 3-axis stabilization to minimize gust response and other oscillations.





heading and altitude.

The development and utilization of control systems may be taken one step further. When a vehicle, such as the orbiter, is required to fly in vastly different environments in the course of a mission, control stick inputs to obtain a given maneuver may require very different control deflections. Variations in dynamic pressure, Mach number, and altitude create changing values of control effectiveness, locations of aerodynamic forces, even stability. The automatic control system can use inputs such as air density, dynamic pressure, Mach number, and existing control deflection to compute precisely how much deflection is required to perform a particular maneuver and how rapidly the deflection should be applied. The system may also consider variations in stability under different flight conditions. It will then command that deflection, measure the response, and make further corrections if necessary, with far greater accuracy and efficiency than a human pilot.

This then is the principle by and for which the fly-by-wire system was developed. In an environment of changing flight conditions and stability where high



control precision is required, the automatic system significantly outperforms the best of pilots.



### III. MATHEMATICAL MODELS OF LINEAR SYSTEM ELEMENTS

The Laplace transform is a major tool in the study and analysis of automatic control systems. It is the procedure by which time domain performance is connected to frequency response and results from the correspondence between the transfer function and the transient response. The transfer function itself is the ratio of the Laplace transform of a system's output to the transform of its input, assuming that all initial conditions are zero. A graphic representation of such an input-output relationship is provided by the block diagram. In the block diagram, of which the transfer function(s) is the heart, inputs and feedbacks are represented by their Laplace transforms, and the paths which the signals follow are depicted.

Several simplifications in computation occur when using the Laplace transform, among which are (1) differentiation in the time domain is represented by multiplication by  $s$  in the Laplace (frequency) domain; (2) integration becomes division by  $s$  (both with regard for initial conditions); and (3) convolution, or complex multiplication, becomes simple multiplication.

The equation linking the time domain to the frequency



domain is

$$\mathcal{L}[f(t)] \triangleq F(s) = \lim_{\substack{t_2 \rightarrow \infty \\ t_1 \rightarrow 0}} \int_{t_1}^{t_2} e^{-st} f(t) dt = \int_{0^+}^{\infty} e^{-st} f(t) dt$$

When the equation of motion for a system can be expressed as a linear differential equation, the Laplace transform reduces the differential equation to an algebraic equation in the Laplace variable,  $s$ . To illustrate, a damped spring-mass system will be used.

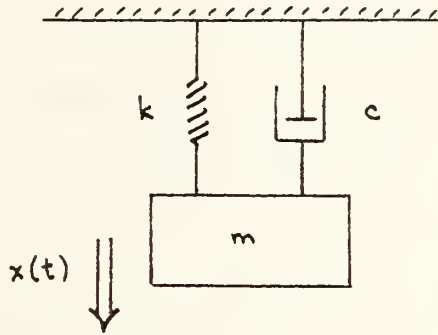


Figure 3-1





Here,  $m\ddot{y} + c\dot{y} + ky = x(t)$ . Each term is replaced by its Laplace transform:

$$m\ddot{y} \rightarrow m \left[ s^2 Y(s) - sy(0) - \frac{dy(0)}{dt} \right]$$

$$c\dot{y} \rightarrow c \left[ sY(s) - y(0) \right]$$

$$ky \rightarrow kY(s)$$

$$x(t) \rightarrow X(s)$$

When coefficients of like powers of  $s$  are collected, the equation becomes

$$\left[ mY(s) \right] s^2 - \left[ my(0) - cY(s) \right] s - \left[ m \frac{dy(0)}{dt} + cy(0) - kY(s) \right] = X(s)$$

The appropriate values of the initial conditions are entered, and a simple quadratic equation in  $s$  has replaced a second order differential equation.

Recalling the definition of a transfer function, all initial conditions are set equal to zero, and the ratio  $Y(s)/X(s)$  is found:

$$\left[ mY(s) \right] s^2 + \left[ cY(s) \right] s + kY(s) = X(s)$$

$$\left[ ms^2 + cs + k \right] Y(s) = X(s)$$

$$\frac{Y(s)}{X(s)} = \frac{1}{ms^2 + cs + k} = G(s) \quad (3-2)$$

where  $G(s)$  is a common symbol for the transfer function.



Figure 3-2 is the block diagram of this system where  $X(s)$  is the input or forcing function,  $Y(s)$  is the output, and  $G(s)$  is the transfer function (also called the plant matrix in multiple input/output systems). In this case,  $G(s)$  has been derived from mass properties of the system, the degree of damping, the spring stiffness, and fundamental laws of motion.

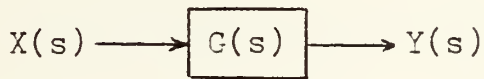


Figure 3-2

In modeling a system,  $G(s)$  will be found in a manner analogous to the above. All that remains in order to find the response to any input (neglecting feedback for the moment) is to multiply the transfer function by the Laplace transform of the input. The response may be left in the frequency domain, which is the usual case in stability analysis, or transformed back into the time domain to study the dynamic characteristics of the system, e.g. rise and settling times, maximum overshoot, etc.

Some of the more common inputs are listed in Table 3-1 with their time- and frequency-domain representations.



The transformations are linear; that is, if  $F(s)$  is the transform of  $f(t)$ , then  $a \cdot F(s)$  is the transform of  $a \cdot f(t)$ .






	time $x(t)$	frequency $X(s)$	graph
unit impulse	$\delta(t)$	1	
unit doublet	$\delta'(t)$	s	
unit step	1	$\frac{1}{s}$	
ramp	t	$\frac{1}{s^2}$	
sinusoidal	$\sin \omega t$	$\frac{\omega}{s^2 + \omega^2}$	

Table 3-1

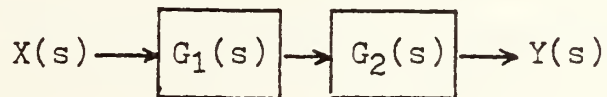
It can be seen in the first column that the unit step is the time derivative of the ramp function, and the unit impulse (represented by the Dirac delta) is the derivative of the unit step. If the latter is not obvious, consider that the derivative of a function is the slope of that function at every point where the function is continuous. At  $t=0$ , the slope of the unit step approaches



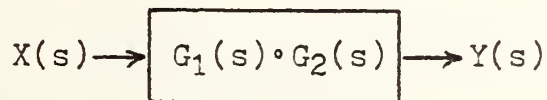
infinity, as does the magnitude of the unit impulse. At  $t=0^+$ , the slope of the unit step is zero, as is the magnitude of the impulse function.

Since an impulse function is an idealization, it must be approximated in the real world. When finding the Laplace transform of this approximation, any arbitrary magnitude may be assigned to the "impulse", as long as its duration is small compared to the time constant of the system. If the duration of the impulse is taken as the inverse of the magnitude, the area under its curve will equal one, hence the unit impulse.

Unless otherwise depicted, successive terms along a block diagram path are multiplied together; witness the correlation between equation (3-2) and Figure 3-2. This is true whether dealing with inputs, successive transfer functions, or other operations such as integration, delay, or differentiation. Diagrammatically,



is identical to



The resulting transfer function  $G(s) = G_1(s) \cdot G_2(s)$ , or





the output  $Y(s) = X(s) \cdot G_1(s) \cdot G_2(s)$ .

A feedback signal, on the other hand, is not multiplied but rather employs a summing junction where certain signals downstream in the diagram are fed back and added to (or subtracted from) the input signal. A typical system with one feedback loop is depicted in Figure 3-3. The derivation of the complete, or closed loop, transfer function follows.

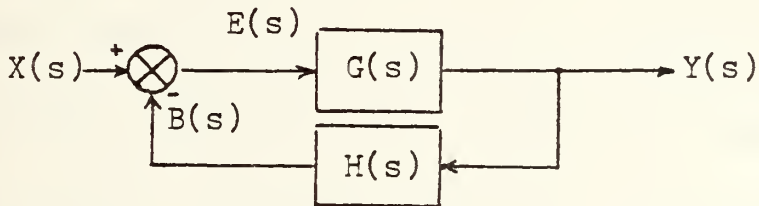


Figure 3-3

$E(s)$  represents an error signal, the difference between the input signal and the feedback signal.  $B(s)$  is called the open loop transfer function; it is the input signal after being modified by any transfer functions and feedback terms up to the summing junction.

In this case

$$B(s) = G(s) \cdot H(s) \cdot E(s).$$

$$\text{Since } Y(s) = G(s) \cdot E(s),$$



$$\text{and } E(s) = X(s) - B(s) = X(s) - G(s) \cdot H(s) \cdot E(s)$$

$$\text{then } E(s) + G(s) \cdot H(s) \cdot E(s) = X(s)$$

$$\text{or } E(s) [1 + G(s) \cdot H(s)] = X(s)$$

$$E(s) = \frac{X(s)}{1 + G(s) \cdot H(s)}$$

Substituting the error signal above into  $Y(s) = G(s) \cdot E(s)$ , the transfer function of the system due to feedback be-

comes 
$$G^*(s) = \frac{Y(s)}{X(s)} = \frac{G(s)}{1 + G(s) \cdot H(s)} \quad .$$

The second order system defined by the damped spring-mass system has the unique definition among its properties that

$$\frac{c}{m} = 2\zeta\omega_n \quad \text{and} \quad \frac{k}{m} = \omega_n^2 \quad \text{where } \zeta = \text{damping ratio}$$

and  $\omega_n =$  undamped (natural) frequency. If the equation of motion is divided through by  $m$ , the result is

$$\ddot{y} + \frac{c}{m} \dot{y} + \frac{k}{m} y = \frac{k}{m} x(t)$$

$$\text{or, } \ddot{y} + 2\zeta\omega_n \dot{y} + \omega_n^2 y = \omega_n^2 x(t)$$

where, for convenience, the input function  $x(t)$  has absorbed a constant  $1/k$ . Taking the Laplace transform as before and letting the initial conditions equal zero,

$$\frac{Y(s)}{s^2 + 2\zeta\omega_n s + \omega_n^2} = X(s)$$

$$\text{or } \frac{Y(s)}{X(s)} = \frac{\omega_n^2}{s^2 + 2\zeta\omega_n s + \omega_n^2} \quad .$$



If, then, the transfer function of a system may be written in the format  $b/(s^2 + as + b)$ , the physical characteristics of the system are immediately evident.

As will be seen in the analysis of the orbiter, the system transfer function may be factored into two such second order terms yielding at once the periods and degrees of damping of both the phugoid and the short period motions. The damping term offers a further clue as to basic or inherent stability of the system. When the roots of the quadratics are obtained from  $s = -\zeta\omega_n \pm \omega_n\sqrt{\zeta^2 - 1}$ , the value of  $\zeta$  determines whether or not those roots lie in the right half plane (RHP) according to Table 3-2.

value of $\zeta$	roots are
$\zeta < 0$	in RHP
$\zeta = 0$	pure imaginary
$0 < \zeta < 1$	complex with negative real parts
$\zeta = 1$	equal, negative, and real
$\zeta > 1$	negative and real

Table 3-2

The significance of a root or roots in the right half plane will be discussed in the section on stability.



#### IV. STABILITY

One of the prime indices of a vehicle's performance is the measure of its stability, or how, how much, and how quickly it responds to external forces or control inputs.

Two types of stability are generally defined, static and dynamic. Static stability is the vehicle's tendency to return to its original flight condition after being disturbed from that condition. A common representation of the three degrees of static stability, positive, negative, and neutral, is shown in Figure 4-1. The ball possessing positive static stability will return to its original position when displaced, the ball with negative static stability will continue to move away from its

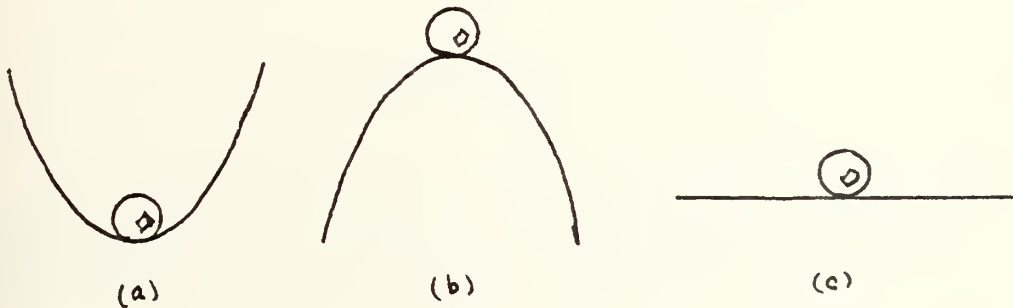


Figure 4-1





original position, and the ball with neutral stability will simply remain in its new position.

The parallel may be drawn with respect to an aircraft's longitudinal (pitch) response when displaced from trimmed flight<sup>7</sup> by a control input or external force. Figure 4-2 illustrates the longitudinal forces acting on a vehicle where  $L$  is the sum of lift forces produced by the wing and tail and is located on the aircraft so as to create the same total moment about the center of mass as would the individual forces.  $C_{m_0}$  is the pitch moment remaining when the lift forces are zero.

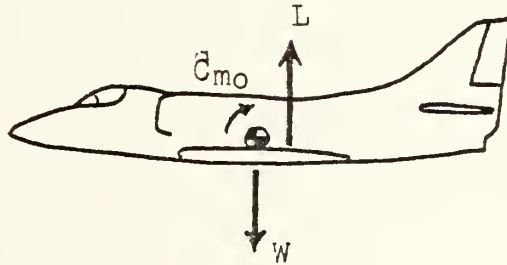


Figure 4-2

---

<sup>7</sup> Trimmed flight is defined as that flight condition where the sum of all moments acting about the longitudinal axis is zero, i.e.,  $C_M = 0$ .



In equilibrium flight, the moment produced by  $L$  is balanced by  $C_{m_0}$ , and no pitch rate is generated. Suppose a gust causes a momentary increase in the angle of attack. If the lift curve slope is positive (that is, a higher angle of attack generates more lift), as are all modern conventional airfoils, the increased lift will cause the total moment about the center of mass to be nose down, or stabilizing. The vehicle will tend to return to its original condition.

If the center of mass should move aft of the lift vector, the aircraft could still be stable if  $C_{m_0}$  were negative (nose down). However, if that gust were to hit this aircraft, the increased lift would cause a nose UP moment, increasing the angle of attack, further increasing the lift, etc. This vehicle then would be clearly unstable.

Three quantities are necessary to this discussion, the lift curve slope, the pitching moment coefficient, examples of which are shown in Figure 4-3, and  $C_{m_0}$ . A vehicle must have a positive lift curve slope ( $\frac{\partial C_L}{\partial \alpha}$ ), a negative pitching moment slope (which means an angle of attack above the trim point causes a pitch down and vice



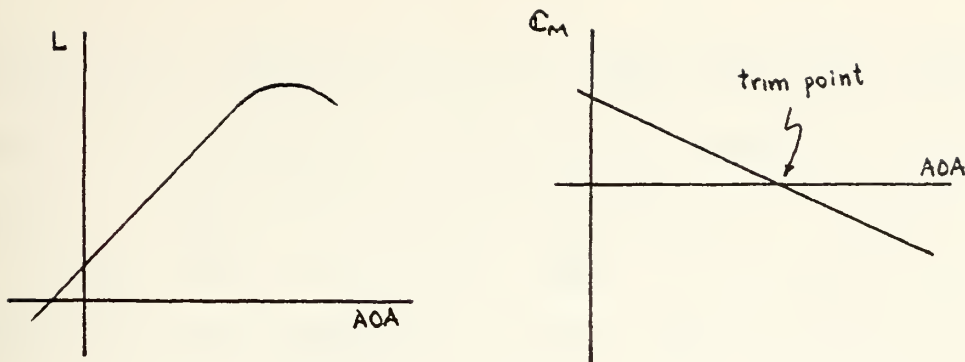


Figure 4-3

versa), and a positive  $C_{m_0}$  in order to be statically stable.  $C_{m_\alpha}$  is negative when the aerodynamic center of the vehicle lies behind the center of mass, and a positive  $C_{m_0}$  is designed into the airframe.

Given that a vehicle has positive static stability, its dynamic stability may be studied<sup>8</sup>. The ball in Figure 4-1(a) is dynamically stable; if displaced from equilibrium, it would return to the bottom, probably overshoot, overshoot again coming back (but at a smaller magnitude), and eventually come to rest. If there were no friction, the system would be dynamically neutrally stable; the amount of overshoot would not vary from cycle to cycle. If, on the other hand, a magnetic

---

<sup>8</sup> An exception to this requirement for positive static stability is the orbiter itself. Early in the re-entry phase, at an angle of attack of  $45^\circ$ , the orbiter is laterally unstable due to the blanking of the vertical stabilizer. However, the presence of a lightly damped Dutch roll gives it positive dynamic stability.



device were installed under the bowl which was timed to attract the ball as it descended and repel it as it ascended, enough velocity could be imparted to the ball to finally shoot it over the side. As long as the force supplied by the magnet was by any degree greater than the forces of friction, the ball would eventually be thrown from the bowl; this is an example of a statically stable but dynamically unstable system.

Each degree of stability can be exemplified by an aircraft. A sharp rap on the control stick of a trimmed aircraft causes a pitch oscillation which quickly damps out and disappears (positive stability). Most aircraft have some degree of Dutch roll, a continuous but mild combination of rolling and yawing (neutral stability). High performance aircraft, whose stability may be marginal under certain conditions, can be susceptible to PIO (pilot induced oscillation) where the pilot plays the rôle of the aforementioned magnetic device and amplifies the pitching motion of the vehicle, with sometimes catastrophic results (negative dynamic stability).

In the more complicated realm of automatic control





systems involving feedback, high precision approach and landing sequences, etc., more than just "positive" or "negative" as regards stability must be known. For one reason or another, it may be desirable to utilize a high gain for a particular feedback signal, but there may be a limit as to how high the gain may be before it causes the system to become unstable. Certain types of inputs, generally frequency related, may cause large increases in the magnitude of response (resonance) and may require a certain amount of feedback to minimize these excursions.

Two of the basic tools used for studying the effects of feedback on a system are the root locus graph and the Bode plot.

The root locus is a locus of roots; the roots are those of the characteristic equation of the system. If the real parts of these roots are all negative, then the solution of the differential equation describing the system will involve negative (decaying) exponents, and the system will be stable. This is the rationale behind requiring roots to be in the left half plane for stability. Feedback gain can change the location of these roots and cause a system to become unstable.



An example is in order. Consider the system shown in Figure 4-4, where the plant transfer function is

$$\frac{(s-2)}{(s+1)(s+2)}$$

and where the feedback is linear and variable in magnitude.

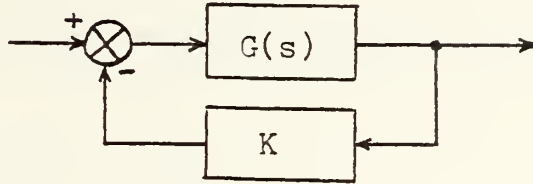


Figure 4-4

The closed loop transfer function becomes

$$\frac{(s-2)}{(s+1)(s+2) + K(s-2)},$$

and the characteristic equation is

$$s^2 + (3+K)s + (2-2K) = 0.$$

The roots, for varying values of K, are given in Table 4-1.

K	root #1	root #2
0	-1	-2
0.5	-0.314	-3.186
1.0	0	-4
1.5	0.212	-4.712
2.0	0.372	-5.372

Table 4-1



Figure 4-5 is a graph of the root locus of the system. It may be seen that, as K exceeds the value of 1, one of the roots moves into the right half plane. That this

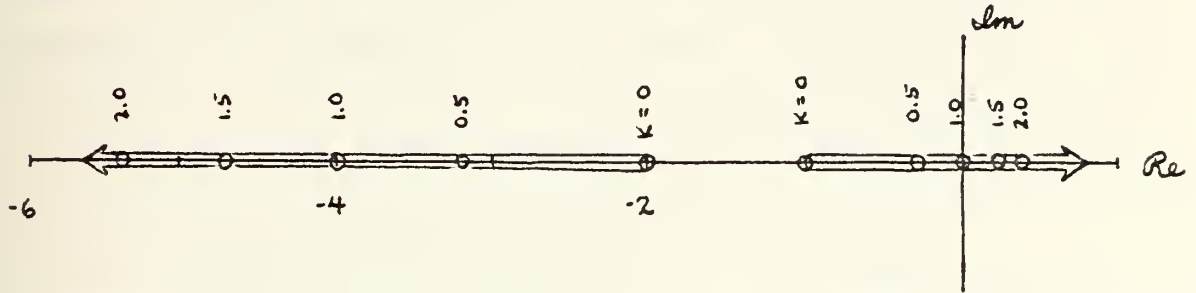


Figure 4-5

results in instability is shown by solving the corresponding differential equation for a value of  $K > 1$ . Let  $K=2$ ; the characteristic equation becomes

$$s^2 + 5s - 2 = 0.$$

Converting this equation to the time domain by taking the inverse Laplace transform yields

$$\ddot{y} + 5\dot{y} - 2y = 0,$$

one of the solutions to which is  $y = e^{0.372t}$ . Since  $y$  is the output, it may be seen that the output increases without bound as the time increases. The system is unstable for this value of feedback gain.



The Bode plot depicts how the system will respond to a sinusoidal input. Gain and phase margins, which are measures of relative stability, are shown directly by the plot, as is the magnitude of response at resonance. By comparison with templates of the proper scale, the degree of damping may be read from the graph.

The standard representation of the magnitude of the response is  $20 \cdot \log |G(j\omega)|$  where  $j\omega$  has replaced  $s$  in the transfer function expression. This magnitude is plotted against the frequency of the input, which is on a logarithmic scale so that wide frequency ranges may be plotted with accuracy. The phase angle,  $\phi$ , is likewise plotted against the logarithmically scaled frequency. A stable, time-invariant system, when energized by a sinusoidal input, will have a steady state output of the same frequency as the input although the magnitude and phase angle will likely be different.

Since the magnitude of the response is plotted in logarithmic form, finding the response curve of a complicated transfer function such as

$$G(s) = \frac{s^2 + 3s + 2}{s^3 + 6s^2 + 19s + 13}$$

is reduced to writing the function as the product of





first-order factors, finding the magnitude of each, and then adding (not multiplying) the logarithms of the magnitudes. From this, it is seen that an increase in gain merely raises the magnitude curve and does not affect the phase angle.

In the above example, writing the transfer function as a function of  $j\omega$ ,

$$G(j\omega) = \frac{(j\omega)^2 + 3j\omega + 2}{(j\omega)^3 + 6(j\omega)^2 + 19(j\omega) + 13} = \frac{(2 - \omega^2) + 3j\omega}{(13 - 6\omega^2) + j(19\omega - \omega^3)} .$$

Letting  $\omega = 0.1$  yields

$$G(j0.1) = \frac{1.99 + j0.3}{12.94 + j1.899} \quad \text{and} \quad |G(j0.1)| = \frac{2.012}{13.079} = 0.1538 .$$

Then  $20 \ln |G(j0.1)| = -37.438$ , the measure of magnitude of the response when the input frequency is 0.1 radian per second.

The phase angle is

$$\varphi = \tan^{-1} \frac{0.3}{1.99} - \tan^{-1} \frac{1.899}{12.94} = 8.57^\circ - 8.35^\circ = 0.22^\circ .$$

Computing the values of the magnitude and phase angle over a wide range of frequencies, say from 0.001 to 10 radians per second, enables the construction of



the Bode diagram.

If the function is factored into

$$G(s) = \frac{(s+1)(s+2)}{(s+3+j2)(s+3-j2)(s+1)}$$

and each term written as a function of  $j\omega$ , the terms become

$$j\omega+1 \quad j\omega+2 \quad [3+j(\omega-2)]^{-1} \quad [3+j(\omega+2)]^{-1} \quad [j\omega+1]^{-1}.$$

The magnitudes at  $\omega = 0.1$  are, respectively,

$$1.005 \quad 2.002 \quad 0.282 \quad 0.273 \quad 0.995.$$

The logarithms of these magnitudes are

$$0.005 \quad 0.694 \quad -1.266 \quad -1.298 \quad -0.005.$$

which, when summed, total  $-1.870$ . Multiplying by 20, as before, yields  $-37.4$ , the same answer.

The sum of the phase angles is

$$5.71^\circ + 2.86^\circ - (-32.3^\circ) - 34.99^\circ - 5.71^\circ = 0.17^\circ,$$

approximately the same answer as before.

The factoring method is desired when the Bode plot is to be approximated by asymptotes, or straight lines which follow the trend of the function. It does not consider damping. The former method is entirely sufficient for plotting the exact function and will be the one used in this study.



A third type of graph used in the analysis of a system is the time response graph, or time history. Any forcing function (not just sinusoidal) for which a Laplace transform exists can be applied to a system, the output calculated, and the output inverted into the time domain. This yields a function of magnitude with respect to time, the plot of which depicts period(s), overshoot(s), rise times, decay times, steady state response, and gives an indication of the degree of damping in the system. Its drawback is that its degree of stability is not easily derived, although it is usually apparent whether or not the response is bounded.

As has been seen, gain will move the locus of roots on a root locus plot, sometimes changing the stability of a system; gain will move the Bode magnitude plot up or down, changing the relative stability. When gain is applied to a system, the time history plot reflects amplification of the magnitude of the response in proportion to the amount of gain, i.e., twice the gain yields twice the magnitude.<sup>9</sup> For example, if 5° of elevator deflection create 50 lbs of force and 1000

---

<sup>9</sup> Since we are dealing with linear systems



ft-lbs of moment, then  $10^\circ$  of deflection will generate 100 lbs of force and 2000 ft-lbs of moment; the pitch rate created by the latter moment will be double that created by the former. However, when the gain to be varied is in a feedback loop, as described above for the root locus and Bode diagrams, the effects on the time history are generally unpredictable. The time history is therefore of limited value in designing a system; its asset is rather in analysis. All three types of plots will be used in this study.





## V. EQUATIONS OF MOTION

In confining the study to the longitudinal case, only the X and Z forces and the pitching moment, M, are of interest. Each of these may have derivatives with respect to (1) forward velocity, u, (2) pitch angle, q, (3) vertical velocity, w, (4) vertical acceleration,  $\dot{w}$ , and (5) elevon deflection,  $\delta_e$ . These derivatives are labelled, respectively,  $X_u$ ,  $X_q$ ,  $X_w$ ,  $X_{\dot{w}}$ ,  $X_{\delta_e}$ ,  $Z_u$ , etc. The lower case subscripts refer to perturbations from steady state.

The linearized equations of motion in state variable format, in terms of the derivatives defined above, are:

$$\begin{aligned}
 \dot{u} &= X_u u + X_w w + X_q q - q^{\theta} + X_{\delta_e} \delta_e \\
 \dot{w} &= Z_u u + Z_w w + (U_0 + Z_f) q + Z_{\delta_e} \delta_e \\
 \dot{q} &= (M_u + Z_u M_{\dot{w}}) u + (M_w + Z_w M_{\dot{w}}) w \\
 &\quad + [M_q + (U_0 + Z_f) M_{\dot{w}}] q + (M_{\delta_e} + Z_{\delta_e} M_{\dot{w}}) \delta_e \\
 \dot{\theta} &= q
 \end{aligned} \tag{5-1}$$



The state variables are written in the format

$$\{x\} = \begin{Bmatrix} u \\ w \\ \dot{\varphi} \\ \theta \end{Bmatrix}$$

and the equations of motion become

$$\begin{Bmatrix} \dot{u} \\ \dot{w} \\ \ddot{\varphi} \\ \ddot{\theta} \end{Bmatrix} = \begin{bmatrix} X_u & X_w & X_{\dot{\varphi}} & -g \\ Z_u & Z_w & (U_0 + Z_{\dot{\varphi}}) & 0 \\ (M_u + Z_u M_{\dot{w}}) & (M_w + Z_w M_{\dot{w}}) & [M_{\dot{\varphi}} + (U_0 + Z_{\dot{\varphi}}) M_{\dot{w}}] & 0 \\ 0 & 0 & 1 & 0 \end{bmatrix} \begin{Bmatrix} u \\ w \\ \dot{\varphi} \\ \theta \end{Bmatrix} + \begin{Bmatrix} X_{\delta_e} \\ Z_{\delta_e} \\ (M_{\delta_e} + Z_{\delta_e} M_{\dot{w}}) \\ 0 \end{Bmatrix} \delta_e$$

$$\text{Or, } \{\dot{x}\} = [A]\{x\} + \{B\} \delta_e$$

where  $[A]$  is the plant matrix and  $\{B\}$  is called the control matrix.

Some justification is in order for the linearization of the system equations of motion. Assumptions are also made to simplify the development and/or to define the scope of the study. Reference is made to Figure 2-1 for sign convention and notation in a body-fixed axis system; linear and angular velocities and applied forces and moments are identified.



The first assumption, which both simplifies the development and defines the environment, is that the earth is fixed in space. In orbital flight, a universal inertial frame is necessary due to the spinning of the earth on its axis and to the more pronounced effects of the gravitational fields of the sun and moon on a spacecraft. However, for the relatively short-term control analysis of this study, a geo-inertial frame of reference is assumed.

The airframe is assumed to be rigid. This enables the description of vehicular motion as a translation of and rotation about the vehicle's center of mass. The method of application of the thermal protection layer of the orbiter requires an absolute minimum of relative motion between and within various sections of the body, so this assumption of rigidity is especially valid.

The mass and mass distribution of the vehicle is assumed to be constant. Actually, since no fuel is being burned in producing thrust and no stores expended during that part of the trajectory under study, this, too, is an especially valid assumption.



For body-fixed axes, the inertial equations of motion (neglecting gravity) are:

$$\begin{aligned}\Sigma F_x &= m(\dot{U} + QW - RV) \triangleq X \\ \Sigma F_z &= m(\dot{W} + PV - QU) \triangleq Z \\ \Sigma M_y &= \dot{Q}I_y + PR(I_x - I_z) + (P^2 - R^2)I_{xz} \triangleq M\end{aligned}$$

The gravity force, acting only at the vehicle's center of mass, produces no moments but does contribute to the external forces; due to gravity,

$$\begin{aligned}\Delta X &= mg \sin(-\Theta) = -mg \sin \Theta \\ \Delta Z &= mg \cos(-\Theta) \cos \Phi = mg \cos \Theta \cos \Phi\end{aligned}$$

The combination of the inertial and gravitational forces on the vehicle yields:

$$\begin{aligned}X &= m(\dot{U} + QW - RV + g \sin \Theta) \\ Z &= m(\dot{W} + PV - QU - g \cos \Theta \cos \Phi) \\ M &= \dot{Q}I_y + PR(I_x - I_z) - R^2 I_{xz} + P^2 I_{xz}\end{aligned}$$

Differentiating these equations yields equations of perturbed motion (where, for example,  $dU = u$ ):

$$\begin{aligned}dX &= m[\dot{u} + W_0 q + Q_0 w - V_0 r - R_0 v + (g \cos \Theta_0) \theta] \\ dZ &= m[\dot{w} + V_0 p + P_0 v - U_0 q - Q_0 u \\ &\quad + (g \cos \Theta_0 \sin \Phi_0) \phi + (g \sin \Theta_0 \cos \Phi_0) \theta] \\ dM &= \dot{q} I_y + (P_0 r + R_0 p)(I_x - I_z) - (2R_0 r - 2P_0 p) I_{xz}\end{aligned} \tag{5-2}$$





where the quantities subscripted zero are the steady state (trimmed) values. To arrive at these equations,  $U$  was replaced by  $U_0 + u$ ,  $P$  by  $P_0 + p$ , etc, and another assumption was made: the disturbances from steady flight are small enough so that the sine of an angle may be replaced by the angle itself and the cosine of an angle equals one. Any products of perturbations are neglected. The "small perturbation" concept has linearized the transcendental equations of the system.

Because of the symmetry of the airframe in the X-Z plane, and because there are no aerodynamic asymmetries such as propeller slipstream, it is assumed that longitudinal forces and moments due to lateral perturbations about the trim condition are negligible. Pitch rate at trim,  $Q_0$ , is defined to be zero. A further simplification, which now has no effect on the system, is that  $P_0 = R_0 = V_0 = \Phi_0 = \text{zero}$ . This yields

$$\delta X = m [\dot{u} + \bar{w}_0 \zeta + g\theta]$$

$$\delta Z = m [\dot{w} - U_0 \zeta]$$

$$\delta M = \dot{q} I_y$$

Since the aerodynamic forces and moments on the vehicle are dependent mainly upon the velocity of the



vehicle with respect to the air and not upon acceleration of the air mass, all derivatives with respect to acceleration are neglected. The exception is  $\dot{w}$ , an important one as it corresponds to the time lag between a vertical velocity perturbation at the leading edge and its effect at the trailing edge. It would not exist if downwash did not exist, but by this very fact, its magnitude cannot be disregarded. The flow is now assumed to be quasi-steady.

Altitude perturbations, being assumed small, allow the neglect of air density and temperature perturbations.

If the body axes are now rotated so that the x-axis points into the relative wind,  $W_0$  may be set equal to zero. This orientation forms a stability axis system. (Since small angle assumptions have been made, perturbations can still be measured in the body-fixed axis system.) Applying this rotation of axes to equations (5-2) and taking the Laplace transform of each yields

$$\begin{aligned}
 (s - X_u)u - (X_{w'}s + X_{w''})w + (-X_{\theta}s + g \cos \theta_0)\theta &= X_{\delta_e} \delta_e \\
 -Z_u u + (s - Z_{w'}s - Z_{w''})w + [(-U_0 - Z_{\theta})s + g \sin \theta_0]\theta &= Z_{\delta_e} \delta_e \\
 -M_u u - (M_{w'}s + M_{w''})w + s(s - M_{\theta})\theta &= M_{\delta_e} \delta_e
 \end{aligned}$$



A vector diagram of the forces acting on the vehicle will aid in the discussion of the derivative terms in the above equations; see Figure 5-1. Note that there is no thrust force present.

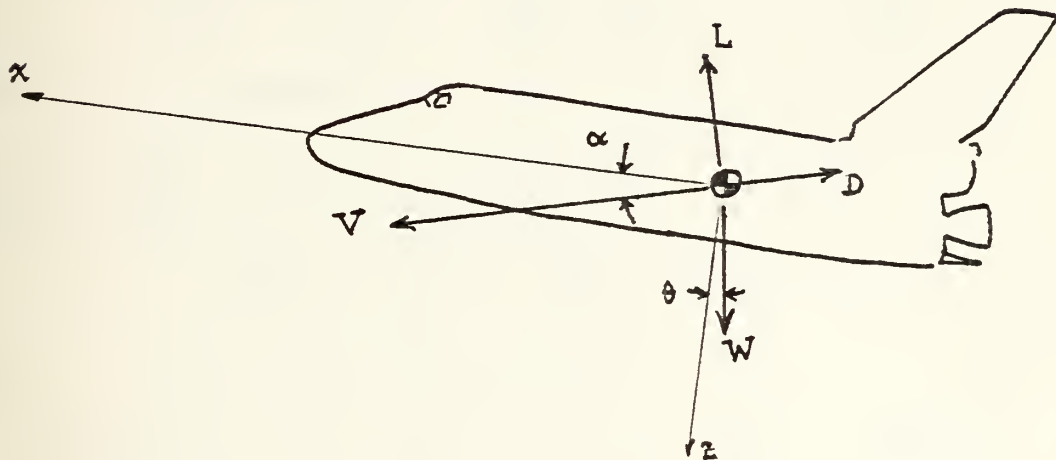


Figure 5-1

The sums of forces in the x- and z-directions is,  
for small  $\alpha$

$$X = L \sin \alpha - D \cos \alpha \approx L \alpha - D$$

$$Z \approx -(L + D \alpha)$$

The velocity,  $\vec{V}$ , is assumed to be equal to  $U_0$ . This assumption is justified by the following treatment:

$$\begin{aligned} \vec{V} &= \sqrt{(U_0 + u)^2 + v^2 + w^2} \\ &= \sqrt{U_0^2 + 2U_0u + u^2 + v^2 + w^2} \end{aligned}$$



Since  $u$ ,  $v$ , and  $w$  are perturbations and are small when compared to  $U_0$ , their products may be neglected:

$$\bar{V} = \sqrt{U_0^2 + 2U_0u} = U_0 \sqrt{1 + u/U_0} \approx U_0$$

Since  $\Delta X = \frac{\partial X}{\partial u} u$ , then

$$\frac{\partial X}{\partial u} u = \left( \frac{\partial L}{\partial u} \alpha_0 + L \frac{\partial \alpha_0}{\partial u} - \frac{\partial D}{\partial u} \right) u = - \frac{\partial D}{\partial u} u$$

where  $\alpha_0$  is assumed to be zero. Using the definitions

$$X_u \triangleq \frac{1}{m} \cdot \frac{\partial X}{\partial u} \quad \text{and} \quad D = \frac{1}{2} \rho U_0^2 S C_D, \quad \text{then}$$

$$\begin{aligned} X_u &= - \frac{\rho S}{2m} \left( U_0^2 \frac{\partial C_D}{\partial u} + 2U_0 C_D \right) \\ &= - \frac{\rho S U_0}{m} \left( \frac{U_0}{2} \frac{\partial C_D}{\partial u} + C_D \right) \end{aligned}$$

$$\text{Similarly} \quad \Delta Z = \frac{\partial Z}{\partial u} u = - \left( \frac{\partial L}{\partial u} + \frac{\partial D}{\partial u} \alpha_0 + \frac{\partial \alpha_0}{\partial u} D \right) u = - \frac{\partial L}{\partial u} u$$

$$Z_u \triangleq \frac{1}{m} \cdot \frac{\partial Z}{\partial u} = - \frac{1}{m} \frac{\partial L}{\partial u}$$

Since lift =  $L = \frac{1}{2} \rho U_0^2 S C_L$ , then

$$Z_u = - \frac{\rho S U_0}{m} \left( \frac{U_0}{2} \frac{\partial C_L}{\partial u} + C_L \right)$$

Finally, where the moment =  $M = \frac{1}{2} \rho U_0^2 S \bar{c} C_m$ ,

$$M_u = \frac{\rho U_0 S \bar{c}}{I_y} \left( \frac{U_0}{2} \frac{\partial C_m}{\partial u} + C_m \right)$$





Using the same substitution and differentiation techniques as above, the rest of the force derivatives are found.

The q-derivatives:

$$X_q = - \frac{\rho U_0 S \bar{z}}{4m} \cdot \frac{\partial C_D}{\partial (\bar{z}^2/2U_0)} \quad 10$$

$$Z_q = - \frac{\rho U_0 S \bar{z}}{4m} \cdot \frac{\partial C_L}{\partial (\bar{z}^2/2U_0)}$$

$$M_q = \frac{\rho U_0 S \bar{z}^2}{4I_y} \cdot \frac{\partial C_m}{\partial (\bar{z}^2/2U_0)}$$

The w-derivatives:

$$X_w = \frac{\rho U_0 S}{2m} \left( C_L - \frac{\partial C_D}{\partial \alpha} \right)$$

$$Z_w = - \frac{\rho U_0 S}{2m} \left( \frac{\partial C_L}{\partial \alpha} + C_D \right)$$

$$M_w = \frac{\rho U_0 S \bar{z}}{2I_y} \cdot \frac{\partial C_m}{\partial \alpha}$$

The  $\dot{w}$ -derivatives:

$$X_{\dot{w}} = - \frac{\rho S \bar{z}}{4m} \cdot \frac{\partial C_D}{\partial (\dot{w}^2/2U_0)}$$

$$Z_{\dot{w}} = - \frac{\rho S \bar{z}}{4m} \cdot \frac{\partial C_L}{\partial (\dot{w}^2/2U_0)}$$

$$M_{\dot{w}} = \frac{\rho S \bar{z}^2}{4I_y} \cdot \frac{\partial C_m}{\partial (\dot{w}^2/2U_0)}$$

---

<sup>10</sup>The non-dimensionalization procedure is discussed later in this chapter.



The  $\delta_e$ -derivatives:

$$Y_{\delta_e} = - \frac{\rho U_0^2 S}{2m} \cdot \frac{\partial C_D}{\partial \delta_e}$$

$$Z_{\delta_e} = - \frac{\rho U_0^2 S}{2m} \cdot \frac{\partial C_L}{\partial \delta_e}$$

$$M_{\delta_e} = \frac{\rho U_0^2 S \bar{z}}{2 I_y} \cdot \frac{\partial C_m}{\partial \delta_e}$$

Since the forces and moments are proportional to, respectively, mass and moment of inertia, the stability derivatives are non-dimensionalized by dividing the force/moment equations by these quantities; hence, the appearance of  $1/m$  and  $1/I_y$  in the results.

Some of the derivatives have particular significance or are named according to their effect on the motion of the system. Others may be neglected for various reasons. A discussion of these items is in order.

The quantity  $\frac{\partial C_D}{\partial u}$  is called the speed damping derivative.

The quantity  $\frac{\partial C_L}{\partial u}$  is generally small except at transonic speeds, the subject of this paper.

The quantity  $\frac{\partial C_m}{\partial u}$  results from aeroelastic effects,



which are being neglected, and from compressibility effects, which are not. It, too, is largest at transonic speeds.

$C_{mq}$  is damping in pitch and is negative for a stable vehicle. Its primary effect is on short period damping.

The quantity  $\frac{\partial C_m}{\partial \alpha}$  is the static stability derivative, the prime indicator of static longitudinal stability. Given an increase in angle-of-attack, the increased lift on the wing (normally, a tail contribution is dominant) will cause a negative pitching moment (nose down) about the center of mass of the vehicle. If this is the case, the center of mass must be forward of the aerodynamic center of the wing, and the vehicle is statically stable. Considering the tailless orbiter, it is expected that  $C_{m_\alpha}$  will be small compared to a conventional aircraft, becoming somewhat more negative (more stable) as the vehicle becomes supersonic and the aerodynamic center moves further aft on the wing.

The quantity  $\frac{\partial C_L}{\partial \alpha}$  is the lift curve slope and is positive and generally linear at angles-of-attack



below stall.

Since a change in drag on a horizontal tail is the main contributor to a change in  $X_{\dot{w}}$ , and since this drag increment is small anyway compared to the total drag,  $X_{\dot{w}}$  is neglected in further discussion.

Because of the time lag between a change in angle-of-attack at the leading edge and the change in pressure distribution at the trailing edge,  $\frac{\partial C_L}{\partial \dot{\alpha}}$  is produced. However, it is a negligible quantity.

The quantity  $\frac{\partial C_m}{\partial \dot{\alpha}}$  will increase short period damping when it is negative, as is normally the case. It is non-dimensionalized as  $\frac{\partial C_m}{\partial (\dot{\alpha} \tau / 2U_0)}$ .

The quantities  $\frac{\partial C_L}{\partial \delta_e}$  and  $\frac{\partial C_D}{\partial \delta_e}$  are both significant in tailless vehicles, the first being always positive, the second smaller and sometimes negative. Their ratio may be likened to  $L/D$ .  $C_{m\delta_e}$  is elevator control effectiveness and, as the name implies, is quite important. It determines how much pitching moment will be generated for a given elevon deflection. It is sensitive to center of mass travel, aerodynamic center travel (as when a vehicle becomes supersonic), and  $C_{L_{max}}$ . It is





a negative quantity for elevons aft of the center of gravity.

Since  $\alpha = \tan^{-1}(w/U_0) \doteq w/U_0$ , the terms  $\alpha$  and  $w$  may be interchanged (as may their derivatives) with due respect for the constant of proportionality.

The non-dimensional stability derivatives introduced on page 61 will be used wherever practical. In accordance with McRuer's definitions, they are called basic derivatives because they do not involve any inertial quantities. They are called non-dimensional because they involve force and moment coefficients rather than the forces and moments themselves. They are useful in that study of the vehicle under different flight conditions is most easily correlated. It may be seen that, for example,  $\frac{\dot{\alpha} \bar{c}}{2U_0}$  is the non-dimensional form of  $\dot{\alpha}$ .

The other type of derivative, of which  $X_u$  is an example, is called a dimensional stability derivative parameter. It will be used in the study of airframe transfer functions.



## VI. COMPUTER METHODS OF ANALYSIS

The concept of state variable analysis was made possible with the advent and refinement of the high speed digital computer. The arithmetical operations involved in dealing with just a  $4 \times 4$  matrix are copious; they include inverting, factoring, solving the equations the matrix represents (which are often differential equations), and applying the results to state variable procedures for obtaining such things as the resolvent matrix, the state transition matrix, and the time response. In addition, most of these results must be computed for many instances of time, say every 0.1 second for 200 seconds, or for a wide range of frequencies in order that meaningful data may be plotted and analyzed.

Before the computer methods can be presented, a description of the underlying state variable theory and mathematics is necessary.

Conventional control theory, exemplified by the damped spring mass system in chapter III (pp 29 et seq.), is adequate for single-input-single-output



operations but is wholly inadequate for multiple-input-multiple-output systems. Each additional parameter introduced as an input or output increases the number of mathematical operations many-fold.

The set of state variables must first be specified. In accordance with the equations of motion (p 53), the set will be  $(u, w, q, \theta)$ . The state vector is seen to be

$$\{x\} = \begin{Bmatrix} u \\ w \\ q \\ \theta \end{Bmatrix}, \text{ the control vector is } u = \delta_e, \text{ and the plant}$$

matrix and control matrix are shown as  $[A]$  and  $\{B\}$  respectively on page 5-2. The state equation for the system is then

$$\{\dot{x}\} = [A]\{x\} + \{B\}u .$$

The Laplace transform is used to solve this non-homogeneous equation of state:

$$sX(s) - \underline{x}(0) = [A]X(s) + \underline{B}U(s)$$

$$sX(s) - [A]X(s) = \underline{x}(0) + \underline{B}U(s)$$

$$[sI - A]X(s) = \underline{x}(0) + \underline{B}U(s)$$

$$X(s) = [sI - A]^{-1} \underline{x}(0) + [sI - A]^{-1} \underline{B}U(s)$$



Since  $(sI-A)^{-1} = \frac{I}{s} + \frac{A}{s^2} + \frac{A^2}{s^3} + \dots$

and  $\mathcal{L}^{-1} [(sI-A)^{-1}] = I + At + \frac{A^2 t^2}{2!} + \frac{A^3 t^3}{3!} + \dots = e^{At}$

then  $X(s) = \mathcal{L} [e^{At}] \underline{x}(0) + \mathcal{L} [e^{At}] \underline{B}U(s)$

Taking the inverse Laplace,

$$\underline{x}(t) = e^{At} \underline{x}(0) + \int_0^t e^{A(t-\tau)} \underline{B}u(\tau) d\tau \quad (6-1)$$

where  $\tau$  is a dummy variable.

The matrix  $e^{At}$  is written as  $\Phi(t)$  and called the state transition matrix. Its Laplace counterpart,  $\Phi(s)$ , is called the resolvent matrix. The first term on the right hand side of equation (6-1) is the time response due to initial conditions; the second term is that due to the input,  $\underline{B}u$ .

Just as in the single-input-single-output system, where  $Y(s) = G(s) \cdot X(s)$ , here,  $X(s) = G(s) \cdot U(s)$ , but  $G(s)$  is now a matrix and is called the transfer matrix. The corresponding closed loop system is depicted in Figure 6-1.

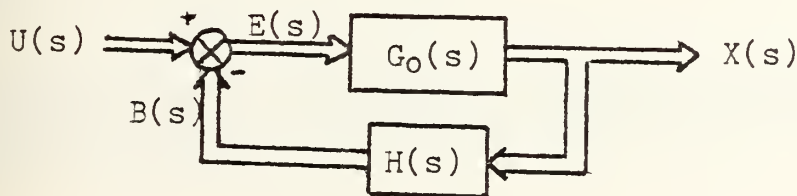


Figure 6-1





As was developed for the single input/output case,

$$B(s) = H(s) \cdot X(s)$$

or, dropping the "(s)" for convenience,

$$B = HG_0E$$

$$\begin{aligned} \text{Since } X &= G_0[U - B] \\ &= G_0[U - HX] \end{aligned}$$

$$\text{then } X + G_0HX = G_0U$$

$$[I + G_0H]X = G_0U$$

$$\text{and } X = [I + G_0H]^{-1} G_0U$$

Writing X as GU shows the closed loop transfer matrix to be  $G(s) = [I + G_0(s) \cdot H(s)]^{-1} \cdot G_0(s)$ .<sup>11</sup>

In order to solve the equations of motion, a computer program will use the above relationships and some form of numerical integration. The programs written by Melsa and Jones<sup>12</sup> were used in this study, the main two of which were BASMAT and RTRESP.

---

<sup>11</sup> Since, in general,  $[A][B] \neq [B][A]$ , care must be exercised in developing the equations by insuring that both sides are pre- or post-multiplied by a matrix in the same order.

<sup>12</sup> J.L. Melsa and S.K. Jones, Computer Programs for Computational Assistance in the Study of Linear Control Theory, 2nd edition, McGraw-Hill, 1973



Given a basic matrix,  $[A]$ , in this case the plant matrix, BASMAT produces

- a. the determinant of  $[A]$ ,  $\det[A]$
- b. the inverse of  $[A]$ ,  $[A]^{-1}$
- c. the characteristic polynomial,  $\det(sI-A)$
- d. the eigenvalues of  $[A]$ ,  $\lambda_i$
- e. the state transition matrix,  $\Phi(t) = e^{At}$
- f. the resolvent matrix,  $\Phi(s) = (sI-A)^{-1}$

Once the state transition matrix is known, the time response may be found by equation (6-1) whether the input is in the form of an initial condition(s), a forcing function, or both. The other Melsa-Jones program, RTRESP (Rational Time RESPONSE), was used for this purpose.

After the mathematical formulation of the time response is obtained, it is left to graph the results to see the time history of the system. In order to facilitate this operation, a program named GRAPH was written, in BASIC language, for execution on the HP9830 computer. See Figure 6-2. An explanation of the variables and operations in GRAPH follows:



```

10 DIM C(9),P(9),Q(9),R(9)
20 FOR I=1 TO 9
30 C(I)=P(I)=Q(I)=R(I)=0
40 NEXT I
50 DISP "HOW MANY REAL ROOTS";
60 INPUT R1
70 DISP "HOW MANY COMPLEX ROOTS";
80 INPUT R2
90 IF R1=0 THEN 140
100 FOR I=1 TO R1
110 DISP "INPUT REAL ROOT # "I
120 INPUT P(I)
130 NEXT I
140 FOR I=R1+1 TO R1+R2 STEP 2
150 DISP "REAL-IMAG PARTS OF CPLX ROOT # "I;
160 INPUT Q(I),R(I)
170 Q(I+1)=Q(I)
180 R(I+1)=-R(I)
190 NEXT I
200 WRITE (15,210)
210 FORMAT 45 "*"
220 PRINT "ROOTS OF CHAR EQN ARE"
230 PRINT "      REAL PART      IMAG PART"
240 FOR I=1 TO R1
250 WRITE (15,310)P(I),0
260 NEXT I
270 PRINT
280 FOR I=R1+1 TO R1+R2
290 WRITE (15,310)Q(I),R(I)
300 NEXT I
310 FORMAT 4X,F10.5,4X,F10.5
320 IF R1=0 THEN 370
330 FOR I=1 TO R1
340 DISP "COEFF OF EXP("P(I)"T)";
350 INPUT C(I)
360 NEXT I
370 FOR I=R1+1 TO R1+R2 STEP 2
380 R(I)=ABS(R(I))
390 DISP "COEFF OF EXP("Q(I)"T)*COS("R(I)"T)";
400 INPUT C(I)
410 DISP "COEFF OF EXP("Q(I)"T)*SIN("R(I)"T)";
420 INPUT C(I+1)
430 NEXT I
440 DISP "MAXIMUM MAGNITUDE OF RESPONSE";
450 INPUT G9

```

Figure 6-2



```

460 SCALE -5,15,-1.1*G9,1.1*G9
470 XAXIS 0,5,0,10
480 YAXIS -0.8,G9/4,-G9,G9
490 LABEL (*,2.5,1.7,0,10/7)
500 FOR X=0 TO 10 STEP 5
510 PLOT X,0,1
520 CPLOT -2.5,-2
530 LABEL (770)X
540 NEXT X
550 FOR Y=-G9 TO G9 STEP 2*G9
560 PLOT 0,Y,1
570 CPLOT -7,-0.3
580 LABEL (780)Y
590 NEXT Y
600 FOR T=0 TO 10 STEP 0.25
610 Y=0
620 GOSUB 1080
630 PLOT T,Y
640 NEXT T
650 PEN
660 DISP "RESET PLOTTER FOR PHUGOID"
670 STOP
680 SCALE -15,215,-1.1*G9,1.1*G9
690 XAXIS 0,25,0,200
700 YAXIS -8,G9/4,-G9,+G9
710 LABEL (*,2.5,2,0,7/10)
720 FOR X=0 TO 200 STEP 50
730 PLOT X,0,1
740 CPLOT -2.5,-2
750 LABEL (770)X
760 NEXT X
770 FORMAT F4.0
780 FORMAT F8.3
790 FOR T=0 TO 10 STEP 0.25
800 Y=0
810 GOSUB 1080
820 PLOT T,Y
830 NEXT T
840 FOR T=10 TO 50 STEP 1
850 Y=0
860 GOSUB 1080
870 PLOT T,Y
880 NEXT T
890 FOR T=50 TO 200 STEP 2
900 Y=0

```

Figure 6-2 (continued)





```

910 COSUB 1080
920 PLOT T,Y
930 NEXT T
940 PEN
950 DISP "INPUT LETTER SIZE FOR LABELLING";
960 INPUT Z
970 LABEL (*,Z,1.7,0,7/10)
980 DISP "YOU ARE IN THE LETTER MODE"
990 LETTER
1000 DISP "ANY MORE LABELLING";
1010 INPUT Z
1020 IF Z=1 THEN 950
1030 DISP "ANY MORE GRAPHS WITH THESE ROOTS";
1040 INPUT Z
1050 IF Z=1 THEN 320
1060 DISP "      - - - - THE END - - - -"
1070 STOP
1080 REM SUBROUTINE TO COMPUTE MAGNITUDE OF RESPONSE
1090 IF R1=0 THEN 1140
1100 FOR I=1 TO R1
1110 IF PC(I)*T<-.015 THEN 1130
1120 Y=Y+CC(I)*EXP(PC(I)*T)
1130 NEXT I
1140 FOR I=R1+1 TO R1+R2 STEP 2
1150 IF QC(I)*T<-.225 THEN 1180
1160 Y=Y+CC(I)*EXP(QC(I)*T)*COS(RC(I)*T)
1170 Y=Y+CC(I+1)*EXP(QC(I)*T)*SIN(RC(I)*T)
1180 NEXT I
1190 RETURN
1200 END

```

Figure 6-2 (continued)



$C_i$ : coefficients of the exponential and sinusoidal terms, the sum of which describe the time response

G9: maximum absolute magnitude of the response; used to scale and label the time history plot

I: counting element

$P_i$ : purely real roots

$Q_i$ : real part of complex roots

$R_i$ : imaginary part of complex roots

R1: number of purely real roots

R2: number of complex roots

T: time; see "X"

X: horizontal (time) axis

Y: vertical (magnitude) axis

Z: yes(1)/no(0) value; used to answer various questions which the program asks of the operator

lines 10-40: dimensions C, P, Q, and R and initializes their value at zero

ll 50-310: inputs roots, categorizes them as real or complex, and prints results

ll 320-430: inputs coefficients of exponential and sinusoidal terms

ll 440-590: scales, draws, and labels the axes of the graph

ll 600-650: plots short period magnitude-vs-time graph, using subroutine 1080

ll 660-940: plots phugoid graph, using subroutine 1080



11 950-1020: allows for labeling

11 1030-1070: allows drawing of other graphs with the same roots

11 1080-1190: subroutine which computes magnitude of response at a given time

line 1200: END statement

The values of the coefficients and roots ( $C_i$ ,  $P_i$ ,  $Q_i$ ,  $R_i$ ) are obtained from the program RTRESP.

The text Aircraft Dynamics and Automatic Control, referenced previously, contains an input/output analysis of an early operational Air Force interceptor, the F-89 Scorpion. In order to validate the GRAPH program, this example was run through the BASMAT and RTRESP programs and the results plotted using GRAPH.

From the given stability derivatives, the plant matrix and control vector were constructed in accordance with the state equations on page 50 ; for

altitude = 20000ft  
weight = 30500lb  
Mach = 0.638  
TAS = 660fps

$X_u$	=	-0.0097	$Z_u$	=	-0.0955	$M_u$	=	0.0
$X_w$	=	0.0016	$Z_w$	=	-1.430	$M_w$	=	-0.0235
$X_{\delta_e}$	=	0.0	$Z_{\delta_e}$	=	-69.8	$M_w$	=	-0.0013
						$M_q$	=	-1.920
						$M_{\delta_e}$	=	-26.009



the plant matrix [A] was

$$\begin{bmatrix} -0.0097 & 0.0016 & 0.0 & -32.2 \\ -0.0955 & -1.430 & 660.0 & 0.0 \\ 0.000124 & -0.0216 & -2.778 & 0.0 \\ 0.0 & 0.0 & 1.0 & 0.0 \end{bmatrix}$$

and the control vector was

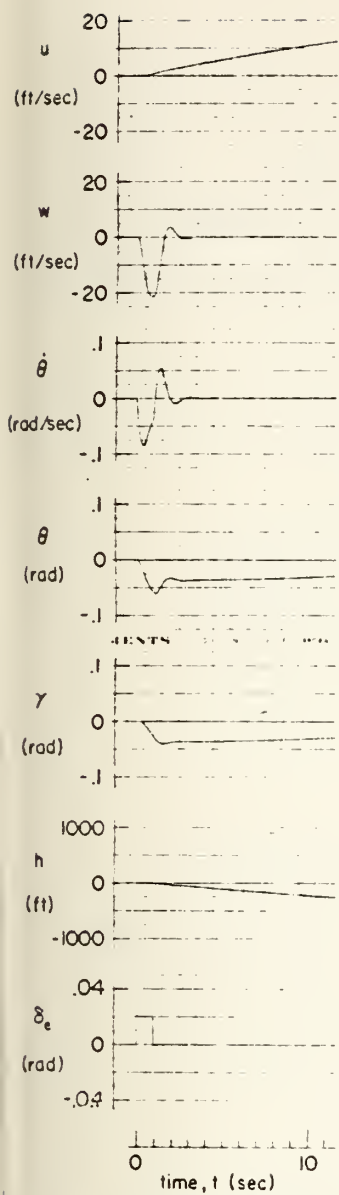
$$\left\{ \begin{array}{c} 0.0 \\ -69.8 \\ -26.009 \\ 0.0 \end{array} \right\}$$

The input to the system consisted of an elevator deflection of 0.02 radian commencing at  $t=0$  with a duration of one second; initial conditions were equal to zero. The text results are shown in Figure 6-3.

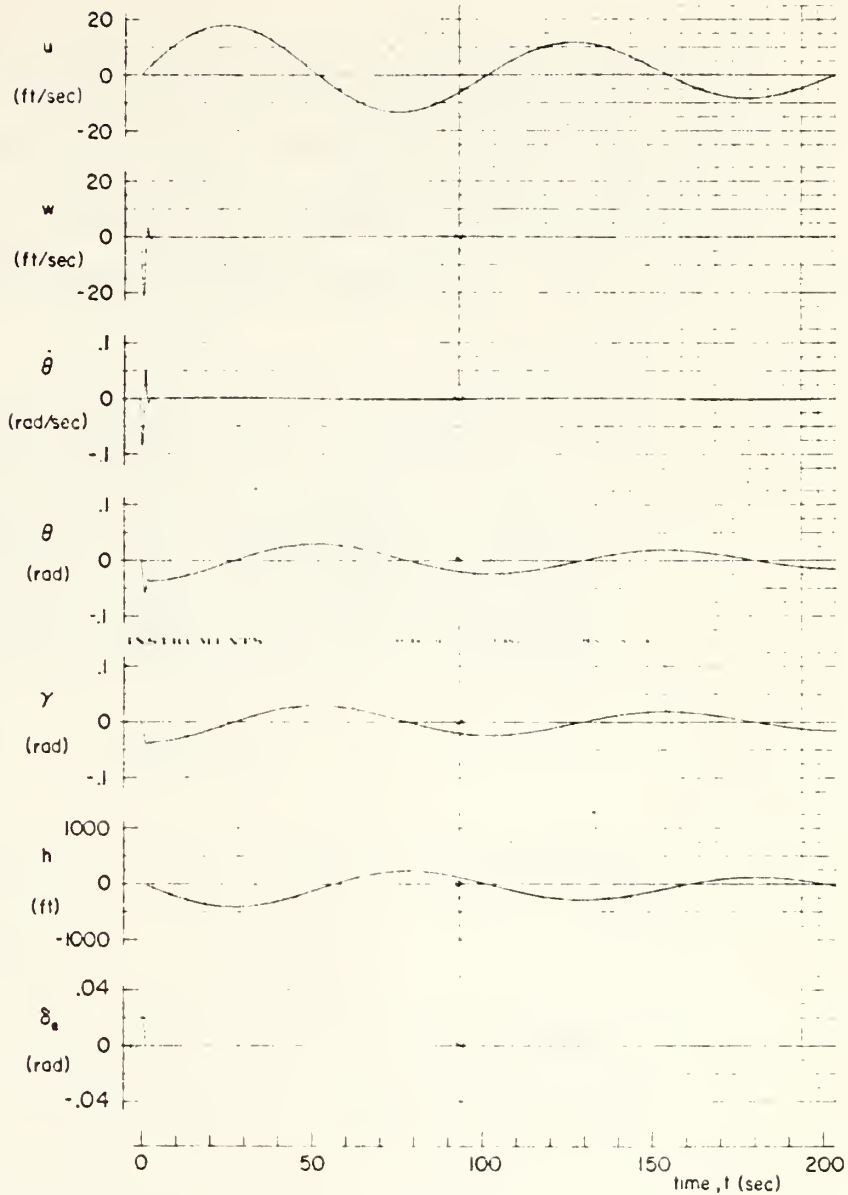
In order to utilize the RTRESP program, a proper Laplace transform of the input had to be found. The first choice was a multiple of the unit impulse, in this case  $0.02 \delta(t)$ . The Laplace of this input is  $0.02(1/s)$ . However, the Melsa-Jones program requires that the denominator of the Laplace of the input be one or more orders greater than that of the numerator. Since this prerequisite could not be satisfied, it was decided to use a step function input and take the derivative with respect to time of the output, since the







a) Short Period



b) Phugoid

Figure 6-3

impulse is the derivative of the step function. The results of the system's matrix analysis are given in



Figure 6-4. The results of the step function input are shown in Figure 6-5, and Table 6-1 shows that the periods and damping ratios of the short period and the phugoid agree quite closely with the text results.

	SHORT PERIOD		PHUGOID	
	BASMAT	text	BASMAT	text
$\omega_n$	4.2693	4.27	0.0629	0.0630
$\zeta$	0.4928	0.493	0.0717	0.0714

Table 6-1

The differentiation of the results of the step function input yielded:

$$\begin{aligned} \text{let } a_1 &= -2.104339 & b_1 &= 3.714746 \\ a_2 &= -0.004510971 & b_2 &= 0.06274506 \end{aligned}$$

$$\begin{aligned} u = & -0.599148 \exp(a_1 t) \cos(b_1 t) \\ & -0.678176 \exp(a_1 t) \sin(b_1 t) \\ & +0.599209 \exp(a_2 t) \cos(b_2 t) \\ & +20.063997 \exp(a_2 t) \sin(b_2 t) \end{aligned}$$



\*\*\*\*\*

THE A MATRIX

```

-9.6999966E-03      1.5999999E-03      0.0      -3.2100007E 01
-9.5499992E-02      -1.4299994E 00      0.000000E 02      0.0
 1.2410000E-04      -2.1599997E-02      -2.7779999E 00      0.0
 0.0                  0.0                  1.000000E 00      0.0

```

THE DETERMINANT OF THE MATRIX

7.2130343E-02

THE INVERSE OF THE MATRIX

```

 1.5259790E-05      -9.6417997E 00      0.203171E 00      0.1707917E 03
 0.0                  -5.5305199E-02      -1.900000E 01      -0.1000791E 01
-3.7259997E-06      2.7993999E-10      -5.000195E-06      0.0000079E-01
-3.1055995E-09      2.0017300E-03      -1.000091E-01      -0.4599999E 00

```

\*\*\*\*\*

THE MATRIX COEFFICIENTS OF THE OPERATOR OF THE RESOLVENT MATRIX

THE MATRIX COEFFICIENT OF S\*\*3

```

 1.0000000E 00      0.0      0.0      0.0
 0.0                1.0000000E 00      0.0      0.0
 0.0                0.0      1.0000000E 00      0.0
 0.0                0.0      0.0      1.0000000E 00

```

Figure 6-4



THE MATRIX COEFFICIENT OF S\*\*2

```

4.20799835 00      1.50000000E-03      0.0      -3.2100007E 01
-9.5499992E-02     2.7876997E 00      0.0000000E 00      0.0
1.24100000E-04     -2.1586667E-02     1.4300000E 00      0.0
0.0                0.0                1.0000000E 00      4.2170001E 00

```

THE MATRIX COEFFICIENT OF S\*\*1

```

1.8228531E 01      4.4447920E-03      -3.1143097E 01      -1.3540754E 02
-1.8339288E-01     2.6047021E-02     6.4010555E 00      3.0750000E 00
2.2402020E-03     -2.003101E-04      1.602007E-02      -3.0060103E-03
1.2410000E-04     -2.1500007E-02     1.4300000E 00      1.0000501E 01

```

THE MATRIX COEFFICIENT OF S\*\*0

```

5.0004065E-02      0.0551000E-01      -4.5045050E 01      -5.0005050E 02
0.5307030E-07      3.0004506E-03      3.0710000E 00      5.0005050E 00
0.0                -2.011001E-02      5.700000E-02      -7.0170707E-02
2.2400000E-03     -2.003101E-04      1.602007E-02      1.7711000E-01

```

\*\*\*\*\*

THE CHARACTERISTIC POLYNOMIAL - IN ASCENDING POWERS OF S

```

7.2136343E-02      1.2110000E-01      1.8000501E 01      4.2170001E 00      1.0000000E 00

```

\*\*\*\*\*

THE EIGENVALUES OF THE A MATRIX  
REAL PART           IMAGINARY PART

```

-2.1043377E 00      -3.7147430E 00
-2.1043377E 00      3.7147430E 00
-4.5110285E-03     -6.2747001E-02
-4.5110285E-03     6.2747001E-02

```

Figure 6-4 (continued)





\*\*\*\*\*

THE ELEMENTS OF THE STATE TRANSITION MATRIX

THE MATRIX COEFFICIENT OF EXP(-0.106330E 00)T\*COS( 3.714746E 00)T

-5.2074035E-05	8.5081075E-07	1.1000170E 00	-1.50000070E-03
1.0030747E-02	1.0000007E 00	-1.0770657E-02	-0.6040513E-02
-1.2310687E-04	1.0704000E-05	1.0000050E 00	-0.0404046E-04
2.1560003E-05	1.1040430E-03	-7.0500058E-02	-5.7177677E-05

THE MATRIX COEFFICIENT OF EXP(-0.106330E 00)T\*SH( 3.714746E 00)T

-2.1243360E-04	-5.0083250E-03	1.3171750E 00	-4.0204005E-04
-2.0048530E-02	1.8104840E-01	1.7705311E 02	-1.4041200E-01
-3.6054340E-05	-5.8148727E-03	-1.8121606E-01	6.7383423E-04
-2.0920542E-05	6.7160025E-04	0.2473000E-01	-2.1027751E-04

THE MATRIX COEFFICIENT OF EXP(-4.511020E-03)T\*COS( 6.274706E-02)T

1.0000525E 00	-8.5682571E-03	-1.1000770E 00	1.5400507E-03
-1.0030255E-02	-7.0112470E-05	1.0001001E-02	0.6040040E-02
1.2310731E-04	-1.8700014E-06	-0.0073707E-05	6.0400047E-04
-2.1550043E-05	-1.1040305E-03	7.0510700E-02	1.0000557E 00

THE MATRIX COEFFICIENT OF EXP(-4.511020E-03)T\*SH( 6.274706E-02)T

-7.1800017E-02	6.0073550E-01	-4.0000304E 01	-5.1210001E 00
9.0256000E-04	-0.0514701E-07	3.0170400E-01	5.100707E 00
-7.6040700E-06	7.5137100E-05	-4.0000041E-03	-0.710605E-02
1.0004000E-03	-1.1500000E-04	4.0700750E-02	8.0000300E-02

D; T=3.00/4.17 21.34.00

Figure 6-4 (continued)



RATIONAL TIME RESPONSE  
 PROBLEM IDENTIFICATION - MCRUER EXAMPLE

\*\*\*\*\*

THE A MATRIX

-0.0097000	0.0016000	0.0	-32.2000000
-0.0955000	-1.4300000	600.0000000	0.0
0.0001240	-0.0210000	-2.7700000	0.0
0.0	0.0	1.0000000	0.0

THE B MATRIX

0.0	-69.0000000	-20.0000000	0.0
-----	-------------	-------------	-----

THE C MATRIX

1.0000000	0.0	0.0	0.0
-----------	-----	-----	-----

FEEDBACK COEFF.

0.0	0.0	0.0	0.0
-----	-----	-----	-----

GAIN = 1.0000000 00

\*\*\*\*\*

INITIAL CONDITIONS - X(0)

0.0	0.0	0.0	0.0
-----	-----	-----	-----

RGAIN = 2.00000000-02

Figure 6-5



NUMERATOR POLYNOMIAL OF R(S) - ASCENDING POWERS OF S  
 1.0000000  
 0.0  
 DENOMINATOR POLYNOMIAL OF R(S) - ASCENDING POWERS OF S  
 1.0000000  
 0.0  
 DENOMINATOR ROOTS ARE  
 REAL PART       IMAG. PART  
 0.0            0.0

\*\*\*\*\*

THE TIME RESPONSE OF THE STATE X(T)

THE VECTOR COEFFICIENT OF EXP(-2.1043300 00)T*COS(3.7147400 00)T	0.0194909
C.2073815            19.0440024            C.6391937	
THE VECTOR COEFFICIENT OF EXP(-2.1043300 00)T*SIN(3.7147400 00)T	0.0215921
-0.0438111            10.6154682            -0.1171410	
THE VECTOR COEFFICIENT OF EXP(-4.5109710-03)T*COS(6.2745010-02)T	0.0774104
-318.8088989            3.1114908            -0.0301704	
THE VECTOR COEFFICIENT OF EXP(-4.5109710-03)T*SIN(6.2745010-02)T	-0.6190052
-13.3704338            0.1375328            -0.0023228	
THE VECTOR COEFFICIENT OF EXP( 0.0            )T	-0.0971559
318.6020508            -22.2811598            0.0001477	

\*\*\*\*\*

Figure 6-5 (continued)



$$w = \begin{aligned} & -1.386301 \exp(a_1 t) \cos(b_1 t) \\ & \quad -92.664985 \exp(a_1 t) \sin(b_1 t) \\ & \quad -0.005406 \exp(a_2 t) \cos(b_2 t) \\ & \quad -0.195852 \exp(a_2 t) \sin(b_2 t) \end{aligned}$$

$$q = \begin{aligned} & -0.520226 \exp(a_1 t) \cos(b_1 t) \\ & \quad +0.102383 \exp(a_1 t) \sin(b_1 t) \\ & \quad +0.000031 \exp(a_2 t) \cos(b_2 t) \\ & \quad +0.002468 \exp(a_2 t) \sin(b_2 t) \end{aligned}$$

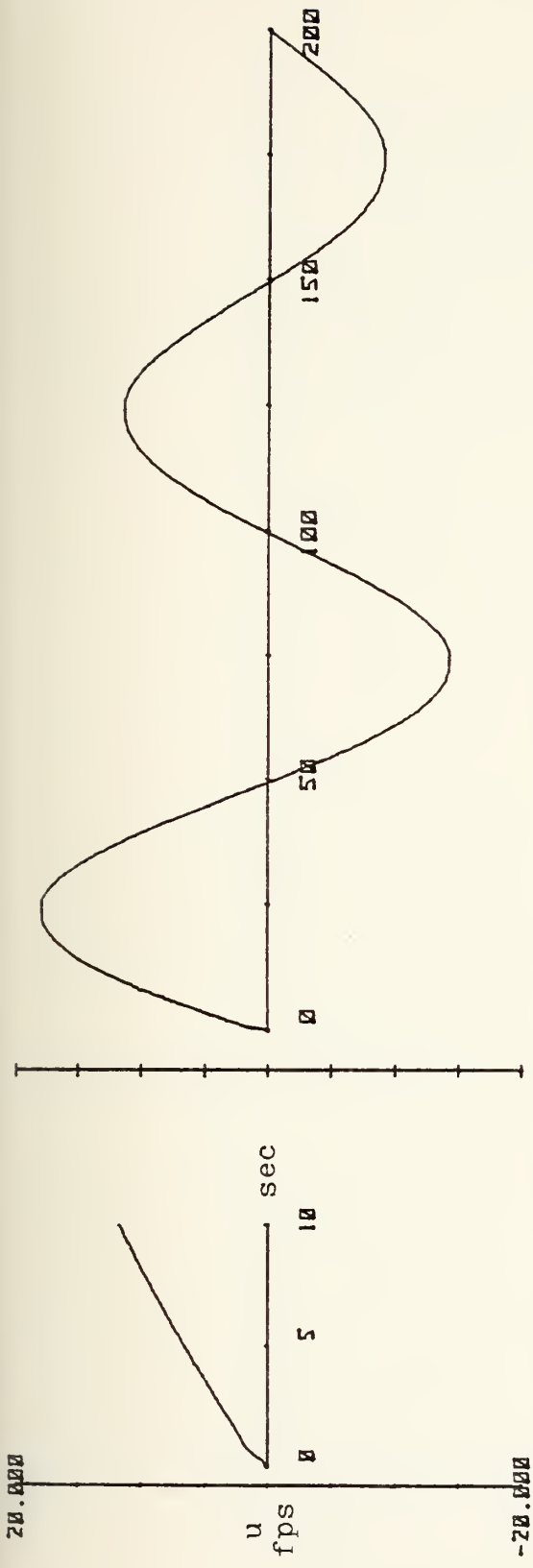
$$\theta = \begin{aligned} & +0.039993 \exp(a_1 t) \cos(b_1 t) \\ & \quad -0.117850 \exp(a_1 t) \sin(b_1 t) \\ & \quad -0.039189 \exp(a_2 t) \cos(b_2 t) \\ & \quad -0.002065 \exp(a_2 t) \sin(b_2 t) \end{aligned}$$

Figure 6-6 shows the time history of this system. The magnitudes of vertical velocity, pitch angle, and to a lesser degree, pitch rate were decidedly in error. Furthermore, the initial condition of zero pitch rate was not reflected in the results.

The discrepancies are due to the improper description of the input. Clearly, the effect of a maximum elevator deflection acting over a short period of time ( $\Delta t \ll 1$ ) is different from a much smaller deflection for one second, hence the magnitude errors. The initial condition error is due to the indefinite integration of the input. When the input is integrated (multiplied by  $s$ ), the denominator loses a root at  $s=0$  and its associated eigenvalue. The time response







phugoid

short period

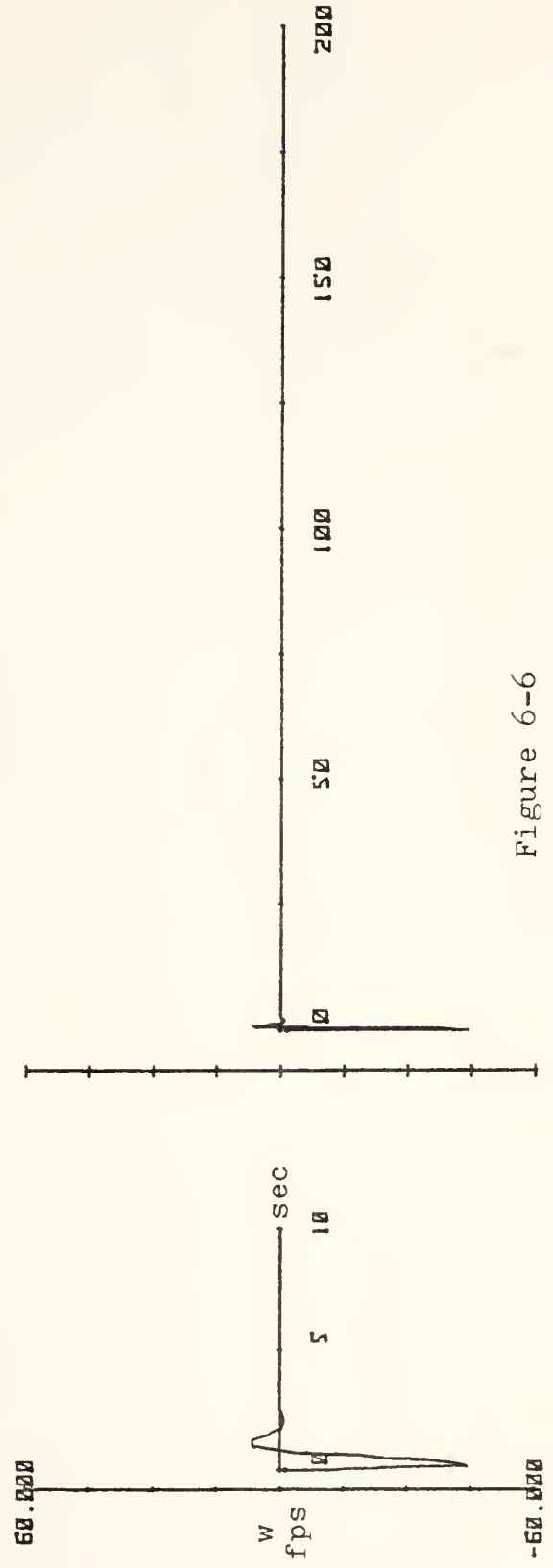
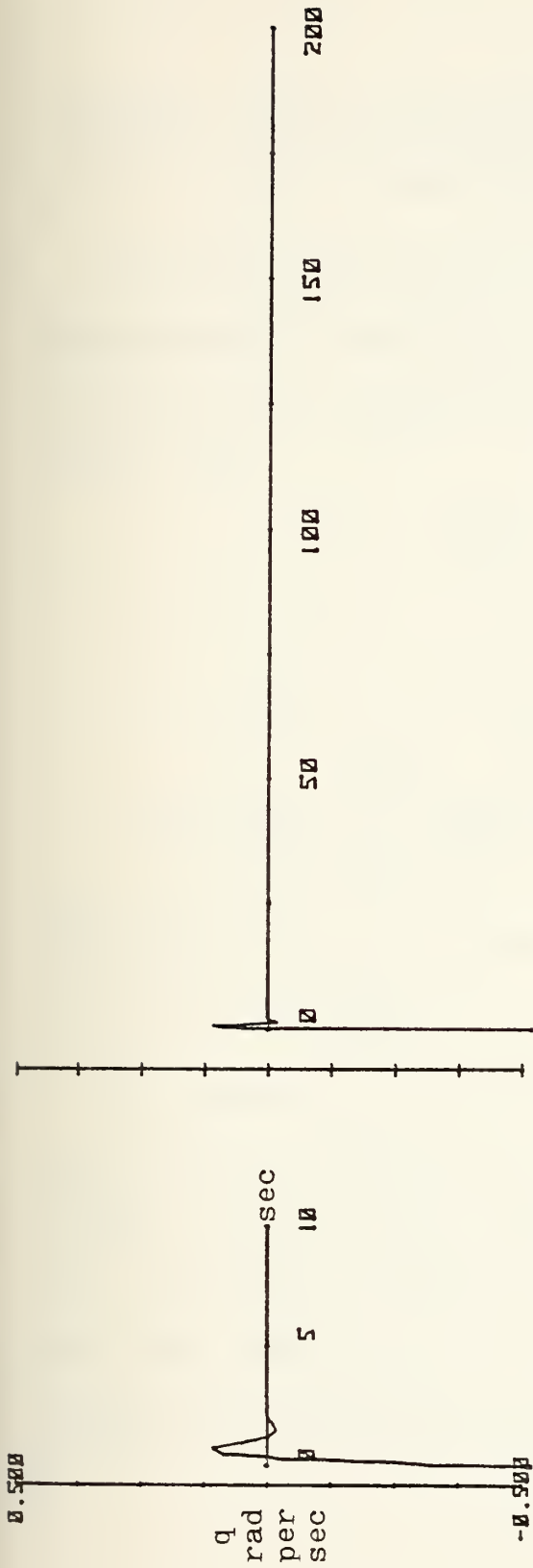
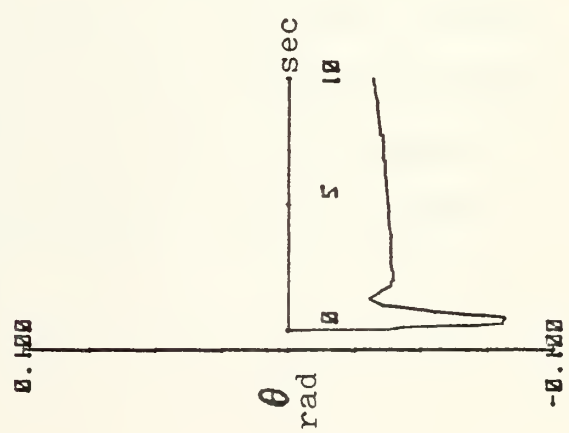


Figure 6-6





short period



phugoid

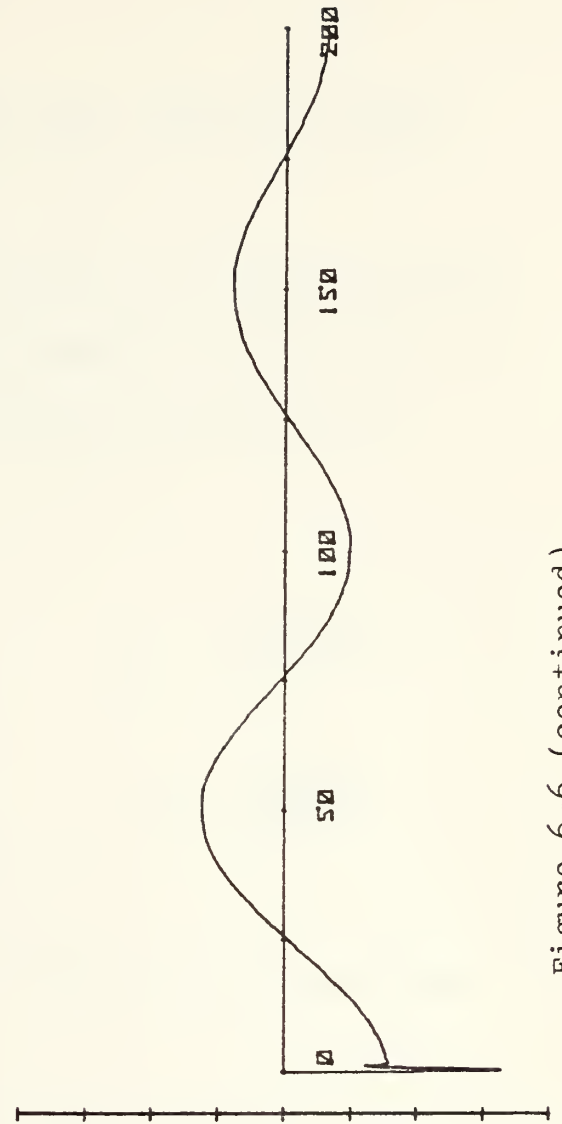
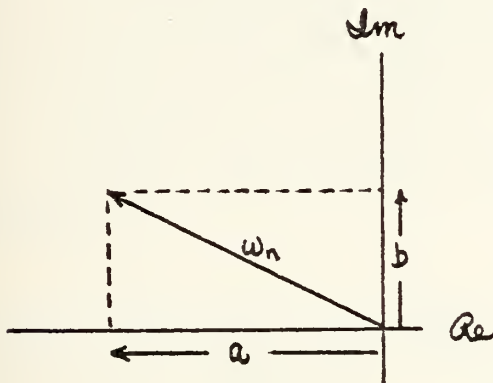


Figure 6-6 (continued)



therefore loses an exponential term, and the initial conditions are not satisfied.

The undamped natural frequencies and damping ratios are calculated from the roots (eigenvalues) of the characteristic equation by considering the roots in vector form.



$$\omega_n = \sqrt{a^2 + b^2}$$

$$\zeta = \frac{a}{\sqrt{a^2 + b^2}}$$

where the roots are expressed as  $\lambda = a + jb$  and were calculated by BASMAT.

The second attempt to duplicate the given input function was to evaluate the results of the step function ( $x_{0.02}$ ) at  $t=1$  and use these values as initial conditions for a zero-input system commencing at  $t=1$ . The values of the state variables at  $t=1$ , calculated from the RTRESP program (see Figure 6-5) were



$$\begin{Bmatrix} u \\ w \\ q \\ \theta \end{Bmatrix} = \begin{Bmatrix} 0.9938 \\ -21.8208 \\ -0.0035 \\ -0.0623 \end{Bmatrix}$$

When these values were run through RTRESP as initial conditions, with the input function now zero, the results were inconsistent with common sense. For example, the response of the system with an initial condition of 0.9938fps of forward velocity perturbation and no input yielded a change in U of over 300fps within ten seconds (the initial velocity of the aircraft was but 660fps).

Using the state transition matrix from BASMAT, a program called ICRESP was written to solve the response due to an initial condition with the equation

$$\underline{x}(t) = \underline{\Phi}(t) \cdot \underline{x}(0) .$$

The results, shown in Figure 6-7, are much more consistent with the earlier figures. In the output portion of the print-out, A1 refers to the real part of the first root, B1 to the imaginary part of the first root, and likewise for A2 and B2. The matrix E is the matrix of coefficients of the state transition matrix,





```

10 DIM EC(16,4),DC(4,1),XC(4,4)
20 MAT READ E
30 DATA -5.2974E-05,0.0085681975,1.1288176,-0.0015909672
40 DATA 0.0100397,1,-0.018779,-0.0942425
50 DATA -0.000123106,1.87941E-06,1,-0.00069424
60 DATA 2.15602E-05,0.00118484,-0.078526,-5.71775E-05
70 DATA -0.000212434,-0.00500833,1.31718,-0.000442043
80 DATA -0.020049,0.18164849,177.653,-0.14041269
90 DATA -3.6054349E-05,-0.0058148727,-0.181217,0.000673834
100 DATA -2.09265E-05,0.000671698,0.224737,-0.000219278
110 DATA 1,-0.00856826,-1.128878,0.00154686
120 DATA -0.010039,-7.91185E-05,0.01062186,0.09424925
130 DATA 0.000123107,-1.8796E-06,-8.88737E-05,0.00069426
140 DATA -2.156E-05,-0.0011849,0.078517,1
150 DATA -0.071893,0.60873556,-40.203644,-513.19824
160 DATA 0.0009086,-0.00605144,0.39170456,5.1588783
170 DATA -7.49E-06,7.5133E-05,-0.004889544,-0.063124955
180 DATA 0.0019604028,-0.000115022,0.00427627,0.0829603
190 MAT READ D
200 DATA 0.9937896,-21.820808,-0.035139,-0.0623077
210 FOR I=1 TO 4
220 FOR J=1 TO 4
230 XC(I,J)=0
240 NEXT J
250 NEXT I
260 FOR I=1 TO 4
270 FOR J=1 TO 4
280 FOR K=1 TO 4
290 XC(I,J)=EC(I+4*J-4,K)*D(K,1)+XC(I,J)
300 NEXT K
310 NEXT J
320 NEXT I
330 PRINT " EXP(A1*T) *      EXP(A1*T) *      EXP(A2*T) *      EXP(A2*T) *
340 PRINT "   COS(B1*T)      SIN(B1*T)      COS(B2*T)      SIN(B2*T)
350 PRINT
360 MAT PRINT X
370 END

```

EXP(A1*T) * COS(B1*T)	EXP(A1*T) * SIN(B1*T)	EXP(A2*T) * COS(B2*T)	EXP(A2*T) * SIN(B2*T)
-0.226584030	0.062817847	1.220327219	20.63436953
-21.80429874	-10.21744129	-0.014495920	-0.202251680
-0.035259095	0.133175189	1.23026E-04	2.45808E-03
-0.023069852	-0.022561160	-0.039232660	-8.61228E-04

Figure 6-7



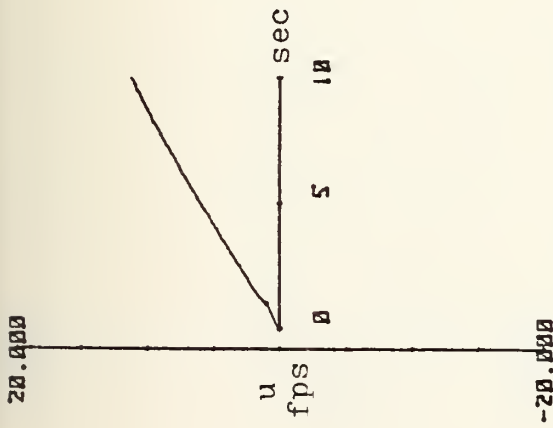
D is the matrix of initial conditions, and X is the matrix of coefficients of the output. The time history plots of the results are shown in Figure 6-8. Since the results were so consistent with the earlier program, it appeared as though the reason these figures were not coinciding with those of the text was that an error existed in one of the two Melsa-Jones programs.

The results of BASMAT (the determinant, the inverse, the characteristic polynomial, the eigenvalues, and the resolvent matrix) were computed by hand and found to be correct. The program RTRESP calculated the same eigenvalues as did BASMAT; its only problem appeared to be in the coefficient of the sine term of the phugoid root in the forward velocity expression when initial conditions are present. The equations of state from RTRESP were verified on the HP9830 by writing a program called STRESP which calculated the response of a system to a step input by using the formula

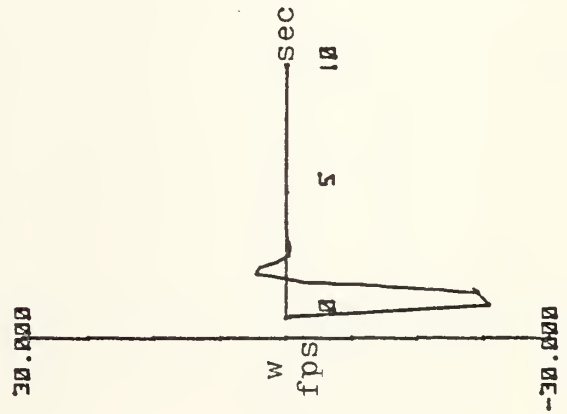
$$\underline{x}(t) = \Phi(t) \cdot \underline{x}(0) + [A]^{-1} [\Phi(t) - I] \{B\} \cdot k$$

where  $[A]$  is the plant matrix,  $\{B\}$  the control vector,  $k$  the gain (magnitude) of the step input, and  $\Phi(t)$  the





short period



phugoid

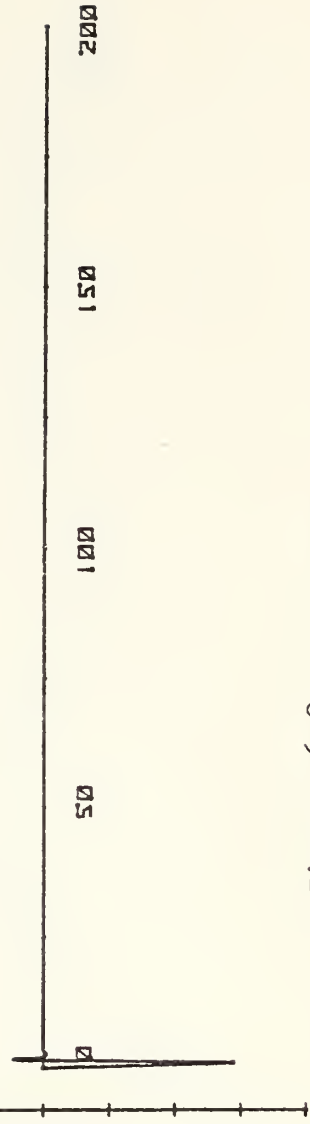
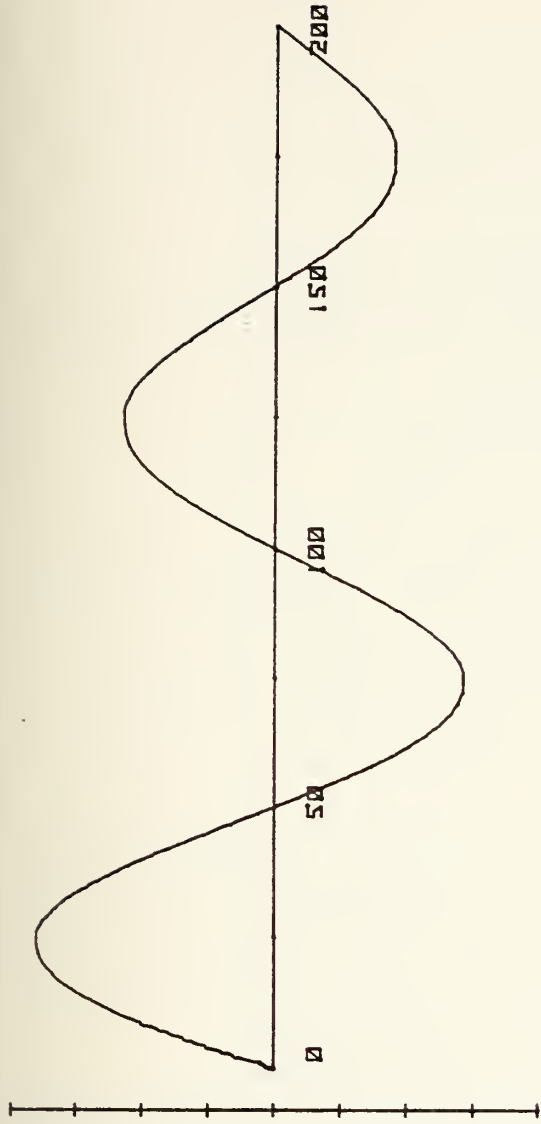
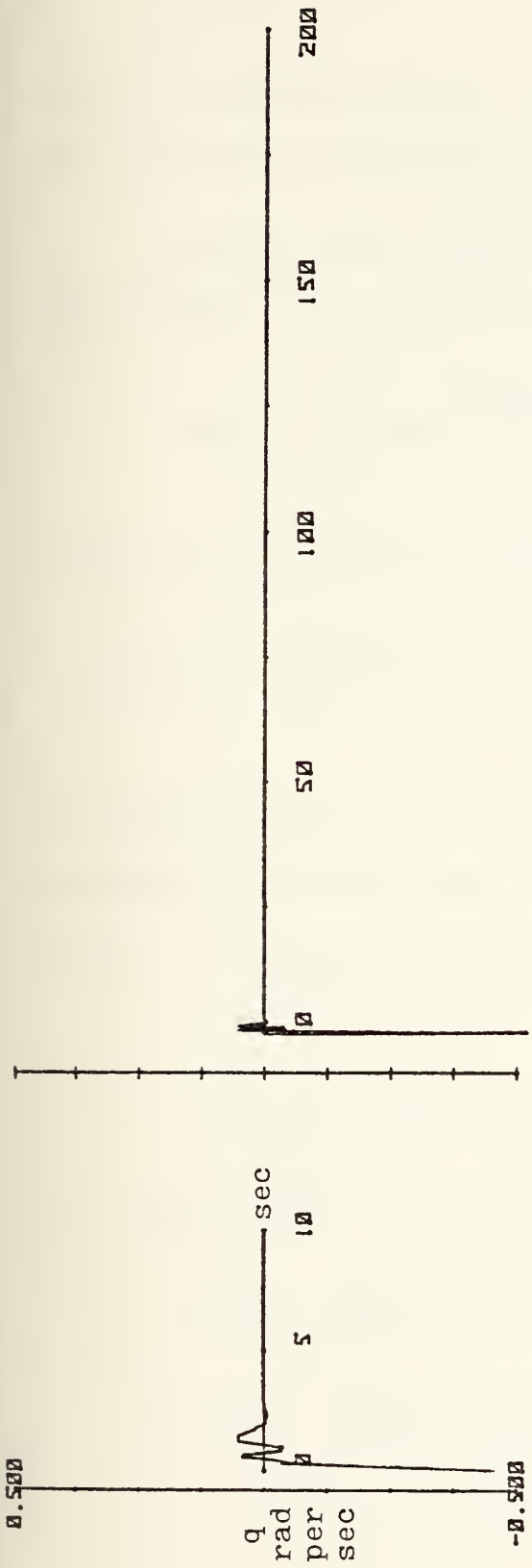


Figure 6-8





short period

phugoid

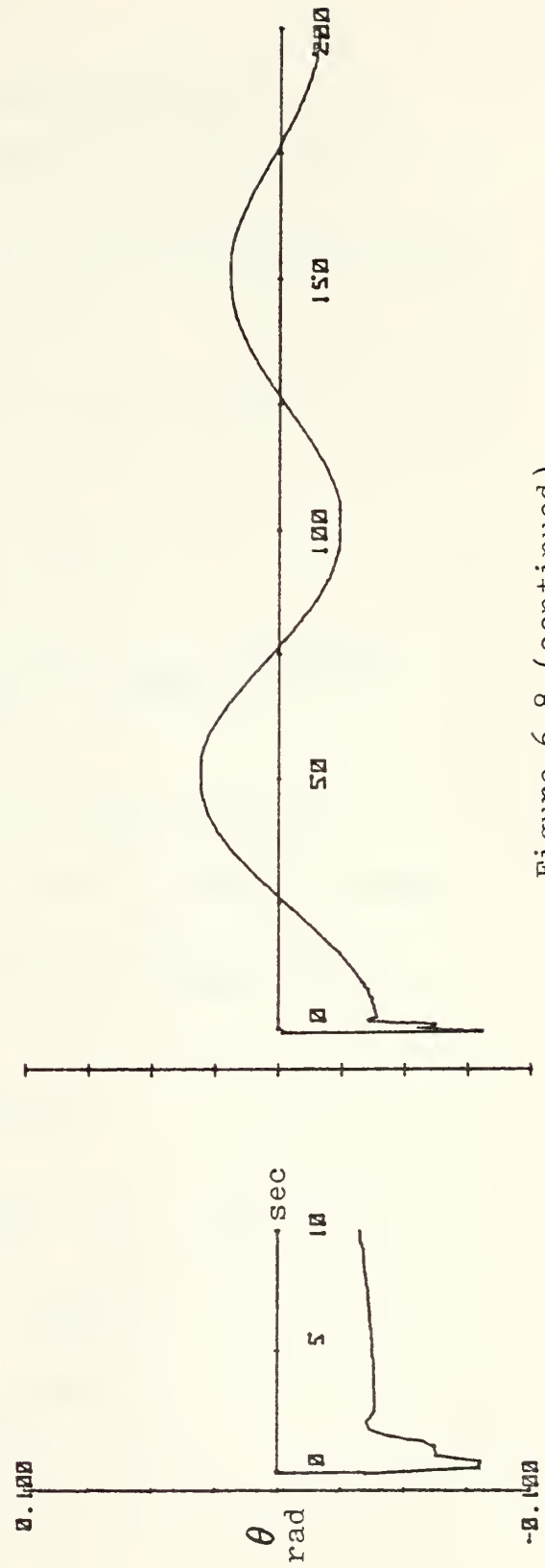


Figure 6-8 (continued)





state transition matrix. In this case,  $\underline{x}(0) = 0$ .

The program and results are shown in Figure 6-9.

Several other approximations to the desired input were tried, the first of which was

$$\delta(t) \approx \frac{1}{\tau} \exp\left[-\pi t^2/\tau^2\right] \quad \text{for } \tau \ll 1$$

Transforming into the Laplace domain,

$$\mathcal{L}[f(t)] = \int_0^{\infty} e^{-st} f(t) dt = \int_0^{\infty} e^{-st} \frac{1}{\tau} \exp\left[-\pi t^2/\tau^2\right] dt$$

The solution was obtained by the use of Bonnet's Theorem (the Second Mean Value theorem) which states that

$$\int_a^b f(t) g(t) dt = f(b) G(b) - \int_a^b G(t) f'(t) dt$$

$$\text{where } G(t) = \int_a^t g(t) dt$$

For  $f(t) = e^{-\alpha t^2}$  where  $\alpha = \frac{\pi}{\tau^2}$  and  $g(t) = e^{-st}$

$$G(t) = \int_0^t e^{-st} dt = \frac{1}{s} - \frac{1}{s} e^{-st}$$

$$\text{and } f'(t) = -2\alpha t e^{-\alpha t^2}$$



```

10 DIM A(4,4),B(4,4),C(4,4),D(4,4),S(4,4)
20 DIM BC(4,4),CC(4,4),DC(4,4),EC(4,4),FC(4,1)
30 DIM WC(4,1),XC(4,1),YC(4,1),ZC(4,1)
40 MAT READ B
50 DATA -5.2974E-05,0.0085681975,1.1288176,-0.0015909672
60 DATA 0.0100397,1,-0.018779,-0.0942425
70 DATA -0.000123186,1.87941E-06,1,-0.00069424
80 DATA 2.15602E-05,0.00118484,-0.078526,-5.71775E-05
90 MAT READ C
100 DATA -0.000212434,-0.00500833,1.31718,-0.000442043
110 DATA -0.020049,0.18164849,177.653,-0.14041269
120 DATA -3.6054349E-05,-0.0058148727,-0.181217,0.000673834
130 DATA -2.09265E-05,0.000671698,0.224737,-0.000219278
140 MAT READ D
150 DATA 1,-0.00856826,-1.128878,0.00154686
160 DATA -0.010039,-7.91185E-05,0.01062186,0.09424925
170 DATA 0.000123187,-1.8706E-06,-8.88737E-05,0.00069426
180 DATA -2.156E-05,-0.0011849,0.078517,1
190 MAT READ E
200 DATA -0.071893,0.60873556,-40.203644,-513.19824
210 DATA 0.0009086,-0.00605144,0.39170456,5.1588783
220 DATA -7.49E-06,7.5133E-05,-0.004889544,-0.063124955
230 DATA 0.0019604028,-0.000115022,0.00427627,0.0829603
240 MAT READ A
250 DATA 0,-9.64173,638.3179,8136.786
260 DATA 0,-0.055395,-42.6289,-81.86226
270 DATA 0,0,0,1
280 DATA -0.031056,0.0029017,-0.194407,-2.45521
290 MAT READ F
300 DATA 0,-69.0,-26.009,0
310 MAT P=A*B
320 MAT Q=A*C
330 MAT R=A*D
340 MAT S=A*E
350 MAT W=P*F
360 MAT W=(0.02)*W
370 MAT X=Q*F
380 MAT X=(0.02)*X
390 MAT Y=R*F
400 MAT Y=(0.02)*Y
410 MAT Z=S*F
420 MAT Z=(0.02)*Z
430 PRINT "THE TIME RESPONSE OF THE STATE, X(T)"
440 PRINT
450 PRINT "VECTOR COEFF OF EXP(-2.104338)T*COS(3.714744)T"

```

Figure 6-9



```

460 PRINT WC[1,1],WC[2,1],WC[3,1],WC[4,1]
470 PRINT
480 PRINT "VECTOR COEFF OF EXP(-2.104338)T*SIN(3.714744)T"
490 PRINT XC[1,1],XC[2,1],XC[3,1],XC[4,1]
500 PRINT
510 PRINT "VECTOR COEFF OF EXP(-0.004511029)T*COS(0.06274706)T"
520 PRINT YC[1,1],YC[2,1],YC[3,1],YC[4,1]
530 PRINT
540 PRINT "VECTOR COEFF OF EXP(-0.004511029)T*SIN(0.06274706)T"
550 PRINT ZC[1,1],ZC[2,1],ZC[3,1],ZC[4,1]
560 END

```

THE TIME RESPONSE OF THE STATE, X(T)

```

VECTOR COEFF OF EXP(-2.104338)T*COS(3.714744)T
 0.233872832      1.91312519      0.039193618      0.019483341

```

```

VECTOR COEFF OF EXP(-2.104338)T*SIN(3.714744)T
-0.045144590     10.41547062     -0.117841383     0.021596520

```

```

VECTOR COEFF OF EXP(-0.004511029)T*COS(0.06274706)T
-018.7879228     0.206305933     -0.039188853     0.077583489

```

```

VECTOR COEFF OF EXP(-0.004511029)T*SIN(0.06274706)T
-03.35349032     0.075818325     -2.06386E-03     -0.619060577

```

Figure 6-9 (continued)



Substituting,

$$\begin{aligned}\int_0^{\infty} f(t) g(t) dt &= f(\infty) G(\infty) - \int_0^{\infty} G(t) f'(t) dt \\ &= \int_0^{\infty} \left( \frac{1}{s} - \frac{1}{s} e^{-st} \right) (2\alpha t e^{-\alpha t^2}) dt \\ &= \frac{2\alpha}{s} \int_0^{\infty} (1 - e^{-st}) e^{-\alpha t^2} dt\end{aligned}$$

$$\int_0^{\infty} e^{-\alpha t^2} e^{-st} dt = \frac{2\alpha}{s} \int_0^{\infty} e^{-\alpha t^2} dt - \frac{2\alpha}{s} \int_0^{\infty} e^{-\alpha t^2} e^{-st} dt$$

Combining terms,

$$\left( \frac{2\alpha}{s} + 1 \right) \int_0^{\infty} e^{-\alpha t^2} e^{-st} dt = \frac{2\alpha}{s} \int_0^{\infty} e^{-\alpha t^2} dt = \frac{2\alpha}{s} \frac{1}{2\sqrt{\alpha}} \sqrt{\pi}$$

$$\int_0^{\infty} e^{-st} e^{-\alpha t^2} dt = \frac{s}{2\alpha + s} \cdot \frac{2\alpha}{s} \sqrt{\frac{\pi}{\alpha}} \cdot \frac{1}{2} = \frac{\alpha}{2\alpha + s} \sqrt{\frac{\pi}{\alpha}}$$

For  $\tau = 0.01$ ,  $\alpha = \frac{\pi}{.0001} = 31416$

$$\int_0^{\infty} e^{-st} e^{-\alpha t^2} dt = \frac{31416}{62832 + s} \sqrt{.0001} = \frac{314.16}{62832 + s}$$





Multiplying by the magnitude of the input, 0.02, yielded

$$0.02 \delta(t) = \frac{6.2832}{62832 + s}$$

The magnitudes of the results of this input were too small, the probable reason being that half of the function  $\exp(\pi t^2/\tau^2)$  lies to the left of the  $t=0$  axis and is contributing nothing to the input.

The application of a 0.001 second delay to this function would place 99% of it to the right of the  $t=0$  axis, countering the problem that existed originally. A time delay of 0.001 seconds corresponds to multiplying the Laplace transform by  $e^{-0.001s}$ . Approximating  $e^{-0.001s}$  by the series

$$1 - 0.001s + \frac{(0.001)^2 s^2}{2!} - \frac{(0.001)^3 s^3}{3!} + \dots,$$



$$R(s) \text{ becomes } \left( \frac{0.000001s^2 - 0.0005s + 0.05}{2} \right) \left( \frac{6.2832}{62832 + s} \right)$$

$$= 79577.5 \left( \frac{s^2 - 500s + 500,000}{s + 62832} \right).$$

Again,  $N(s)$  is of greater order than  $D(s)$ .

The correct answer was finally reached when a variation of an earlier idea (using the response at  $t=1$  from a step function as initial conditions) was pursued. In this case, the two steps were combined into one by summing two step functions, one commencing at  $t=0$ , the other at  $t=1$  and negative in sign. The graphical representation and summation is shown in Figure 6-14.

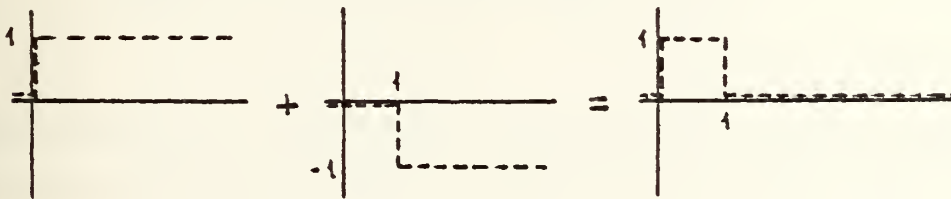


Figure 6-14

In the time domain, the result is written

$$r(t) = 1(t) - 1(t - \tau), \text{ where } \tau = 1.$$



The Laplace was easily found and was

$$R(s) = \frac{1}{s} - \frac{1}{s} e^{-\tau s}$$

Searching for an approximation of  $e^{-s}$  which would satisfy the requirement for the order of the numerator to be smaller than the order of the denominator led to<sup>13</sup>

$$\begin{aligned} e^{-s} &= \frac{1 - \frac{s}{2} + \frac{s^2}{8} - \frac{s^3}{48} + \dots}{1 + \frac{s}{2} + \frac{s^2}{8} + \frac{s^3}{48} + \dots} \\ &= \frac{48 - 24s + 6s^2 - s^3 + \dots}{48 + 24s + 6s^2 + s^3 - \dots} \end{aligned}$$

Substituting into  $R(s) = 0.02(\frac{1}{s} - \frac{1}{s} e^{-s})$  yielded

$$R(s) = 0.04 \left[ \frac{24 + s^2}{48 + 24s + 6s^2 + s^3} \right]$$

The results of the RTRESP computations and the time history plots are shown in Figures 6-15 and 6-16. Their agreement with the text figures confirmed the accuracy of the RTRESP (for other than initial condition inputs) and GRAPH programs and provided a valid approximation of a finite impulse-type input.

---

<sup>13</sup>Ogata, Modern Control Engineering, Prentice-Hall, 1970, p 414



\*\*\*\*\*

THE A MATRIX

-0.0097000	0.0011000	0.0	-32.2000000
-0.0955000	-1.4360000	0.0000000	0.0
0.0001240	-0.0210000	-2.7700000	0.0
0.0	0.0	1.0000000	0.0

THE B MATRIX

0.0	-0.0000000	-0.0000000	0.0
-----	------------	------------	-----

THE C MATRIX

1.0000000	0.0	0.0	0.0
-----------	-----	-----	-----

FEEDBACK COEFF.

0.0	0.0	0.0	0.0
-----	-----	-----	-----

GAIN = 1.0000000 00

\*\*\*\*\*

INITIAL CONDITIONS - Y(0)

0.0	0.0	0.0	0.0
-----	-----	-----	-----

PGAIN = 4.0000000D-02

NUMERATOR POLYNOMIAL OF P(S) - ASCENDING POWERS OF S

24.0000000	0.0	1.0000000
------------	-----	-----------

Figure 6-15





REAL PART IMAC. PART

0.0  
0.0  
-4.8980705  
4.8980705

NUMERATOR POLYNOMIAL OF R(S) - ASCENDING POWERS OF S  
48.0000000 24.0000000 0.0000000 1.0000000

DENOMINATOR ROOTS ARE  
REAL PART IMAC. PART

-1.4030284 -3.0140790  
-1.4030284 3.0140790  
-3.1021433 0.0

\*\*\*\*\*

THE TIME RESPONSE OF THE STATE X(T)

THE VECTOR COEFFICIENT OF EXP(-2.1047300 S)T\*COS(5.7147460 C)T  
-0.4502925 89.5680930 -1.0780185 0.1906888

THE VECTOR COEFFICIENT OF EXP(-2.1047300 S)T\*SIN(5.7147460 C)T  
-1.0682787 -175.2880471 -0.5249722 -0.1821001

THE VECTOR COEFFICIENT OF EXP(-4.5109710-03)T\*COS(0.2745000-02)T  
-0.0308005 0.0043945 -0.0010298 -0.0391895

THE VECTOR COEFFICIENT OF EXP(-4.5109710-03)T\*SIN(0.2745000-02)T  
20.1149222 -0.1923828 0.0025139 -0.0033010

THE VECTOR COEFFICIENT OF EXP(-1.4030280 S)T\*COS(3.0140790 C)T  
1.2740306 6.0007056 0.0125071 -0.0083148

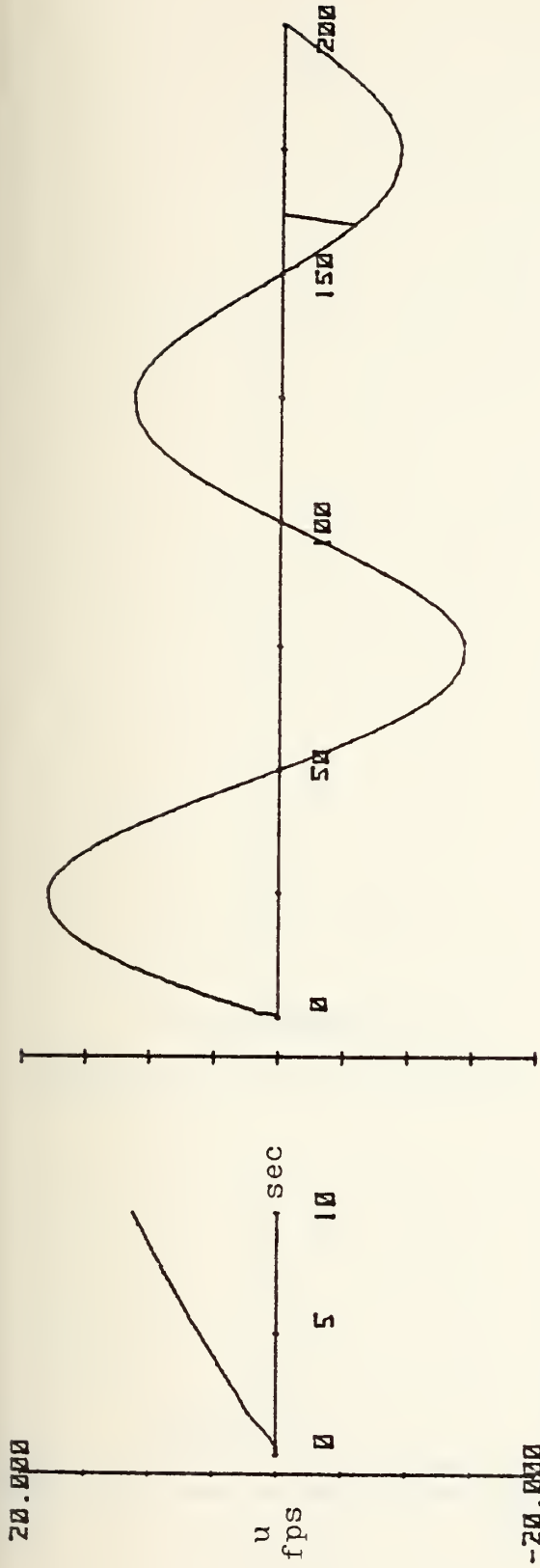
THE VECTOR COEFFICIENT OF EXP(-1.4030280 S)T\*SIN(3.0140790 C)T  
1.1051407 149.1347351 -0.0514089 0.1092617

THE VECTOR COEFFICIENT OF EXP(-3.1021430 S)T  
-0.7932087 -0.1000449 0.0055351 -0.0031830

\*\*\*\*\*

Figure 6-15 (continued)



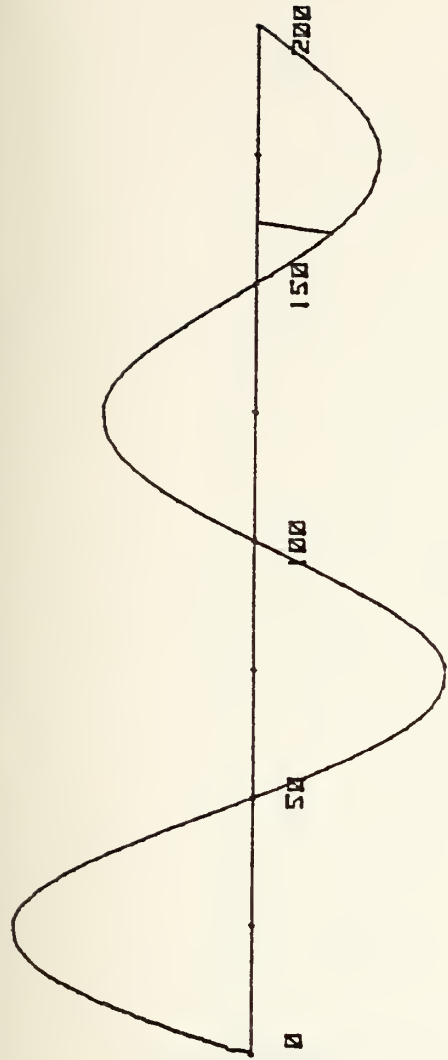


-20.000

short period

20.000

phugoid

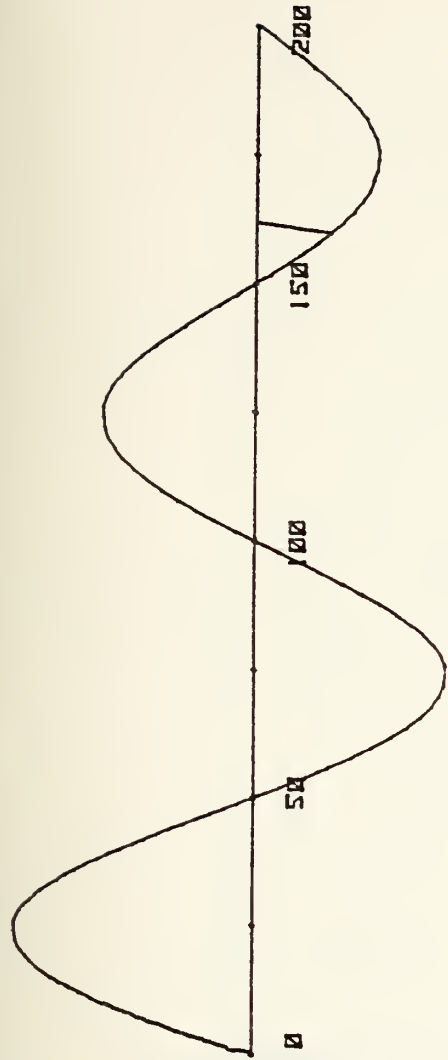


-20.000

short period

20.000

phugoid

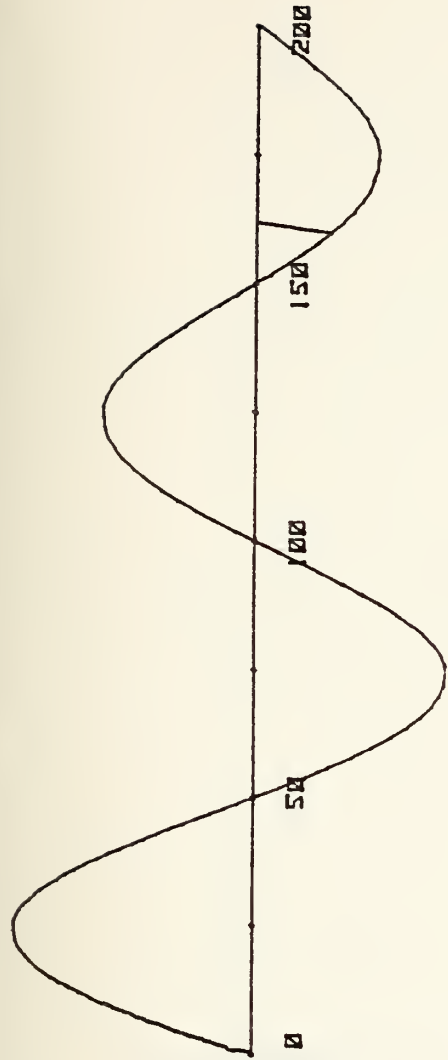


-20.000

short period

20.000

phugoid



-20.000

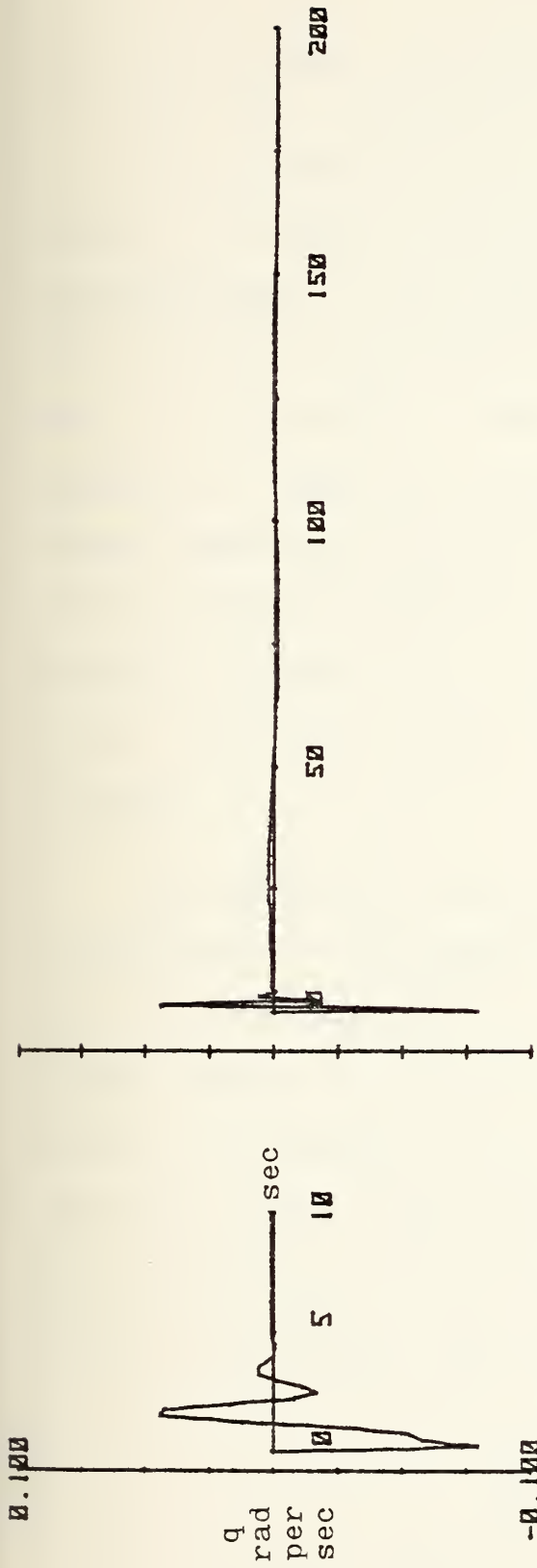
short period

20.000

phugoid

Figure 6-16





short period

phugoid

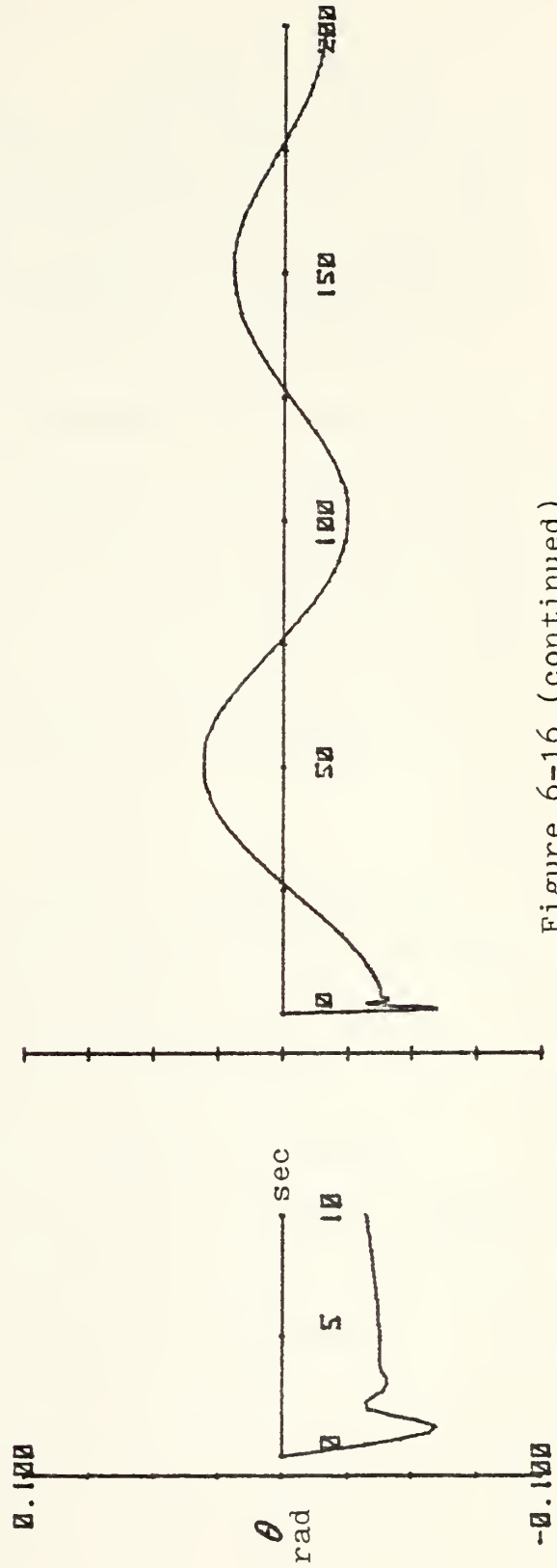


Figure 6-16 (continued)



## VII. LONGITUDINAL FEEDBACK

The primary purpose in using feedback in a control system is to reduce the system's sensitivity to external perturbations. In the open loop system, the area of main concern is calibration; in the closed loop system, it is stability. Use of feedback can enhance the rapidity of response, reduce errors of response, and increase damping to satisfactory levels; it can also overcorrect errors or decrease damping to the point where an otherwise stable system becomes unstable. It is of interest, then, to be able to "measure" the stability of a system.

The stability of a system may be ascertained by an analysis of the characteristic equation of the system, that is, the denominator of its transfer function. Simply stated, if the real part of every root of the equation is negative in sign, the system is stable. That this is so is manifested by the relationship between the roots of the characteristic equation and the solution of the differential equation which it represents.





For a multiple input/output system, the feedback effects on the transfer functions must be dealt with by matrix manipulation

The solution to the system of differential equations

$$\dot{\underline{x}} = [A]\underline{x} + \{b\}u \cdot$$

was seen to be, in the Laplace domain,

$$x(s) = [sI-A]^{-1} \{b\}u(s) = [\Phi(s)]\{b\}u(s).$$

The open loop transfer function was then

$$G_o(s) = \frac{x(s)}{u(s)} = [\Phi(s)]\{b\}$$

where  $\Phi(s)$  is the resolvent matrix. In a 4x4 system, the transfer function is written



$$G_O(s) = \frac{\begin{bmatrix} \varphi_{11} & \varphi_{12} & \varphi_{13} & \varphi_{14} \\ \varphi_{21} & \varphi_{22} & \varphi_{23} & \varphi_{24} \\ \varphi_{31} & \varphi_{32} & \varphi_{33} & \varphi_{34} \\ \varphi_{41} & \varphi_{42} & \varphi_{43} & \varphi_{44} \end{bmatrix} \begin{Bmatrix} b_1 \\ b_2 \\ b_3 \\ b_4 \end{Bmatrix}}{\Delta} = \begin{Bmatrix} \sum \varphi_{1j} b_j / \Delta \\ \sum \varphi_{2j} b_j / \Delta \\ \sum \varphi_{3j} b_j / \Delta \\ \sum \varphi_{4j} b_j / \Delta \end{Bmatrix}$$

$j = 1, \dots, 4$

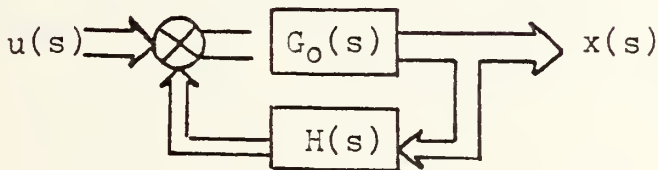
The last quantity will be written

$$\begin{Bmatrix} G_1 \\ G_2 \\ G_3 \\ G_4 \end{Bmatrix}_{\text{open}} \quad \text{where } \Delta = \det[sI - A]$$

Applying the feedback signal to a particular parameter, for example,  $x_3$ , yields

$$H = [0 \ 0 \ h \ 0]$$

where the block diagram is



(The solid arrows are used to signify a multiple input/output system.) The closed loop transfer function is



$$G(s) = \frac{G_o(s)}{1 + G_oH}$$

In matrix format,  $\{G(s)\} = [I + G_oH]^{-1} \{G_o(s)\}$ .

To find this matrix product, the matrices were taken term by term:

$$[I + G_oH] = \begin{bmatrix} 1 & 0 & hG_1 & 0 \\ 0 & 1 & hG_2 & 0 \\ 0 & 0 & 1+hG_3 & 0 \\ 0 & 0 & hG_4 & 1 \end{bmatrix}$$

$$[I + G_oH]^{-1} = \frac{\begin{bmatrix} 1+hG_3 & 0 & -hG_1 & 0 \\ 0 & 1+hG_3 & -hG_2 & 0 \\ 0 & 0 & 1 & 0 \\ 0 & 0 & -hG_4 & 1+hG_3 \end{bmatrix}}{\Delta'}$$

where  $\Delta' = \det [I + G_oH] = 1 + hG_3$ .

Finally,

$$[I + G_oH]^{-1} \{G_o(s)\} = \frac{\begin{Bmatrix} G_1 \\ G_2 \\ G_3 \\ G_4 \end{Bmatrix}_{open}}{\Delta'} = \frac{\begin{Bmatrix} \sum b_j \varphi_{1j} \\ \sum b_j \varphi_{2j} \\ \sum b_j \varphi_{3j} \\ \sum b_j \varphi_{4j} \end{Bmatrix}}{(1+hG_3) \Delta} = \frac{\begin{Bmatrix} \sum b_j \varphi_{1j} \\ \sum b_j \varphi_{2j} \\ \sum b_j \varphi_{3j} \\ \sum b_j \varphi_{4j} \end{Bmatrix}}{\left(1 + h \frac{\sum b_j \varphi_{3j}}{\Delta}\right) \Delta}$$

$$= \frac{\begin{Bmatrix} \sum b_j \varphi_{1j} \\ \sum b_j \varphi_{2j} \\ \sum b_j \varphi_{3j} \\ \sum b_j \varphi_{4j} \end{Bmatrix}}{\Delta + h \sum b_j \varphi_{3j}}$$



The closed loop transfer function is then

$$\{G_c(s)\} = \frac{\begin{pmatrix} b_1 \varphi_{11} + b_2 \varphi_{12} + b_3 \varphi_{13} + b_4 \varphi_{14} \\ b_1 \varphi_{21} + b_2 \varphi_{22} + b_3 \varphi_{23} + b_4 \varphi_{24} \\ b_1 \varphi_{31} + b_2 \varphi_{32} + b_3 \varphi_{33} + b_4 \varphi_{34} \\ b_1 \varphi_{41} + b_2 \varphi_{42} + b_3 \varphi_{43} + b_4 \varphi_{44} \end{pmatrix}}{\Delta + h(b_1 \varphi_{31} + b_2 \varphi_{32} + b_3 \varphi_{33} + b_4 \varphi_{34})}$$

In the general form, the first subscript of  $\varphi$  in the denominator will vary as the feedback parameter is varied. Regardless of the form or magnitude of  $h$ , only the denominator is affected; the numerator is a function solely of the openloop resolvent matrix,  $\bar{\Phi}(s)$ , and the control vector,  $\{b\}$ .

The most important characteristic of the transfer function is that the frequency response may be obtained by letting  $s = j\omega$ , where  $\omega$  is the applied sinusoidal forcing function. That this is so is shown by assuming that the output contains a sinusoidal component of the same frequency as the input in the form

$$A \cdot R(\omega) \cdot \sin[\omega t + \varphi(\omega)]$$

where  $A$  is a constant,  $R(\omega)$  is the magnitude, and  $\varphi(\omega)$





is the phase angle between the input and the response.

For an input of  $A \sin \omega t$ , the Laplace of which is

$$\frac{A\omega}{s^2 + \omega^2}$$

the output is

$$y(s) = G(s)r(s) = \frac{A\omega G(s)}{s^2 + \omega^2} = \frac{A\omega G(s)}{(s + j\omega)(s - j\omega)}$$

Using partial fraction expansion:

$$y(s) = \frac{Z_1}{s + j\omega} + \frac{Z_2}{s - j\omega} + \text{transient terms}$$

Assuming the transient solution is stable allows the transient terms to be dropped, so

$$Z_1 = \left. \frac{A\omega G(s)}{s - j\omega} \right|_{s = -j\omega} = \frac{-AG(-j\omega)}{2j}$$

$$Z_2 = \left. \frac{A\omega G(s)}{s + j\omega} \right|_{s = +j\omega} = \frac{AG(j\omega)}{2j}$$

Solving for  $y(t)$  by taking the inverse Laplace transform:

$$y(t) = \frac{-AG(-j\omega)}{2j} e^{-j\omega t} + \frac{AG(j\omega)}{2j} e^{+j\omega t} \quad (7-1)$$

Since  $G(j\omega)$  is complex, write it as

$$G(j\omega) = X(\omega) + jY(\omega) \quad \text{and} \quad G(-j\omega) = X(\omega) - jY(\omega)$$



where  $|G(j\omega)| = \sqrt{X^2(\omega) + Y^2(\omega)}$  and  $\arg G(j\omega) = \tan^{-1} \frac{Y(\omega)}{X(\omega)}$ .

Substitute into equation (7-1):

$$\begin{aligned}
 y(t) &= -\frac{A}{2j} [X(\omega) - jY(\omega)] e^{-j\omega t} + \frac{A}{2j} [X(\omega) + jY(\omega)] e^{+j\omega t} \\
 &= \frac{AX(\omega)}{2j} (e^{j\omega t} - e^{-j\omega t}) + \frac{AY(\omega)}{2j} (e^{j\omega t} + e^{-j\omega t}) \\
 &= AX(\omega) \sin \omega t + AY(\omega) \cos \omega t \\
 &= A [X^2(\omega) + Y^2(\omega)]^{1/2} \sin [\omega t + \alpha(\omega)]
 \end{aligned}$$

where  $\alpha = \tan^{-1} \frac{Y(\omega)}{X(\omega)}$ .

This is the same form as the assumed input, so that  $R(s)$  becomes  $\sqrt{X^2(\omega) + Y^2(\omega)} = |G(j\omega)|$  and the phase angle  $\varphi(\omega)$  becomes  $\tan^{-1} Y(\omega)/X(\omega) = \arg G(j\omega)$ .

It becomes a simple matter to apply a feedback to a plant matrix, obtain the transfer functions in each of the variables, and plot the magnitude of the responses to a sinusoidal input against the frequency of that



input. This plot is termed a Bode (Bō'-dee) plot, named for its developer, H.W. Bode. One of the important uses of the plot is in measuring the stability of a system.

In order to facilitate construction of a Bode plot, and in order to avoid relying upon asymptotic approximations of magnitude and phase angle, a program named BODE was written for the HP9830 computer/plotter. Using, as input, the stability derivatives and the type and magnitude of feedback, the program prints out the resulting transfer functions (in the Laplace domain), repeats the feedback inputs, and, for given limits of frequency and magnitude, constructs the Bode diagram on semi-log paper. The feedback form may be linear, integration (1/s), or differentiation (s).

The program, listed in Figure 7-2, is explained:

```
line 10    dimensions open and closed loop matrices
ll 20-60   defines variables in terms of stability
           derivatives;
           XU = Xu
           XW = Xw
           XDE = Xde
           MWDOT = Mw , etc.
line 70    iterates program for x1, x2, x3, and x4
           (u,w,q,θ) outputs
```



```

10 DIM N(8,3),SL(8,3)
20 REM X1,X2,X3 ARE XU,XV,XDE
30 REM Z1,Z2,Z3 ARE ZU,ZV,ZDE
40 REM M1,M2,M3 ARE MU,MV,MWDOT
50 REM M4,M5,M6 ARE MA,MO,MDE
60 REM X4 IS X0
70 FOR J=1 TO 4
80 WRITE (15,90)
90 FORMAT 45"%"
100 PRINT
110 DEG
120 T3=0
130 U0=1016.9
140 G=82.073
150 X1=-0.0097
160 X2=0.0016
170 X3=0
180 X4=0
190 Z1=-0.0955
200 Z2=-1.43
210 Z3=-59.8
220 M1=-3
230 M2=-0.6235
240 M3=-0.0013
250 M4=U0+M2
260 M5=-1.52
270 M6=-20.1
280 FOR I=1 TO 7
290 D(I)=0
300 FOR K=1 TO 7
310 N(I,K)=0
320 NEXT K
330 NEXT I
340 D(5)=1
350 N(3,4)=M6+Z3*M3
360 N(4,2)=Z3
370 N(4,1)=X3
380 D(4)=-M5-Z2-X1
390 N(2,4)=X3*(Z1*M3+M1)+Z3*(M2-X1*M3)-M6*(X1+Z2)
400 N(3,2)=X3*Z1-Z3*(X1+M5)+M6*U0
410 N(3,1)=-X3*(Z2+M5)+Z3*X2+X4+M6
420 D(3)=Z2*M5-X2*Z1+X1*(M5+Z2)-M4-M1*X4
430 N(1,4)=X3*(Z1*M2-Z2*M1)+Z3*(M1*X2-M2*X1)+M6*(Z2*X1-X2*Z1)
440 N(2,2)=X3*(U0+M1-Z1*M5)+Z3*X1*M5-U0+M6*X1+X4*(M6*Z1-M1*Z3)
450 N(2,1)=X3*(Z2*M5-M4)-Z3*(X2*M5+G*M3)-M6+G+M6*X2*U0-M6+Z3*X4
460 D(2)=-X1*(Z2*M5-M4)+Z1*(X2*M5+G*M3)-M1*(X2*U0-G)+X4*(M1*Z2-M2*Z1)
470 N(5,4)=N(5,3)=0
480 N(4,3)=M6
490 N(3,3)=-M6*X1-M6*Z2+M1*X3+M2*Z3
500 N(2,3)=M6*X1*Z2+M2*X3*Z1+M1*X2*Z3-M1*X3*Z2-M6*X2*Z1-M2*X1*Z3

```

Figure 7-2





```

510 N[I,J]=0
520 N[I,2]=G*(23*N[I,1]+M1*Z1)
530 N[I,1]=G*(M5+L1*(23*M2)
540 D[I]=G*(Z1*M2-N1+Z2)
550 DISP "IS FDBK 0, LINEAR, S, OR 1/S";
560 INPUT Z
570 IF Z=0 THEN 940
580 IF Z=1 THEN 610
590 IF Z=2 THEN 680
600 IF Z=3 THEN 790
610 DISP "INPUT FEEDBACK GAIN";
620 INPUT K
630 PRINT "FEEDBACK IS LINEAR"
640 FOR I=1 TO 7
650 D[I]=D[I]-N[I,J]*K
660 NEXT I
670 GOTO 960
680 DISP "INPUT FEEDBACK GAIN";
690 INPUT K
700 PRINT "FEEDBACK FORM IS K*S"
710 FOR I=7 TO 1 STEP -1
720 S[I+1,J]=N[I,J]*K
730 NEXT I
740 S[1,J]=0
750 FOR I=1 TO 7
760 D[I]=D[I]-S[I,J]
770 NEXT I
780 GOTO 960
790 DISP "INPUT FEEDBACK GAIN";
800 INPUT K
810 PRINT "FEEDBACK FORM IS K/S"
820 FOR I=7 TO 1 STEP -1
830 D[I+1]=D[I]
840 NEXT I
850 D[1]=0
860 FOR I=1 TO 7
870 D[I]=D[I]-N[I,J]*K
880 NEXT I
890 FOR I=7 TO 1 STEP -1
900 N[I+1,J]=N[I,J]
910 NEXT I
920 N[1,J]=0
930 GOTO 960
940 PRINT "FEEDBACK IS NOT APPLIED"
950 GOTO 970
960 PRINT "FEEDBACK GAIN IS "K
970 PRINT "TRANSFER FUNCTION COEFFICIENTS (INCREASING POWERS OF S)"
980 PRINT
990 PRINT "COEFFICIENTS OF NUMERATOR"
1000 FOR I=1 TO 7

```

Figure 7-2 (continued)



```

1010 PRINT NL G, JJ
1020 NEXT I
1030 PRINT
1040 PRINT "COEFFICIENTS OF DENOMINATOR (CHAR EDH):"
1050 FOR I=1 TO 7
1060 PRINT DC I
1070 NEXT I
1080 DISP "PLACE PAPER ON PLOTTER";
1090 STOP
1100 DISP "INPUT <G/> MAX (DB)";
1110 INPUT G9
1120 DISP "INPUT OMEGA MINIMUM";
1130 INPUT O0
1140 GOSUB 1650
1150 FOR L=LGT(O0)+1 TO LGT(O0)+5
1160 X=10^L
1170 FOR W=X/10 TO X STEP X/50
1180 XC JJ=(NC 1, JJ)-NC 3, JJ)*W^2+NC 5, JJ)*W^4-NC 7, JJ)*W^6)+2
1190 XL JJ=XC JJ+(NC 2, JJ)+W-NC 4, JJ)*W^3+NC 6, JJ)*W^5)+2
1200 XC JJ=SQR(XC JJ)
1210 YC JJ=(DC 1)-DC 3)*W^2+DC 5)*W^4)+2
1220 YL JJ=YC JJ+(DC 2)*W-DC 4)*W^3+DC 6)*W^5)+2
1230 YC JJ=SQR(YC JJ)
1240 RC JJ=XC JJ/YC JJ
1250 IF 20*LGT(RC JJ)<G9-140 THEN 1270
1260 PLOT LGT(W), 20*LGT(RC JJ)
1270 NEXT W
1280 NEXT L
1290 PEN
1300 PLOT LGT(O0)+0.1, G9-1, 1
1310 LABEL (*, 1.2, 1.7, 0, 7/10) "DECIBELS"
1320 PLOT LGT(O0)+2.2, G9-140, 1
1330 LABEL (*, 1.2, 1.7, 0, 7/10) "RADIANS/SECOND"
1340 PEN
1350 GOSUB 1910
1360 FOR L=LGT(O0)+1 TO LGT(O0)+5
1370 X=10^L
1380 FOR W=X/10 TO X STEP X/50
1390 T9=T3
1400 Q1=NC 2, JJ)+W-NC 4, JJ)*W^3+NC 6, JJ)*W^5
1410 Q2=NC 1, JJ)-NC 3, JJ)*W^2+NC 5, JJ)*W^4-NC 7, JJ)*W^6
1420 Q3=DC 2)*W-DC 4)*W^3+DC 6)*W^5
1430 Q4=DC 1)-DC 3)*W^2+DC 5)*W^4-DC 7)*W^6
1440 GOSUB 2000
1450 T3=T1-T2
1460 IF ABS(T3-T9)<180 THEN 1500
1470 T3=T3+360
1480 IF ABS(T3-T9)<180 THEN 1500
1490 T3=T3-720
1500 IF T3<-300 THEN 1520

```

Figure 7-2 (continued)



```

1510 PLOT LGT(W),T3
1520 NEXT W
1530 NEXT I
1540 PEN
1550 DISP "INPUT LETTER SIZE";
1560 INPUT Z
1570 LABEL (+,2,2,0,7/10)
1580 DISP "YOU ARE IN THE LETTER MODE"
1590 LETTER
1600 DISP "ANY OTHER LETTERING";
1610 INPUT Z
1620 IF Z=1 THEN 1550
1630 NEXT _
1640 STOP
1650 SCALE LGT(00)-0.5,LGT(00)+5.5,G9-140,G9+5
1660 DISP "CHECK ALIGNMENT OF PLOTTER"
1670 PLOT LGT(00),G9-140,1
1680 STOP
1690 PLOT LGT(00)+5,G9,1
1700 DISP "RE-CHECK ALIGNMENT?";
1710 INPUT Z
1720 IF Z=0 THEN 1740
1730 GOTO 1660
1740 YAXIS LGT(00),20,G9-140,G9
1750 LABEL (+,1,1.7,0,7/10)
1760 FOR Y=G9-140 TO G9 STEP 20
1770 PLOT LGT(00),Y,1
1780 CPLOT -5,-0.3
1790 LABEL (1800)Y
1800 FORMAT F4.0
1810 NEXT Y
1820 FOR X=LGT(00)+1 TO LGT(00)+5
1830 PLOT X,G9-140,1
1840 CPLOT -4.5,-1.5
1850 LABEL (1860)10*X
1860 FORMAT F8.2
1870 NEXT X
1880 PEN
1890 RETURN
1900 STOP
1910 SCALE LGT(00)-0.5,LGT(00)+5.5,-325,425
1920 DISP "RE-CHECK ALIGNMENT OF PLOTTER";
1930 PLOT LGT(00),-300,1
1940 STOP
1950 PLOT LGT(00)+5,400,1
1960 STOP
1970 LABEL (+,1.2,1.7,0,7/10)
1980 FOR Y=-200 TO 100 STEP 100
1990 PLOT LGT(00)+4.7,Y,1
2000 CPLOT 0,-0.3

```

Figure 7-2 (continued)



```

2010 LABEL (2050)Y
2020 NEXT Y
2030 PLOT LGT(100)+4.95,95,1
2040 LABEL (+,1.2,1.7,0,7/10)"DEG"
2050 FORMAT F4.0
2060 RETURN
2070 STOP
2080 IF Q1>0 AND Q2<0 THEN 2130
2090 IF Q1<0 AND Q2<0 THEN 2150
2100 IF Q1<0 AND Q2>0 THEN 2170
2110 T1=ATN(Q1/Q2)-180
2120 GOTO 2180
2130 T1=ATN(Q1/Q2)
2140 GOTO 2180
2150 T1=ATN(Q1/Q2)
2160 GOTO 2180
2170 T1=180+ATN(Q1/Q2)
2180 IF Q3>0 AND Q4<0 THEN 2230
2190 IF Q3<0 AND Q4<0 THEN 2250
2200 IF Q3<0 AND Q4>0 THEN 2270
2210 T2=ATN(Q3/Q4)
2220 RETURN
2230 T2=180+ATN(Q3/Q4)
2240 RETURN
2250 T2=180+ATN(Q3/Q4)
2260 RETURN
2270 T2=360+ATN(Q3/Q4)
2280 RETURN
2290 END

```

Figure 7-2 (continued)



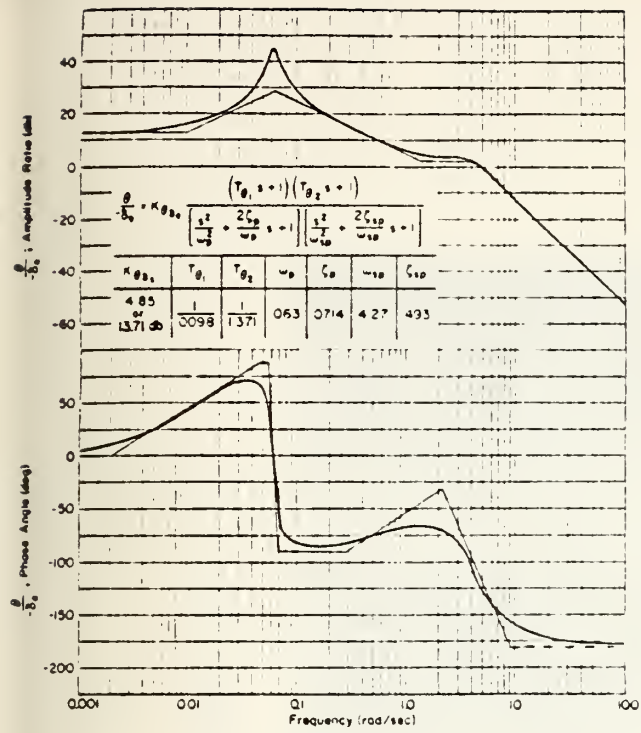


11 80-110 format  
 11 120-270 assigns values to variables, initializes  
     T3 (phase angle, used for comparison)  
 11 280-330 initializes numerator and denominator  
     coefficients to zero  
 11 340-540 computes values of numerator and denomi-  
     nator coefficients  
 11 550-1070 inputs feedback type and magnitude, com-  
     putes and prints closed loop numerator and  
     denominator coefficients  
 11 1080-1640 inputs frequency and magnitude limits  
     (of response), labels graph, and plots  
     magnitude and phase angle against applied  
     frequency  
 11 1650-1900 subroutine for scaling and labelling  
     magnitude graph  
 11 1910-2070 subroutine for scaling and labelling  
     phase angle graph  
 11 2080-2280 subroutine which computes phase angle  
     correct for sign and quadrant  
 line 2290 END statement

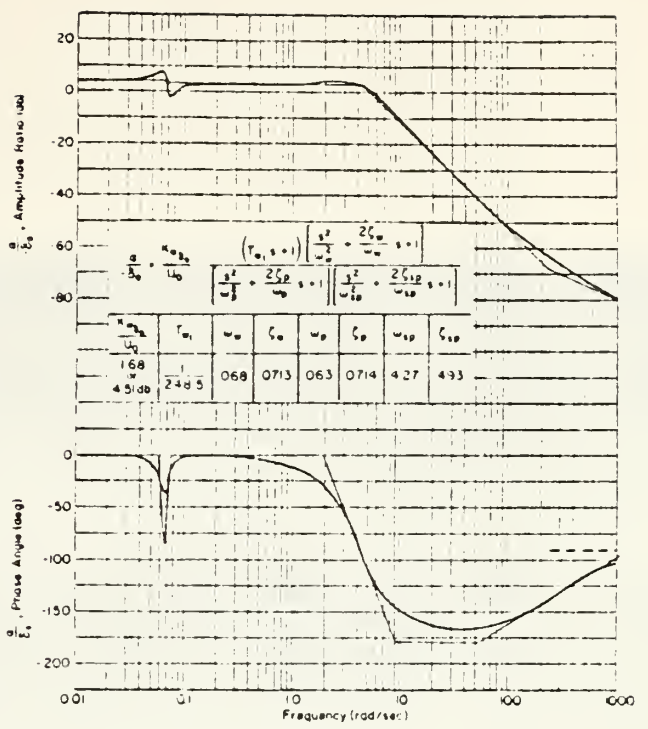
To verify the program, the M<sup>C</sup>Ruer example was again  
 used. The text results are shown in Figure 7-3. The  
 BODE results are shown in Figures 7-4, 7-5, and 7-6 for  
 the three parameters common to both programs,  $\theta$ ,  $\alpha$ , and  
 u.

The comparison of the  $\alpha$  values of the text and the  
 graph of w from BODE needs some explanation. The text's

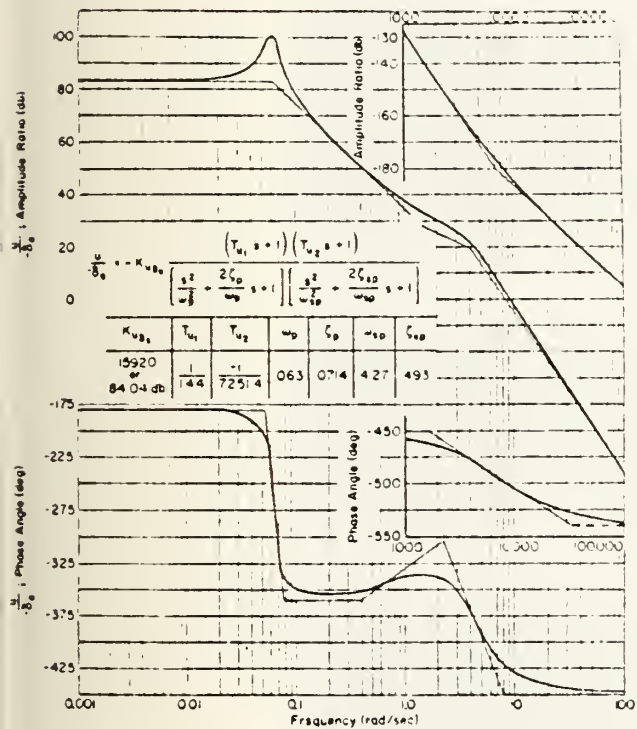




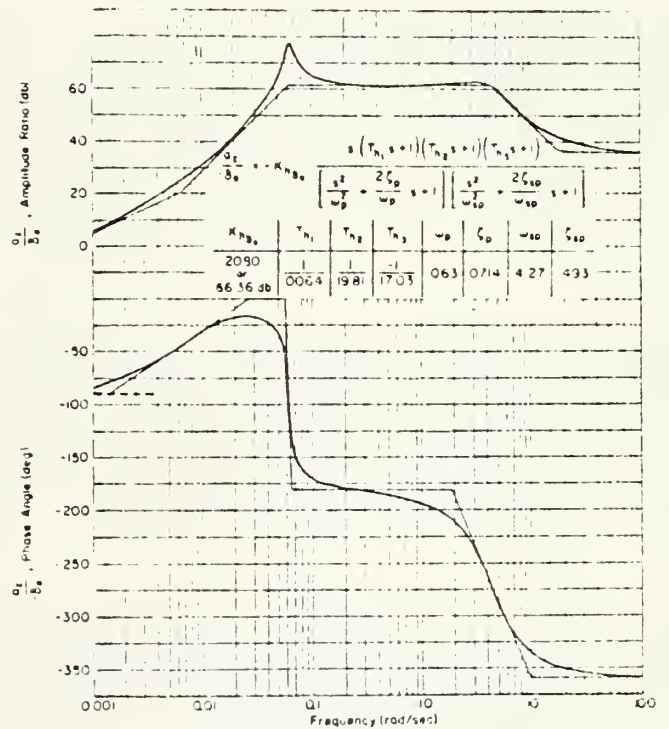
a)  $\frac{\theta}{\delta_e}$



b)  $\frac{a}{\delta_e}$



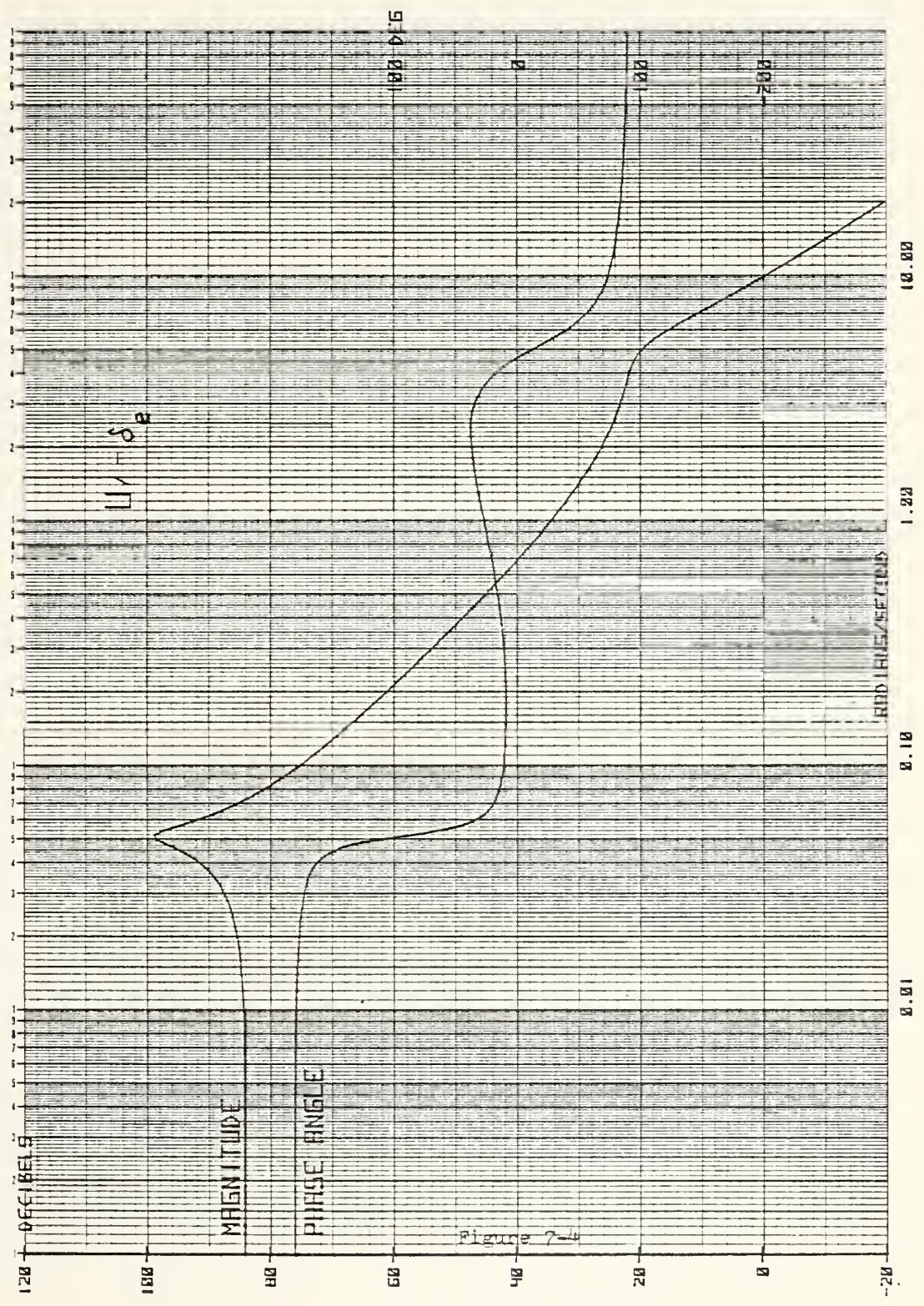
c)  $\frac{u}{\delta_e}$



d)  $\frac{z}{\delta_e}$

Figure 7-3







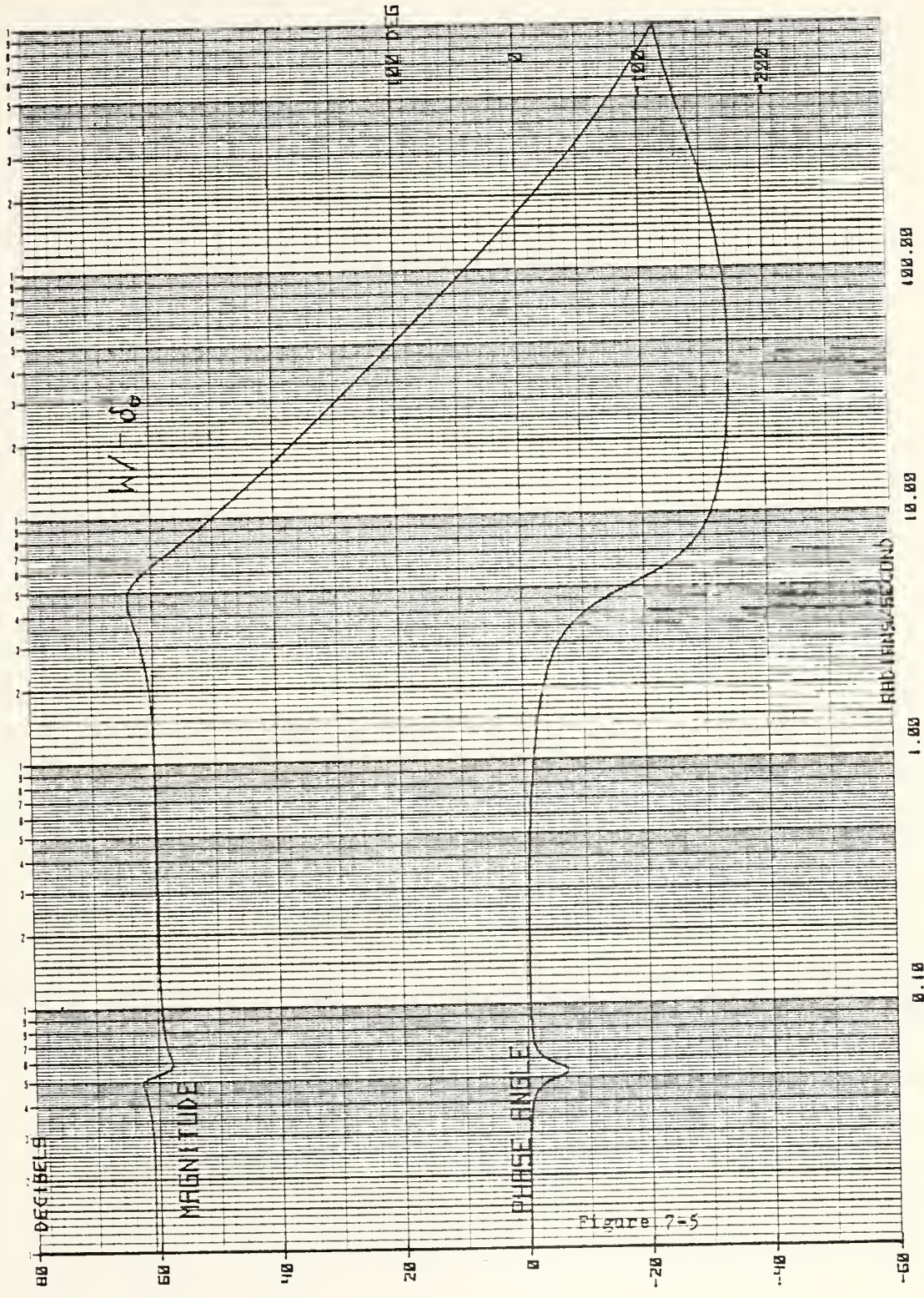
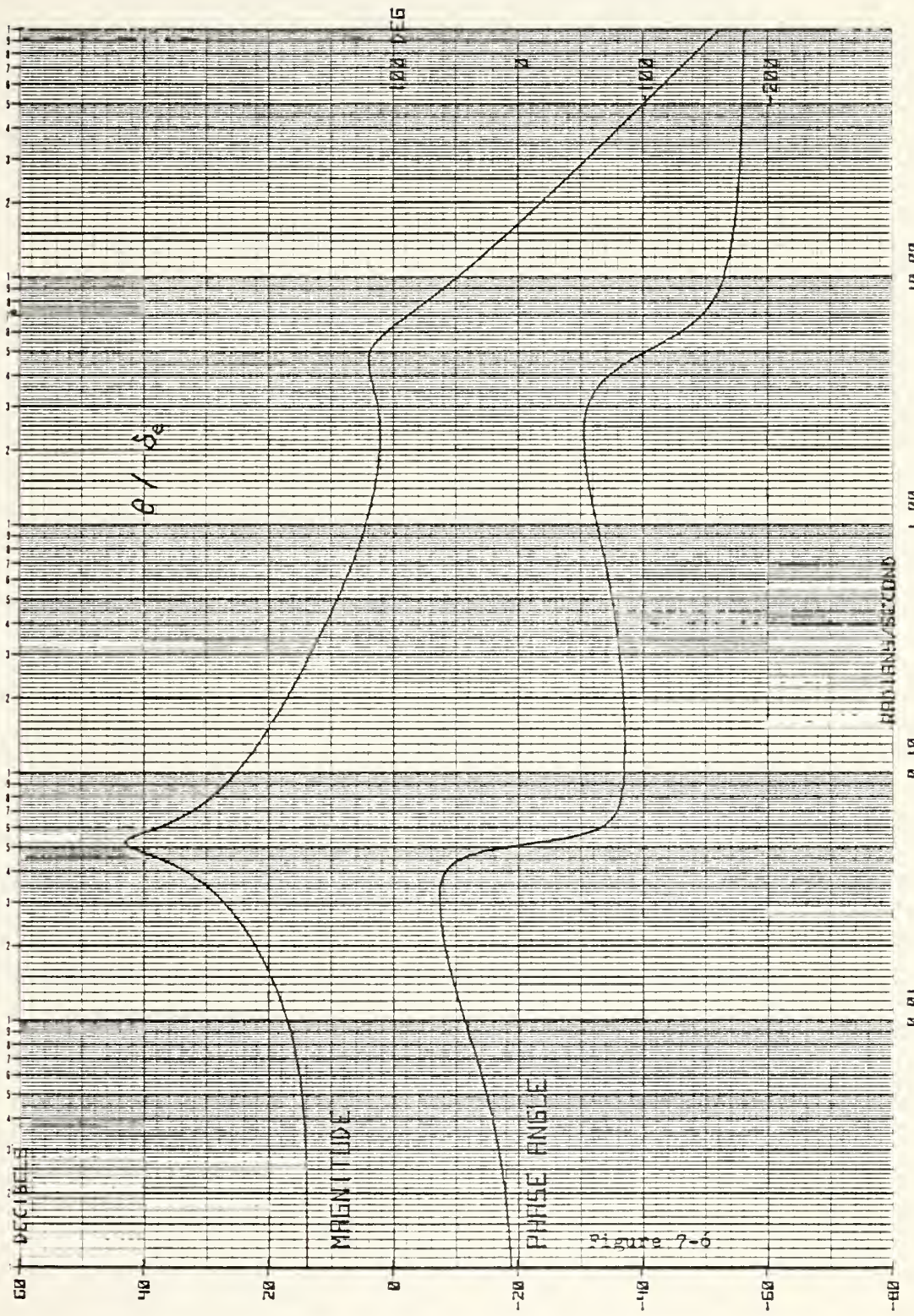


Figure 7-5









magnitude for  $\alpha$  at low frequency is  $\sim 4.0$ ; the results of BODE showed the magnitude of  $w$  at low frequency to be  $\sim 61$ , a 57 decibel difference. For  $U_0 = 660$ ,

$$w = \alpha U_0 = 660\alpha$$

$$\log(w) = \log(660) + \log(\alpha).$$

Since  $\log(660) = 56.4$ , the 57 db difference is correct.

Table 7-2 compares the results of the BODE program's transfer function coefficients with those of the text.

<u>NUMERATORS</u>	
u	BODE $0.11168s^2 - 791.5148s - 1144.4512$ text $0.1103s^2 - 799s - 1151$
w	BODE $69.8s^3 + 26675.783s^2 + 258.7485s + 79.94357$ text $69.8s^3 + 17350s^2 + 168.6s + 80.2$
e	BODE $26.00926s^2 + 35.93499s + 0.35011$ text $26.12s^2 + 36.1s + 0.351$
<u>DENOMINATOR</u>	
	BODE $s^4 + 3.3597s^3 + 26.6754s^2 + 0.26271s + 0.07198$ text $s^4 + 4.22s^3 + 18.28s^2 + 0.2097s + 0.0724$

Table 7-2



Inasmuch as the text figures appeared to be slide-rule accuracy, the results of BODE were considered more accurate. The BODE graphs, which were computed with zero feedback, compared very favorably with the text, and the program may be considered verified.

The transfer functions may also be written as functions of the stability derivatives, and, in this way, the effects of various types of feedback may be predicted. Writing the equations of motion (equations 5-1) in the Laplace domain:

$$\begin{array}{rclcl}
 (s-X_u)u & -X_w w & -X_q q + g\theta & = & X_{f_e} \\
 -Z_{uu}u + (s-Z_w)w & & -U_0 q & = & Z_{f_e} \\
 -M_{uu}u & -M_w w + (s-M_q)q & & = & M_{f_e} \\
 & & -q + s\theta & = & 0
 \end{array}$$

Use of Cramer's rule allows for the solution of each variable in terms of the stability derivatives. That is:

$$\frac{u(s)}{\delta_e(s)} = \frac{
 \begin{vmatrix}
 X_{f_e} & -X_w & -X_q & g \\
 Z_{f_e} & s-Z_w & -U_0 & 0 \\
 M_{f_e} & -M_w & s-M_q & 0 \\
 0 & 0 & -1 & s
 \end{vmatrix}
 }{\Delta}$$



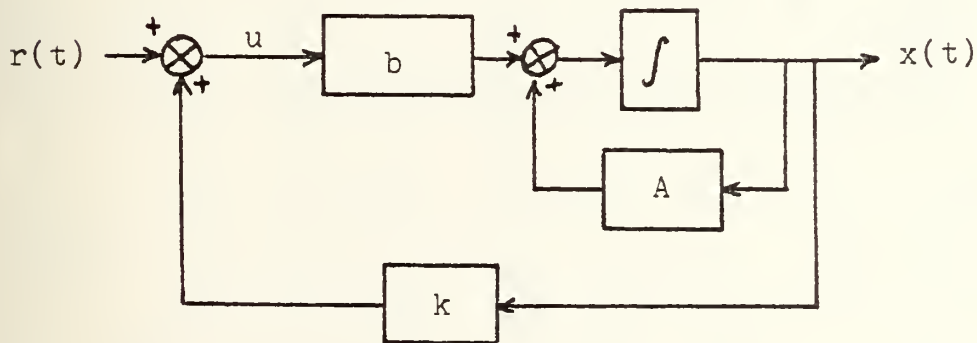
where  $\Delta = \begin{vmatrix} s - X_u & -X_w & -X_q & q \\ -Z_u & s - Z_w & -U_0 & 0 \\ -M_u & -M_w & s - M_q & 0 \\ 0 & 0 & -1 & s \end{vmatrix}$

The transfer functions for  $w(s)/\delta_e(s)$ ,  $q(s)/\delta_e(s)$ , and  $\theta(s)/\delta_e(s)$  are similarly found. Compiling the coefficients for each of the numerators yields Table 7-3.

The time history response may be obtained by substituting the error signal for the input term to the plant matrix. In other words, where, for the open loop system,

$$\dot{\underline{x}}(t) = [A]\underline{x} + \{b\}u,$$

in the closed loop system



$$u = r - kx, \text{ and } \dot{\underline{x}}(t) = [A]\underline{x} + \{b\}(r - [k]\{x\}).$$

Rewriting,

$$\dot{\underline{x}}(t) = (A - bk^T)\underline{x} + \underline{b}r.$$





Table 7-3

NUMERATORS

	$s^3$	$s^2$	$s^1$	$s^0$
u	$X_w Z$ $-X_{\mathcal{E}} (Z_w + M_q)$	$X_{\mathcal{E}} (Z_w M_q - M_w U_0)$ $-Z_{\mathcal{E}} X_w M_q$ $+M_{\mathcal{E}} (X_w U_0 - g)$	$X_{\mathcal{E}} (Z_w M_q - M_w U_0)$ $-Z_{\mathcal{E}} X_w M_q$ $+M_{\mathcal{E}} (X_w U_0 - g)$	$g(Z_w M_{\mathcal{E}} - Z_{\mathcal{E}} M_w)$
w	$X_{\mathcal{E}} Z_u + M_{\mathcal{E}} U_0$ $-Z_{\mathcal{E}} (X_u + M_q)$	$X_{\mathcal{E}} (M_u U_0 - Z_u M_q)$ $+Z_{\mathcal{E}} (X_u M_q - X_q M_u)$ $+M_{\mathcal{E}} (X_q Z_u - X_u U_0)$	$X_{\mathcal{E}} (M_u U_0 - Z_u M_q)$ $+Z_{\mathcal{E}} (X_u M_q - X_q M_u)$ $+M_{\mathcal{E}} (X_q Z_u - X_u U_0)$	$g(Z_{\mathcal{E}} M_u - Z_u M_{\mathcal{E}})$
q	$X_{\mathcal{E}} M_u + Z_{\mathcal{E}} M_w$ $-M_{\mathcal{E}} (X_u + Z_w)$	$X_{\mathcal{E}} (Z_u M_w - Z_w M_u)$ $+Z_{\mathcal{E}} (X_w M_u - X_u M_w)$ $+M_{\mathcal{E}} (X_u Z_w - X_w Z_u)$	$X_{\mathcal{E}} (Z_u M_w - Z_w M_u)$ $+Z_{\mathcal{E}} (X_w M_u - X_u M_w)$ $+M_{\mathcal{E}} (X_u Z_w - X_w Z_u)$	
$\theta$	$M_{\mathcal{E}}$		$X_{\mathcal{E}} M_u + Z_{\mathcal{E}} M_w$ $-M_{\mathcal{E}} (X_u + Z_w)$	$X_{\mathcal{E}} (Z_u M_w - M_u Z_w)$ $+Z_{\mathcal{E}} (X_w M_u - X_u M_w)$ $+M_{\mathcal{E}} (X_u Z_w - X_w Z_u)$

DENOMINATOR

$$\Delta = s^4 - (X_u + Z_w + M_q)s^3 + (X_u Z_w + X_u M_q + Z_w M_q - X_q M_u - X_w Z_u - M_w U_0)s^2 + (X_q Z_w M_u + X_w Z_u M_q - X_u Z_w M_w - X_w M_u U_0 + X_u M_w U_0 + M_u g)s + g(Z_u M_w - Z_w M_u)$$



As originally formulated,

$$[A] = \begin{bmatrix} X_u & X_w & X_q & -g \\ Z_u & Z_w & U_0 + Z_q & 0 \\ M_u & M_w & M_q & 0 \\ 0 & 0 & 1 & 0 \end{bmatrix}$$

and

$$\{B\} = \begin{Bmatrix} X_{\delta_e} \\ Z_{\delta_e} \\ M_{\delta_e} \\ 0 \end{Bmatrix}$$

Assuming the input to be zero ( $r = 0$ ), the effects of a speed error feedback can be seen by letting  $[k] = [k_u \ 0 \ 0 \ 0]$

and solving for  $[A - \underline{b}k^T]$ :

$$\{B\}[k] = \begin{bmatrix} X_{\delta_e} k_u & 0 & 0 & 0 \\ Z_{\delta_e} k_u & 0 & 0 & 0 \\ M_{\delta_e} k_u & 0 & 0 & 0 \\ 0 & 0 & 0 & 0 \end{bmatrix}$$

$$[A - \underline{B}k^T] = \begin{bmatrix} X_u - X_{\delta_e} k_u & X_w & X_q & -g \\ Z_u - Z_{\delta_e} k_u & Z_w & U_0 + Z_q & 0 \\ M_u - M_{\delta_e} k_u & M_w & M_q & 0 \\ 0 & 0 & 1 & 0 \end{bmatrix}$$



This is the new plant matrix from which the eigenvalues may be calculated and roots plotted. As  $k_u$  is varied, the roots move, and this movement is the critical factor in retaining, gaining, or improving stability. Plotting the roots also shows how variations in  $k$  affect the undamped natural frequencies and damping ratios and gives a rough idea of the sensitivity of the system.

In order that the roots of a given system subject to feedback could be quickly ascertained, a program named FDBK was written for the HP9830. Using as inputs the resolvent matrix of the open loop system, the control vector  $\{b\}$ , the coefficients of the open loop characteristic equation, and the type and magnitude (gain) of the feedback, the program computes  $[A - bk^T]$ , finds and prints the new roots, and calculates the resulting frequencies, periods, and damping ratios. See Figure 7-7 for a listing of FDBK. The REMark statements in the listing provide an explanation of the procedures used.

Figure 7-8 is an example of the program's output. In this case, the M<sup>C</sup>Ruer example was again used with no feedback applied; the results were in agreement with the example.



```

10 REM THIS PROGRAM TAKES A 4X4 RESOLVENT MATRIX FROM DATA
20 REM STATEMENTS, CONSTRUCTS THE OPEN-LOOP TRANSFER FUNCTION,
30 REM AND FINALLY, BY APPLYING FEEDBACK FROM ANY ONE OF THE
40 REM FOUR PARAMETERS, CONSTRUCTS THE CLOSED-LOOP TRANSFER
50 REM MATRIX; THE FEEDBACK MAY BE LINEAR, K/S, K*S, OR NOT
60 REM APPLIED AT ALL. ANY VALUE OF FEEDBACK GAIN MAY BE USED.
70 DIM A[4,4],B[4,4],C[4,4],D[4,4],E[4,4],F[4,4],M[4]
80 REM INITIALIZE COEFFS TO ZERO
90 FOR I=1 TO 4
100 FOR J=1 TO 4
110 A[I,J]=B[I,J]=C[I,J]=D[I,J]=E[I,J]=F[I,J]=0
120 NEXT J
130 G[I]=H[I]=I[I]=J[I]=K[I]=M[I]=0
140 NEXT I
150 S=T=U=V=W=X=Y=X9=Y9=0
160 PRINT
170 WRITE (15,180)
180 FORMAT 45"*"
190 FORMAT 22"*"
200 PRINT
210 REM ENTER RESOLVENT MATRIX IN INCREASING POWERS OF S
220 MAT READ B
230 DATA 0,0.7567,-46.046,-627.429
240 DATA 0,0.004061,3.0646,5.91353
250 DATA 0,0,0,-0.07797
260 DATA 0.00242,-0.00023,0.01401,0.1893
270 MAT READ C
280 DATA 19.4854,0.004448,-31.144,-135.5619
290 DATA -0.18365,0.02695,6.401856,3.075099
300 DATA 0.00242,-0.00023,0.01401,-0.0039928
310 DATA 0.000124,-0.0235,1.4397,19.52637
320 MAT READ D
330 DATA 4.21,0.0015,0,-32.2
340 DATA -0.0955,2.7897,660,0
350 DATA 0.000124,-0.0235,1.4397,0
360 DATA 0,0,1,4.2197
370 MAT READ E
380 DATA 1,0,0,0
390 DATA 0,1,0,0
400 DATA 0,0,1,0
410 DATA 0,0,0,1
420 REM ENTER CONTROL VECTOR (B)
430 MAT READ M
440 DATA 0,-69.8,-26.009,0
450 REM ENTER COEFFICIENTS OF ORIGINAL CHARACTERISTIC EQUATION
460 REM IN INCREASING POWERS OF S
470 READ N0,N1,N2,N3,N4
480 DATA 0.07797,0.19329,19.52637,4.2197,1
490 DISP "IS FDBK 0. LINEAR, K*S, OR K/S";
500 INPUT L

```

Figure 7-7





```

510 DISP "WHICH PARAMETER DESIRED FOR FDBK";
520 INPUT Z
530 DISP "ENTER GAIN";
540 INPUT K
550 IF Z#1 THEN 570
560 PRINT "FEEDBACK PARAMATER IS HORIZ VELOCITY"
570 IF Z#2 THEN 590
580 PRINT "FEEDBACK PARAMETER IS VERT VELOCITY"
590 IF Z#3 THEN 610
600 PRINT "FEEDBACK PARAMETER IS PITCH RATE"
610 IF Z#4 THEN 630
620 PRINT "FEEDBACK PARAMETER IS PITCH ANGLE"
630 PRINT "GAIN = "K
640 REM MULTIPLY PHI(S) TIMES B (CONTROL VECTOR) TO FORM
650 REM NUMERATOR OF G0(S) (OPEN LOOP TX FN)
660 FOR I=1 TO 4
670 FOR J=1 TO 4
680 HC[I]=B[I,J]*MC[J]+HC[I]
690 IC[I]=C[I,J]*MC[J]+IC[I]
700 JC[I]=D[I,J]*MC[J]+JC[I]
710 KC[I]=E[I,J]*MC[J]+KC[I]
720 NEXT J
730 NEXT I
740 REM DENOMINATOR OF G0(S) IS THE CHARACTERISTIC EQN (SEE
750 REM LINES 440-470). NUMERATOR OF CLOSED-LOOP TRANSFER
760 REM MATRIX IS THE SAME AS THAT OF THE OPEN-LOOP MATRIX.
770 REM THE DENOMINATOR IS OF THE FORM H TIMES SUM(B(J)+PHI
780 REM (Z,J) PLUS CHAR EQN OF PLANT MATRIX.
790 FOR J=1 TO 4
800 T=B[Z,J]+MC[J]+T
810 U=C[Z,J]+MC[J]+U
820 V=D[Z,J]+MC[J]+V
830 W=E[Z,J]+MC[J]+W
840 X=F[Z,J]+MC[J]+X
850 NEXT J
860 IF L=0 THEN 990
870 IF L=1 THEN 1030
880 IF L=2 THEN 1110
890 IF L=3 THEN 900
900 PRINT "FEEDBACK MODE IS K/S"
910 PRINT
920 S=T*K
930 T=U*K
940 U=V*K
950 V=W*K
960 W=X*K
970 X=0
980 GOTO 1200
990 PRINT "FEEDBACK IS NOT APPLIED"
1000 PRINT

```

Figure 7-7 (continued)



```

1010 T=U=V=W=X=Y=0
1020 GOTO 1200
1030 PRINT "FEEDBACK MODE IS LINEAR"
1040 PRINT
1050 T=T*K
1060 U=U*K
1070 V=V*K
1080 W=W*K
1090 X=X*K
1100 GOTO 1200
1110 PRINT "FEEDBACK MODE IS K*S"
1120 PRINT
1130 Y=X*K
1140 X=W*K
1150 W=V*K
1160 V=U*K
1170 U=T*K
1180 T=0
1190 GOTO 1200
1200 REM SUMMING TERMS IN DENOMINATOR OF CLOSED-LOOP TX MATRIX
1210 S=S
1220 T=T+N0
1230 U=U+N1
1240 V=V+N2
1250 W=W+N3
1260 X=X+N4
1270 Y=Y
1280 WRITE (15,190)
1290 PRINT
1300 PRINT "THE COEFFICIENTS OF THE NUMERATOR OF THE CLOSED-LOOP TX
1310 PRINT " (FROM S+(0) TO S+(3))"
1320 PRINT
1330 FOR I=1 TO 4
1340 PRINT "COEFFS OF G("I")"
1350 WRITE (15,1470)H[I],I[I],J[I],K[I]
1360 PRINT
1370 NEXT I
1380 WRITE (15,190)
1390 PRINT
1400 PRINT "COEFFICIENTS OF THE DENOMINATOR ARE:"
1410 PRINT " (FROM S+(-1) TO S+(5))"
1420 PRINT
1430 WRITE (15,1470)S,T,U,V
1440 WRITE (15,1470)W,X,Y
1450 PRINT
1460 WRITE (15,190)
1470 FORMAT 4F15.7
1480 IF S=0 AND Y=0 THEN 1530
1490 GOTO 2140
1500 STOP

```

Figure 7-7 (continued)



```

1510 REM
1520 REM
1530 PRINT
1540 REM THIS PROGRAM CALCULATES THE COMPLEX ROOTS OF A FOURTH
1550 REM ORDER POLYNOMIAL USING THE MODIFIED BAIRSTOW METHOD.
1560 R9=1
1570 S9=1
1580 A4=X
1590 A3=W
1600 A2=Y
1610 A1=U
1620 A0=T
1630 B4=A4
1640 B3=A3+R9*B4
1650 B2=A2+R9*B3+S9*B4
1660 B1=A1+R9*B2+S9*B3
1670 B0=A0+S9*B2
1680 IF ABS(B0)>1E-02 THEN 1700
1690 IF ABS(B1)<1E-02 THEN 1730
1700 S9=-A0/B2
1710 R9=-(A1+S9*B3)/B2
1720 GOTO 1630
1730 IF (R9^2+4*S9)<0 THEN 1780
1740 X1=(R9+SQR(P9^2+4*S9))/2
1750 X2=(R9-SQR(P9^2+4*S9))/2
1760 X5=X6=0
1770 GOTO 1810
1780 X1=X2=R9/2
1790 X5=SQR(ABS(R9^2+4*S9))/2
1800 X6=-X5
1810 IF (B3^2-4*B4*B2)<0 THEN 1860
1820 X3=(-B3+SQR(B3^2-4*B4*B2))/2
1830 X4=(-B3-SQR(B3^2-4*B4*B2))/2
1840 X7=X8=0
1850 GOTO 1890
1860 X3=X4=-B3/2
1870 X7=SQR(ABS(B3^2-4*B4*B2))/2
1880 X8=-X7
1890 PRINT "THE EIGENVALUES ARE"
1900 PRINT
1910 PRINT "      REAL PART      IMAG PART"
1920 WRITE (15,1990)X1,X5
1930 WRITE (15,1990)X2,X6
1940 WRITE (15,1990)X3,X7
1950 WRITE (15,1990)X4,X8
1960 PRINT
1970 PRINT
1980 WRITE (15,190)
1990 FORMAT 3X,F10.5,5X,F10.5
2000 FIXED 4

```

Figure 7-7 (continued)



```
2010 PRINT
2020 PRINT "MODE I FREQUENCY IS "SQR(X1+2+X5+2)"RADIANS PER SECOND"
2030 PRINT "          PERIOD IS "2*PI/SQR(X1+2+X5+2)"SECONDS"
2040 PRINT "    DAMPING RATIO IS "-X1/SQR(X1+2+X5+2)
2050 PRINT
2060 PRINT "MODE II FREQUENCY IS "SQR(X3+2+X7+2)"RADIANS PER SECOND"
2070 PRINT "          PERIOD IS "2*PI/SQR(X3+2+X7+2)"SECONDS"
2080 PRINT "    DAMPING RATIO IS "-X3/SQR(X3+2+X7+2)
2090 PRINT
2100 FORMAT 5F12.5
2110 X9=X
2120 Y9=Y
2130 STOP
```

Figure 7-7 (continued)





\*\*\*\*\*

FEEDBACK PARAMETER IS PITCH RATE  
GAIN = 0  
FEEDBACK IS NOT APPLIED

\*\*\*\*\*

THE COEFFICIENTS OF THE NUMERATOR OF THE CLOSED-LOOP TX FN ARE:  
(FROM S+(0) TO S+(3))

COEFFS OF G( 1 )  
1144.7927540      809.7138256      -0.1116800      0.0000000

COEFFS OF G( 2 )  
-79.9906392      -168.3869827      -17360.6610600      -69.8000000

COEFFS OF G( 3 )  
0.0000000      -0.3483321      -35.8048573      -26.0090000

COEFFS OF G( 4 )  
-0.48337      -35.8048573      -26.0090000      0.0000000

\*\*\*\*\*

COEFFICIENTS OF THE DENOMINATOR ARE:  
(FROM S+(0) TO S+(5))

0.0000000      0.0779700      0.1932900      19.5263700  
4.2197000      1.0000000      0.0000000

\*\*\*\*\*

THE EIGENVALUES ARE

REAL PART	IMAG PART
-0.30455	0.06308
-0.00455	-0.06308
-2.10532	3.87967
-2.10532	-3.87967

\*\*\*\*\*

MODE I FREQUENCY IS 0.0632 RADIANS PER SECOND  
PERIOD IS 99.3505 SECONDS  
DAMPING RATIO IS 0.0716

MODE II FREQUENCY IS 4.4141 RADIANS PER SECOND  
PERIOD IS 1.4234 SECONDS  
DAMPING RATIO IS 0.4770

Figure 7-8



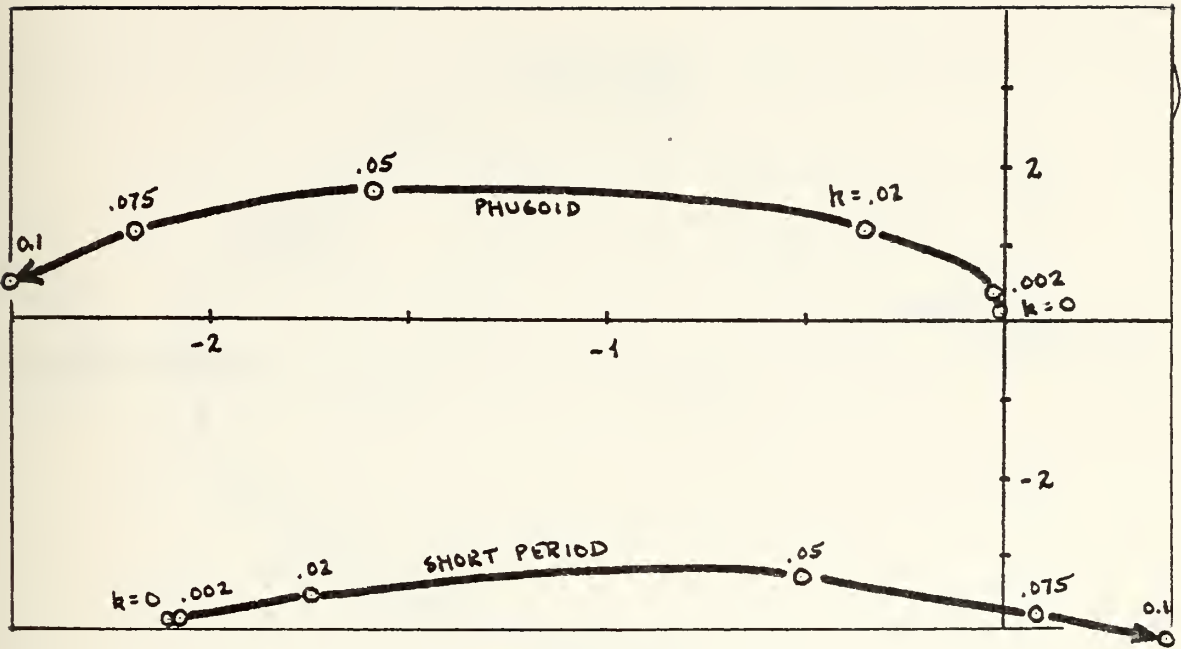
Figure 7-9 (a,b,c,d) shows how the roots vary as the feedback gain is varied and as different parameters are fed back. Complex conjugates are not shown where their omission would be confusing. These results are tabulated for more careful scrutiny in Table 7-4.

Figure 7-10(a) depicts the time history of the MCRuer F-89 aircraft subject to an initial condition of vertical velocity = 10 fps. No control inputs are postulated. The parameter chosen to display system response is pitch angle; it was chosen because of its good definition of short period and phugoid motion.

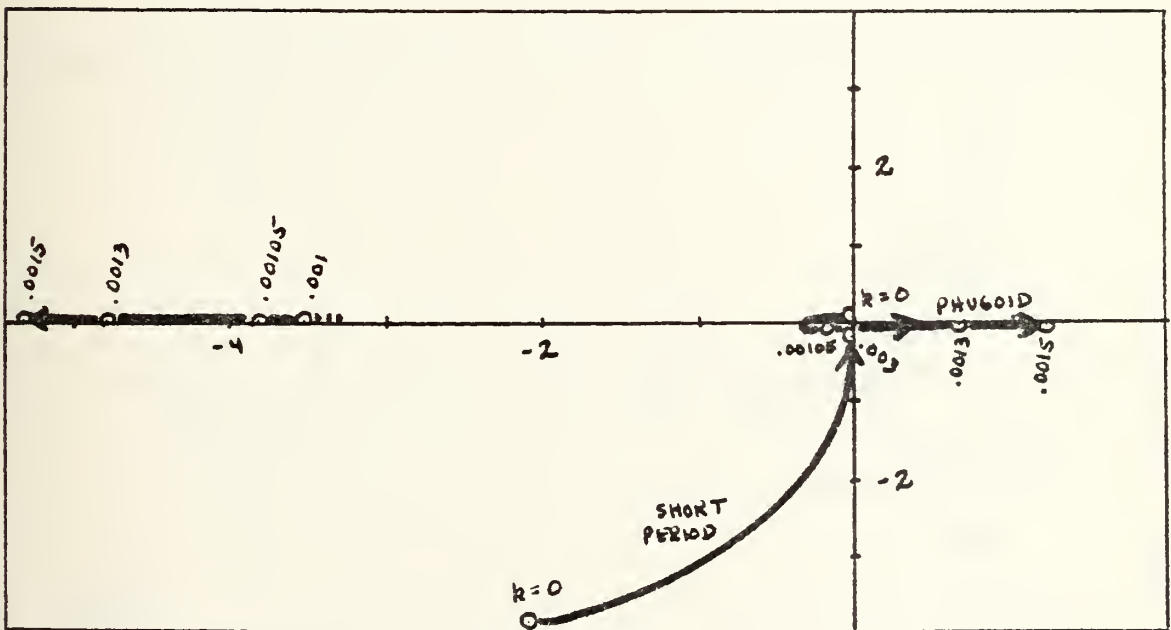
Feedback of horizontal velocity error can substantially increase phugoid damping before the short period mode is much affected. However, a further increase in the gain of this error signal will drive the short period to instability. The sensitivity of the system in this regime is shown by Figure 7-10(b); here, with  $k_u = 0.02$ , the short period motion is less than critically damped and oscillates several times before dying out. The damping effect on the phugoid is readily apparent.

Feedback of vertical velocity (or angle of attack),





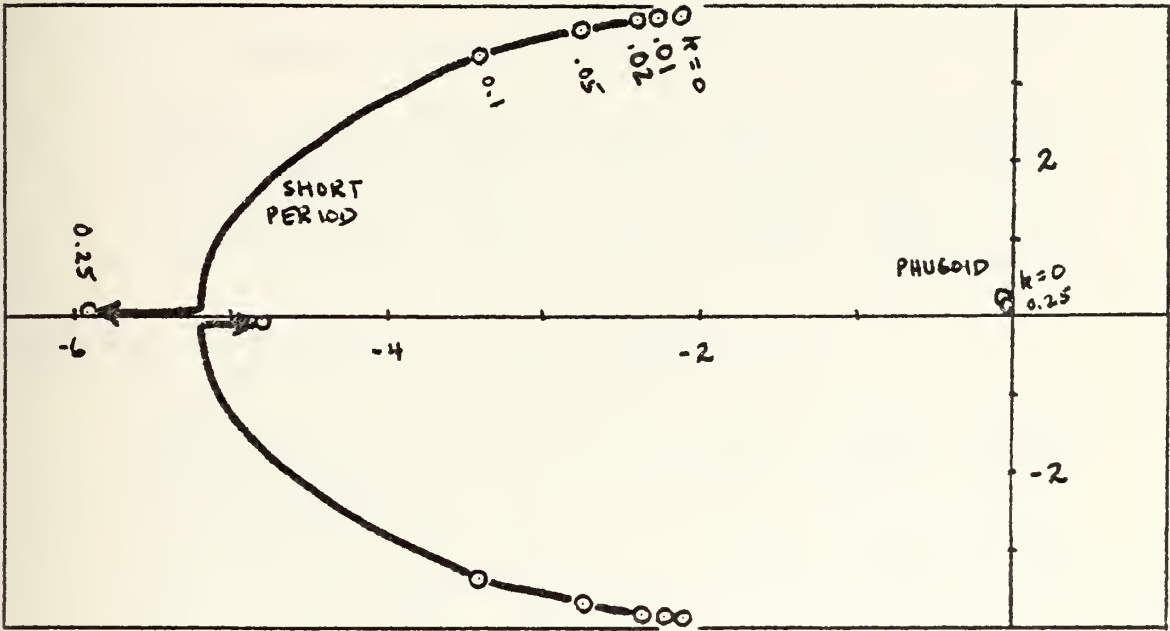
(a)  $k_u$  feedback



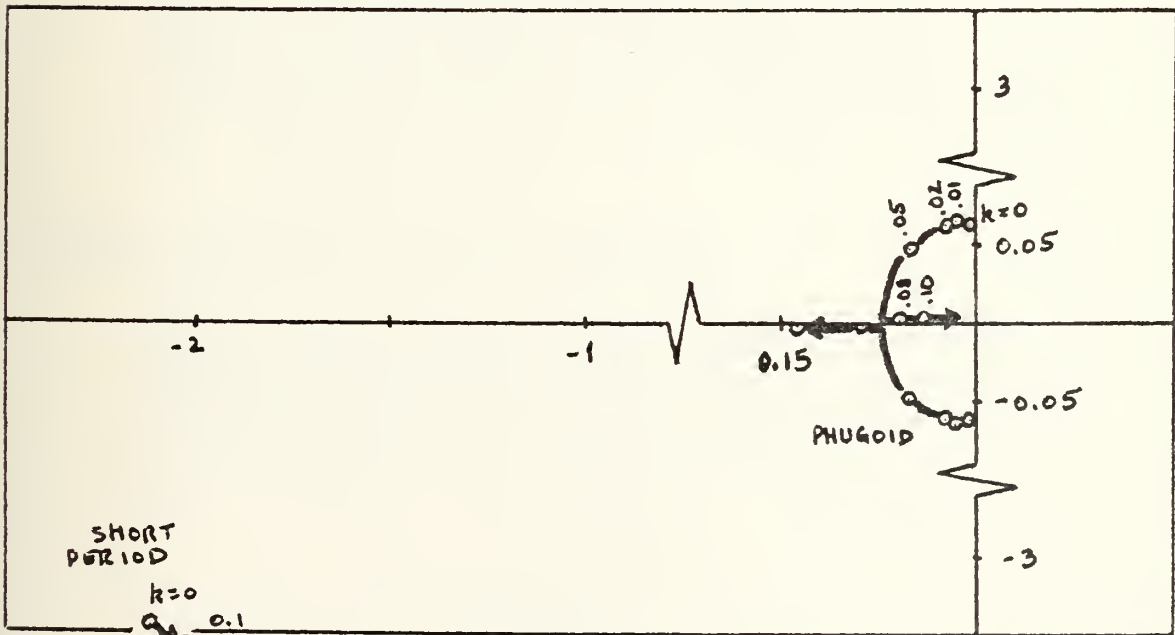
(b)  $k_w$  feedback

Figure 7-9





(c)  $k_q$  feedback



(d)  $k_\theta$  feedback

Figure 7-9 (continued)





Feedback parameter: HORIZONTAL VELOCITY (u)

gain	0	0.002	0.02	0.05	0.075	0.1
T(sp)	1.42	1.44	1.60	1.89	1.67	1.52
$\zeta$ (sp)	0.477	0.475	0.444	0.154	-0.02	-0.10
T(ph)	99.35	17.86	5.16	2.76	2.55	2.43
$\zeta$ (ph)	0.072	0.097	0.297	0.702	0.888	0.980

Feedback parameter: VERTICAL VELOCITY (w)

gain	0	0.001	.00105	.0013	.0015	.003
T(sp)	1.42	1.77	1.65	1.32	1.18	0.78
$\zeta$ (sp)	0.477	1	1	1	1	1
T(ph)	99.35	165.17	75.04	68.11	78.43	89.15
$\zeta$ (ph)	0.072	1	1	0.108	0.082	0.072
T <sub>3</sub>	-	254.69	112.48	-	-	-
$\zeta$ <sub>3</sub>	-	-1	-1	-	-	-
T <sub>4</sub>	-	10.54	20.14	9.56	5.10	1.55
$\zeta$ <sub>4</sub>	-	1	1	-1	-1	-1

Feedback parameter: PITCH RATE (q)

gain	0	0.01	0.02	0.05	0.1	0.25
T(sp)	1.42	1.41	1.40	1.36	1.31	1.31
$\zeta$ (sp)	0.477	0.502	0.526	0.598	0.710	1
T(ph)	99.35	100.25	101.14	103.75	107.97	119.69
$\zeta$ (ph)	0.072	0.072	0.073	0.074	0.076	0.084
T <sub>3</sub>	-	-	-	-	-	1.06
$\zeta$ <sub>3</sub>	-	-	-	-	-	1

Feedback parameter: PITCH ANGLE ( $\theta$ )

gain	0	0.01	0.02	0.05	0.08	0.1
T(sp)	1.42	1.42	1.41	1.39	1.37	1.36
$\zeta$ (sp)	0.477	0.473	0.469	0.456	0.445	0.437
T(ph)	99.35	97.71	96.18	92.16	73.18	45.98
$\zeta$ (ph)	0.072	0.211	0.343	0.702	1	1
T <sub>3</sub>	-	-	-	-	107.12	163.04
$\zeta$ <sub>3</sub>	-	-	-	-	1	1

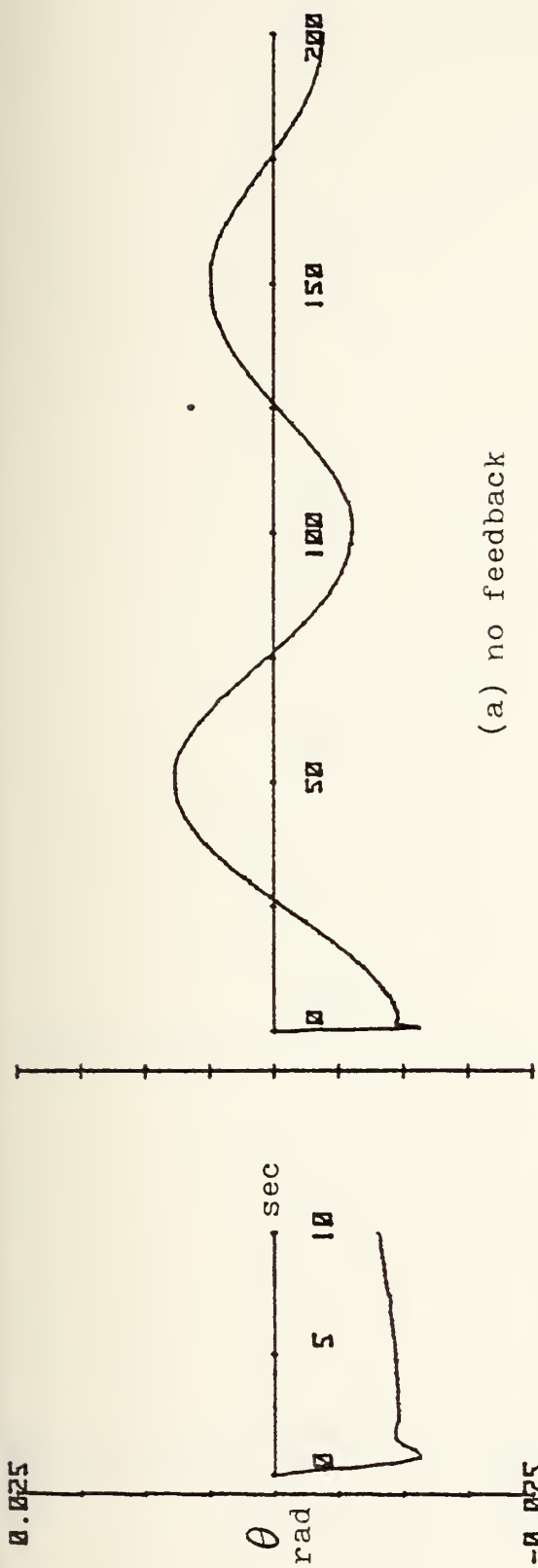
Table 7-4



if the gain is small, will increase the frequency and damping ratio of the short period mode. Since the angle of attack signal is 1/660th of the vertical velocity signal, it would be a better parameter from which to obtain an error signal. Increasing the gain of this feedback will cause a third mode to go unstable; however, its period is so great that no problem would be anticipated in controlling it manually. A further increase in gain will cause a fourth mode of significantly shorter period to go unstable. Since its period decreases rapidly with an increase in gain, it may be assumed that values of gain in this region are to be avoided. Figure 7-10 (c) shows a time history of pitch angle versus time with  $k_w = 0.0001$  and  $w_0 = 10\text{fps}$ .

Feedback of pitch rate has almost no effect upon the phugoid motion but appreciably increases the short period damping. This very desirable feature makes this parameter useful in speed, altitude, and attitude hold modes for auto-pilots. Figure 7-10(d) shows a time history of pitch angle against time with  $k_q = 0.1$  and  $w_0 = 10\text{fps}$ .

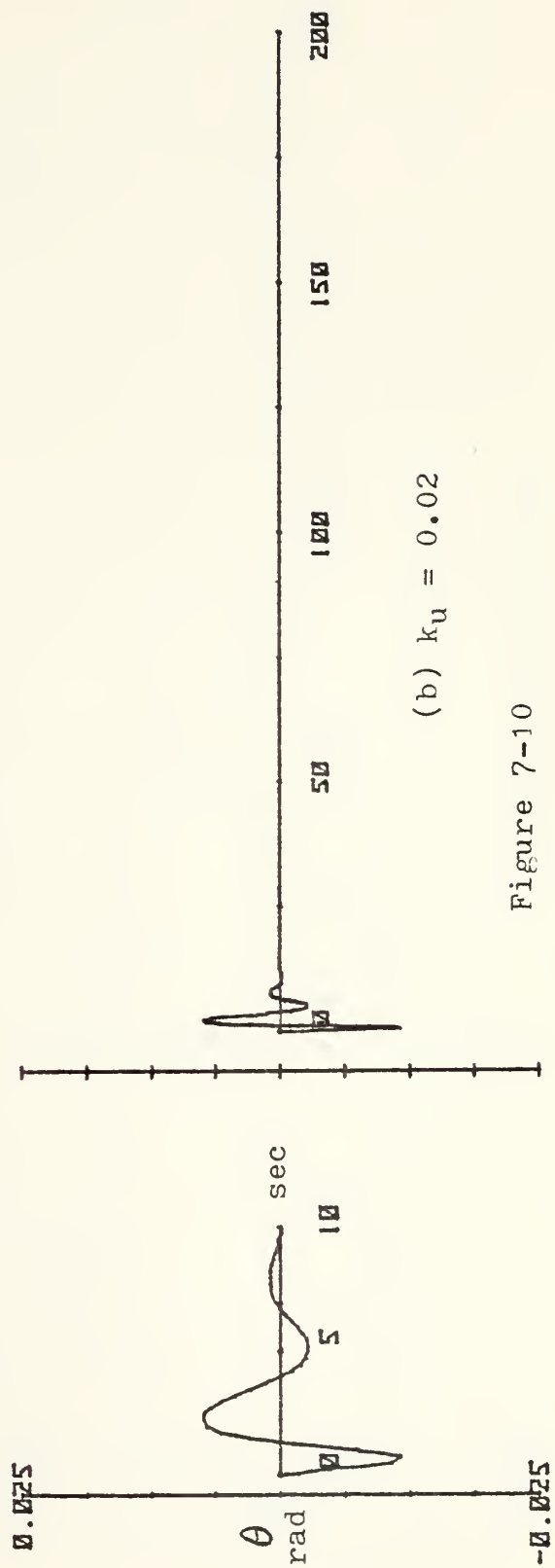




(a) no feedback

phugoid

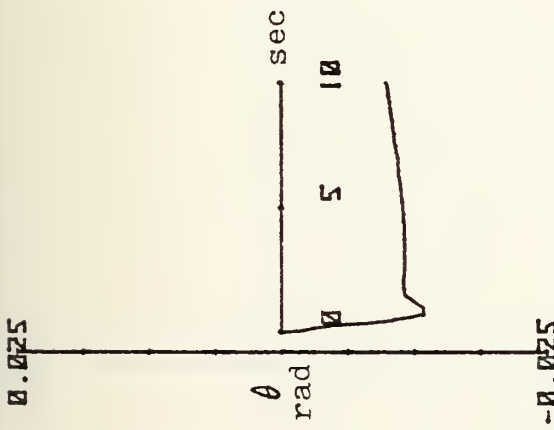
short period



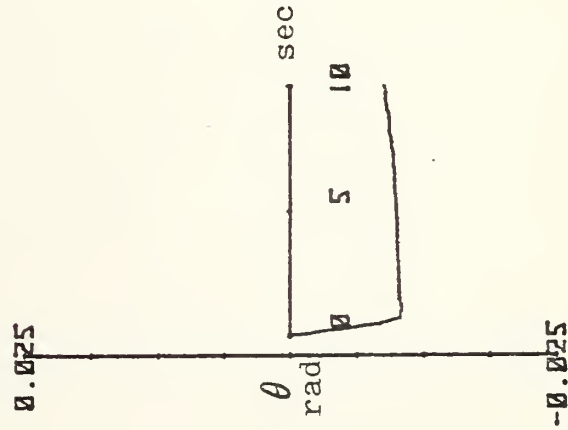
(b)  $k_u = 0.02$

Figure 7-10





short period



phugoid

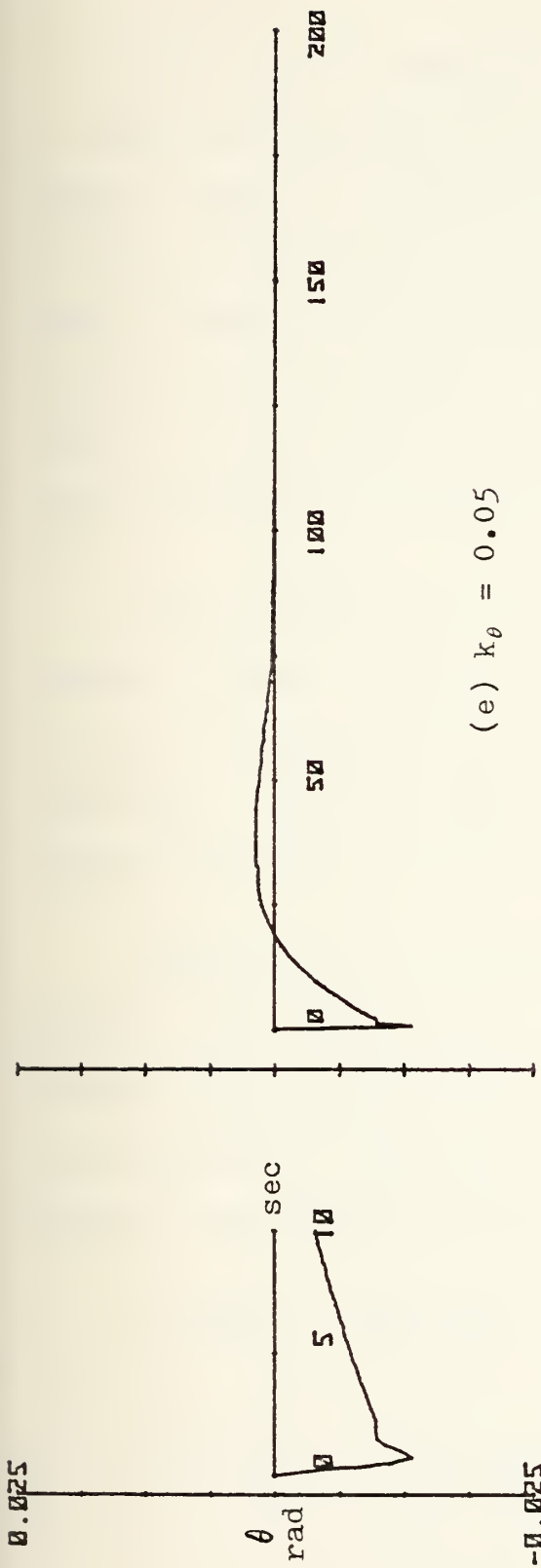
(c)  $k_w = 0.0001$

(d)  $k_q = 0.02$

Figure 7-10 (continued)



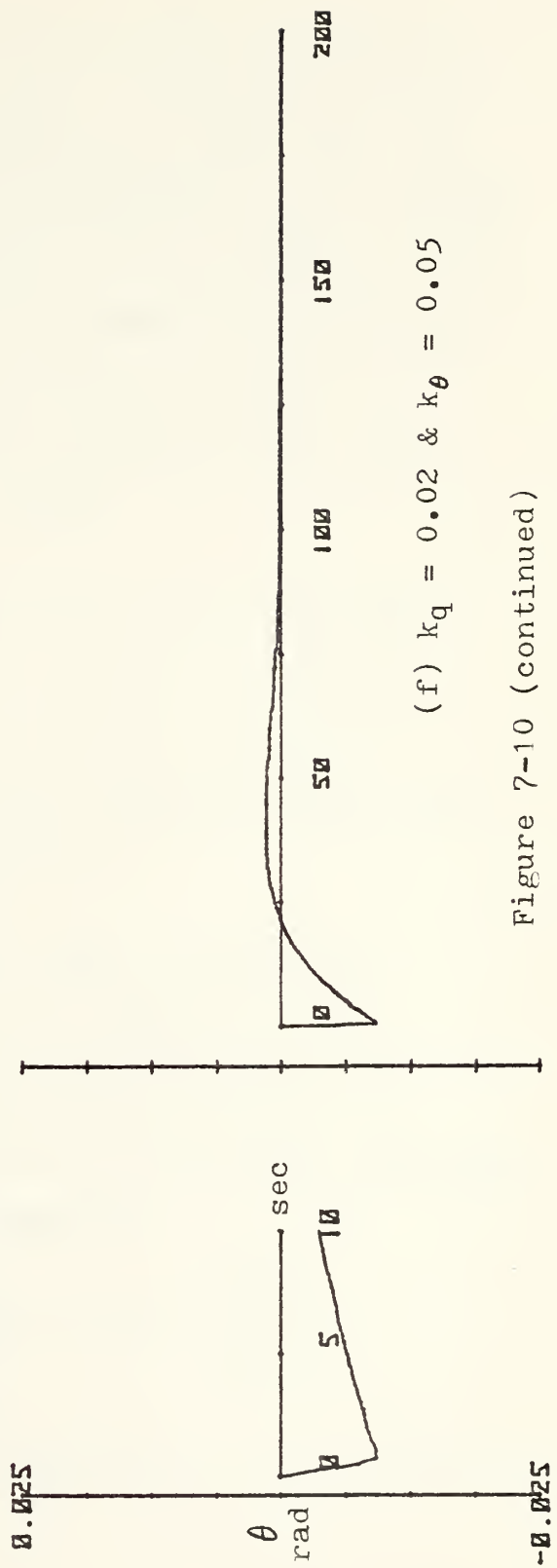




(e)  $k_{\theta} = 0.05$

phugoid

short period



(f)  $k_q = 0.02$  &  $k_{\theta} = 0.05$

Figure 7-10 (continued)



Pitch angle feedback is also an excellent method of improving longitudinal response. In this case, the phugoid damping is significantly increased at the expense of short period damping. If short period damping is marginal to begin with, use of this feedback may cause an instability in that mode. Figure 7-10(e) shows the effects of  $k_\theta = 0.05$  on the time history of the pitch angle perturbations with  $w_0 = 10\text{fps}$ .

Use of both pitch rate and pitch angle feedback together should provide an ideal system with maximum increase in damping ratios and minimum increase in frequency. Using the same feedback gains as above, the response is shown in Figure 7-10(f).

The equations of state for each of the above examples were obtained by entering BASMAT with the modified plant matrix  $[A - \underline{b}\underline{k}^T]$  and multiplying the resulting state transition matrix by the initial condition vector in accordance with the equation

$$\underline{\dot{x}}(t) = \Phi(t)\underline{x}(0) \quad \text{where} \quad \underline{x}(0) = \begin{Bmatrix} 0 \\ 10 \\ 0 \\ 0 \end{Bmatrix}.$$

One further conclusion was reached in this treatment



of feedback: the two parameters which are most affected in phugoid motion, forward velocity and pitch angle, were the two whose feedback most affected that motion. Their effect on the short period was minimal. Likewise, the two parameters which are relatively constant in the phugoid but which vary considerably in the short period, angle of attack and pitch rate, had little effect on the phugoid but significantly damped the short period.



## VIII. THE ORBITER

The Aerodynamic Design Data Book was obtained from NASA's Lyndon B. Johnson Space Center in order to obtain data necessary to calculate the stability derivatives and to acquire the block diagram of the longitudinal control system (automatic mode) of the space shuttle orbiter.

The environment chosen for the study was the area at which the Mach number was 1.05. This area was chosen because the aerodynamics are undergoing rapid change here, and it would provide a testing challenge for programming and solution.

The stability derivatives were found by plotting the force and moment coefficients with respect to velocity ( $U$ ) and angle of attack and then measuring the slope; see Figures 8-1 through 8-6. By choosing points close together where the slope was rapidly changing, piecewise linearity could be assumed between them. The results are shown in Table 8-1. The derivatives with respect to  $\delta_e$  were also taken from the publication; the graph of  $\Delta C_{D_e}$  -vs-  $\delta_e$  is shown, as an example, in Figure 8-7. The  $\delta_e$  derivatives are listed in Table 8-2.





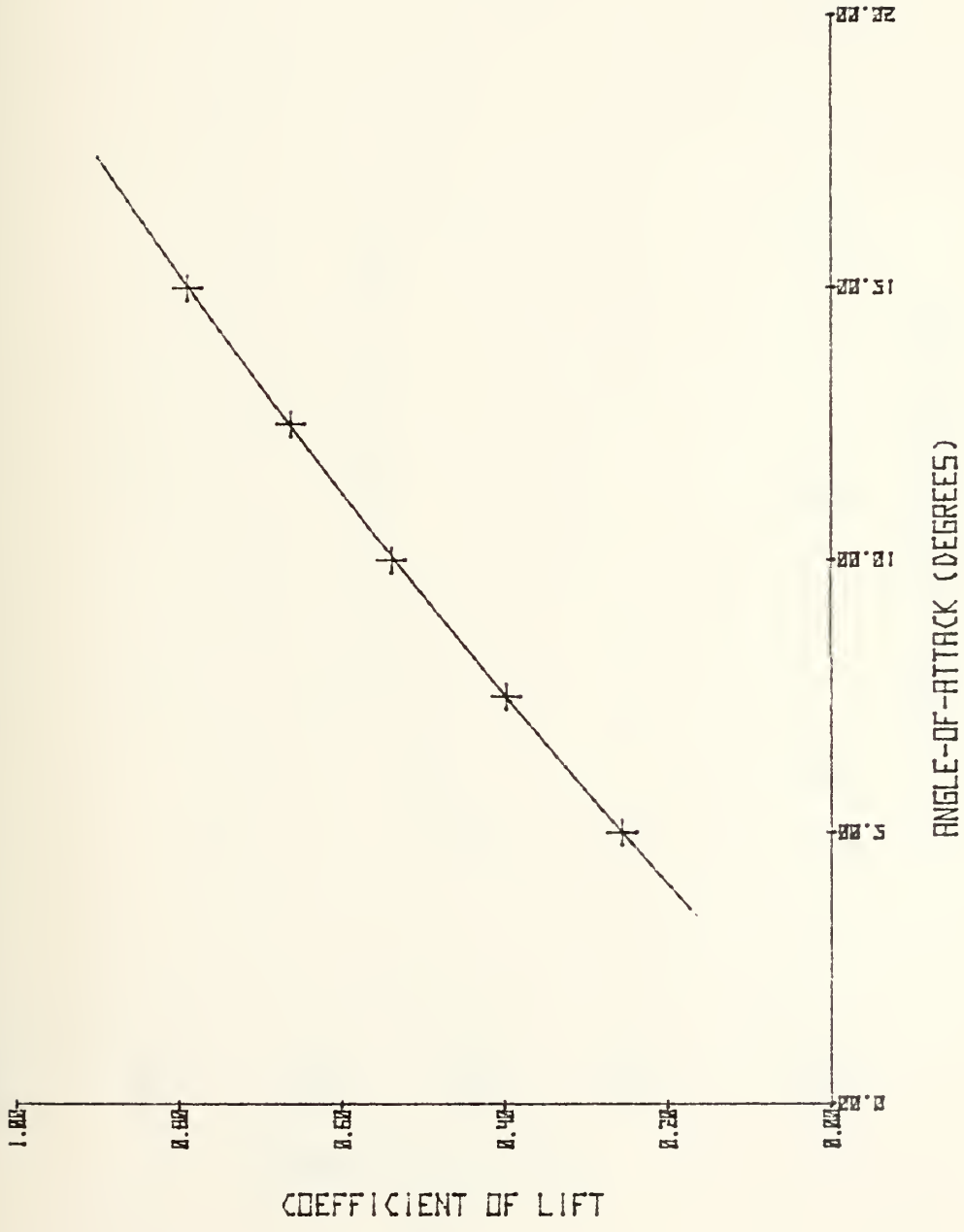
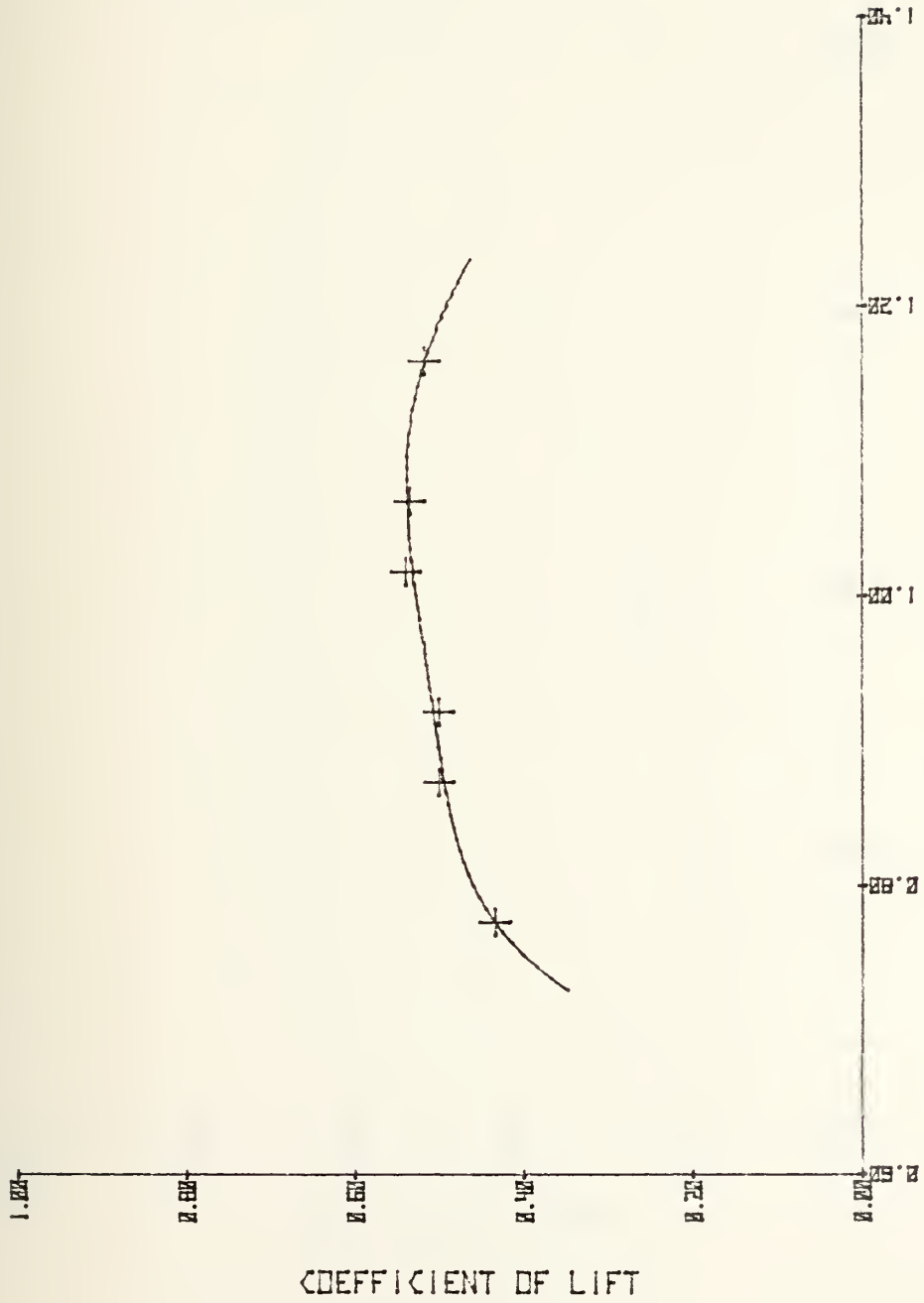


Figure 8-1

AOA --VS-- COEFF OF LIFT (MACH=1.05)





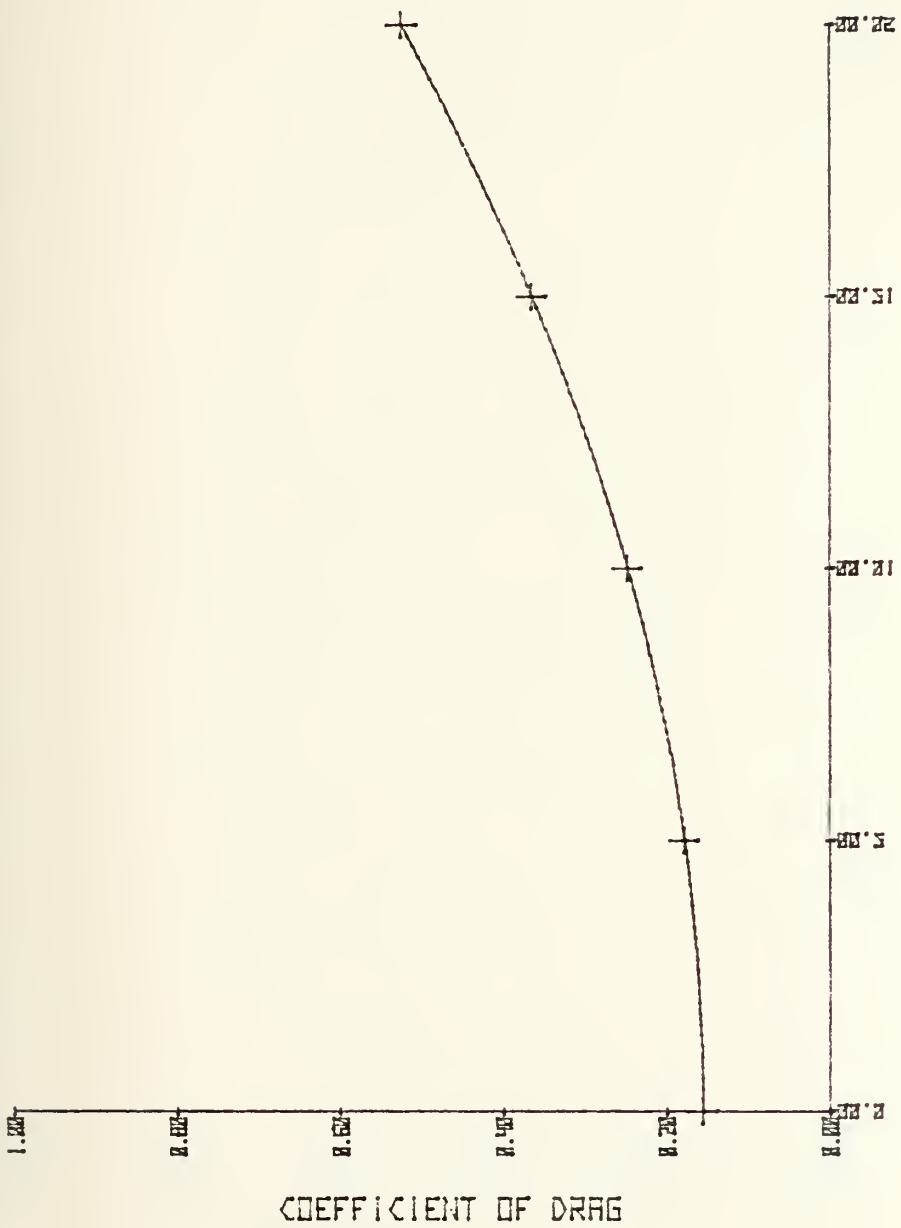
MACH	VEL (FPS)	$C_L$
0.80	774.8	0.434
0.90	871.6	0.500
0.95	920.0	0.500
1.05	1016.9	0.539
1.10	1065.3	0.534
1.20	1162.2	0.517

HORIZ. VELOCITY (FPS) X 10<sup>3</sup>

Figure 8-2

VEL - VS - COEFF OF LIFT (AOA = 10 DEG)





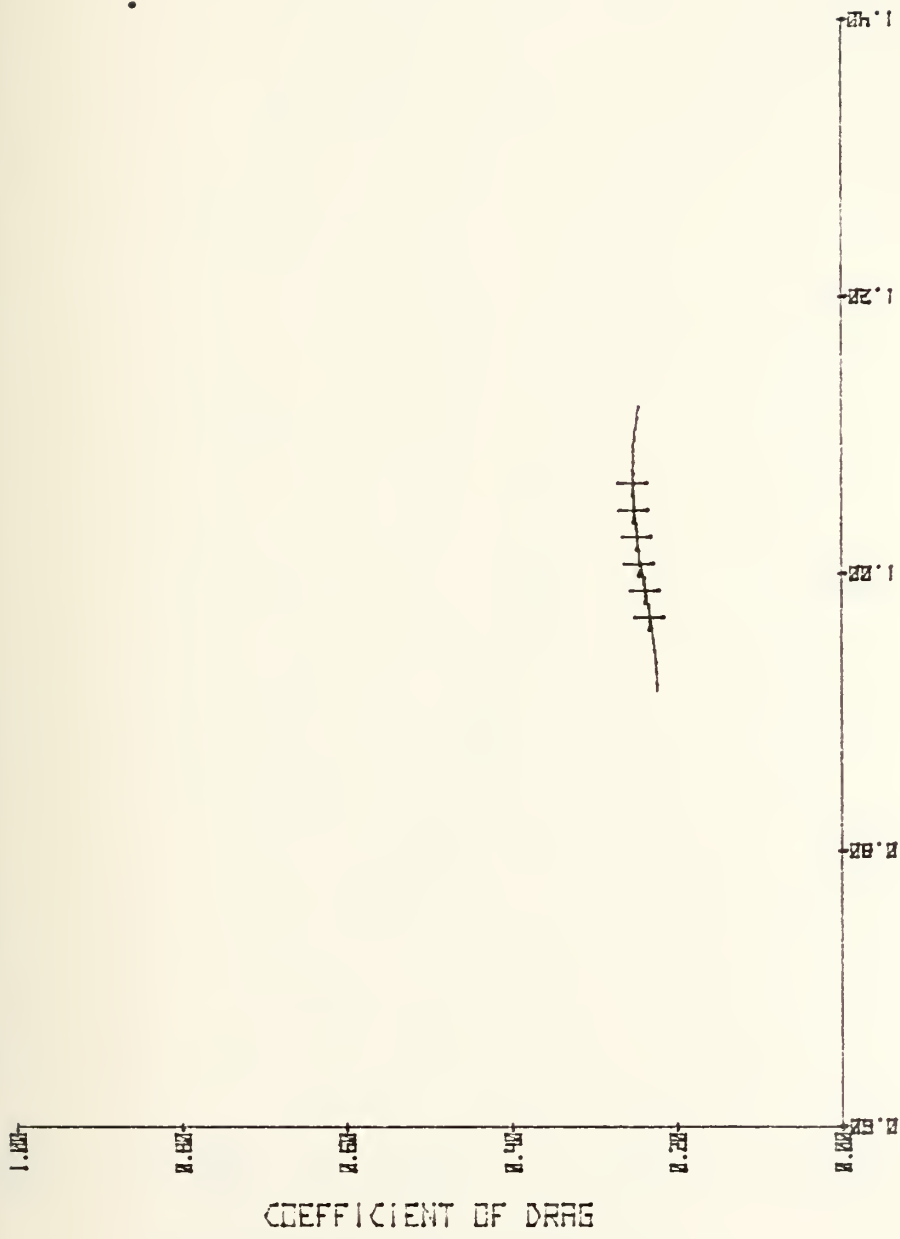
AOA (DEG)	$C_D$
0	0.156
5	0.179
10	0.248
15	0.365
20	0.525

ANGLE-OF-ATTACK (DEGREES)

Figure 8-3

AOA -VS- COEFF OF DRAG (MACH=1.05)





MACH	VEL (FPS)	$C_D$
1.00	968.5	0.233
1.02	987.8	0.238
1.04	1007.2	0.245
1.06	1026.6	0.248
1.08	1045.9	0.252
1.10	1065.3	0.253

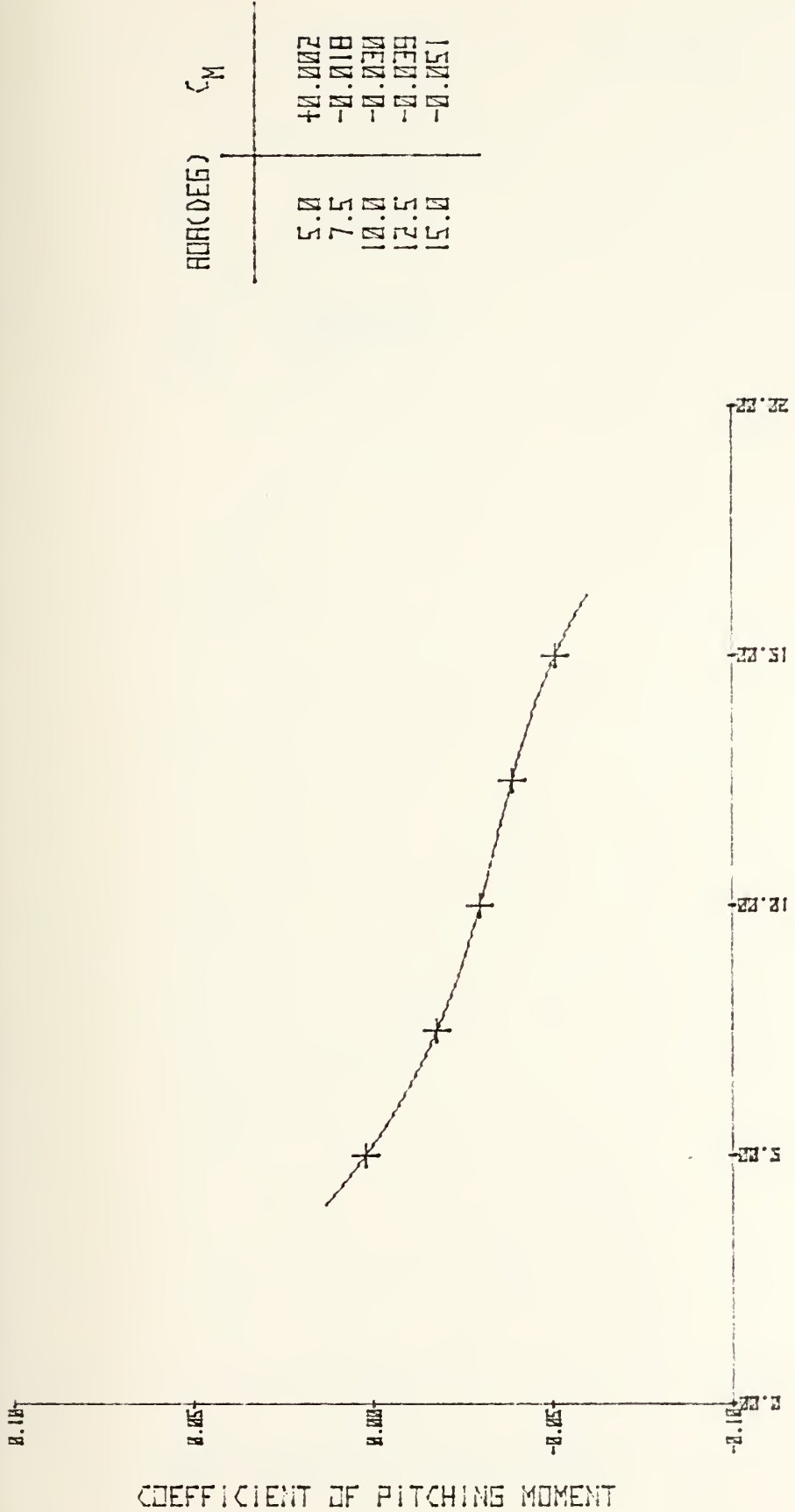
HORIZ. VELOCITY (FPS) X 10<sup>3</sup>

Figure 8-4

VEL. VS. COEFF OF DRAG (AOA = 10 DEG)







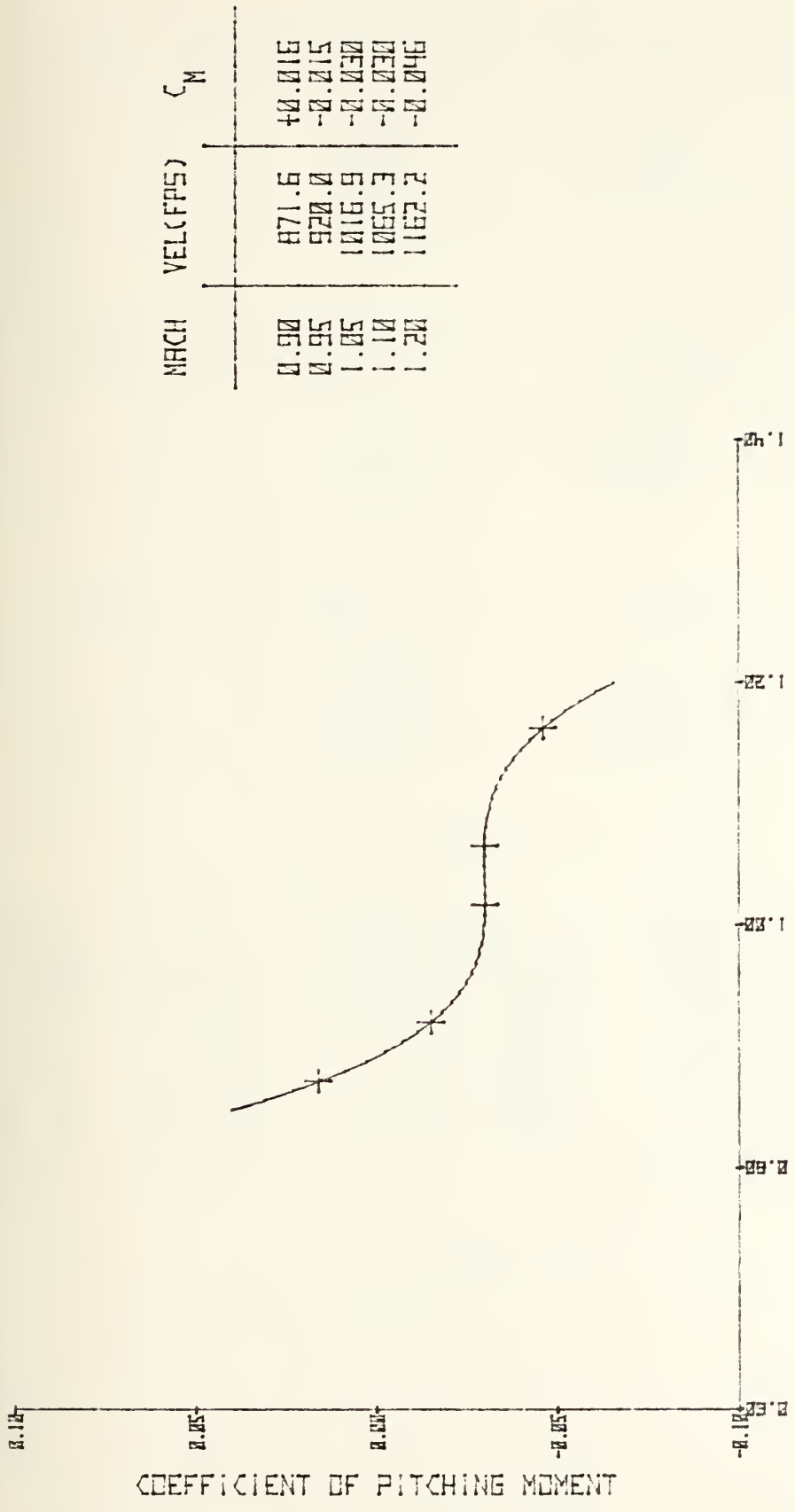
ROA(DEG)	C <sub>M</sub>
5.0	0.002
7.5	0.018
10.0	0.039
12.5	0.059
15.0	0.074

ANGLE-OF-ATTACK (DEGREES)

Figure 8-5

ROA --VS-- PITCHING MOMENT COEFF (MACH=1.05)





HORIZ. VELOCITY (FPS) X 10<sup>3</sup>

Figure 8-6

VEL -VS- PITCHING MOMENT COEFF. (AOA=10 DEG)



AOA (deg)	$C_{L\alpha}$
5	0.0564
7.5	0.0564
10	0.0528
12.5	0.0500
15	0.0500

U (fps)	$C_{L_u}$
920.1	0.0
1016.9	7.23E-4
1065.3	-1.24E-4
1162.2	-1.75E-4

AOA (deg)	$C_{D\alpha}$
5	0.0046
10	0.0138
15	0.0234
20	0.0320

U (fps)	$C_{D_u}$
968.5	5.79E-4
1016.9	3.10E-4
1065.3	1.24E-4
1113.7	-2.10E-5

AOA (deg)	$C_{M\alpha}$
7.5	-0.0080
10	-0.0048
12.5	-0.0036
15	-0.0048

U (fps)	$C_{M_u}$
920.1	-6.40E-4
1016.9	-1.55E-4
1065.3	0.0
1162.2	-1.65E-4

Table 8-1

$\delta_e$	$C_{L\delta_e}$
-20°	0.0057
-17.5	0.0072
-15	0.0076
-10	0.0086
0	0.0108
20	0.0142

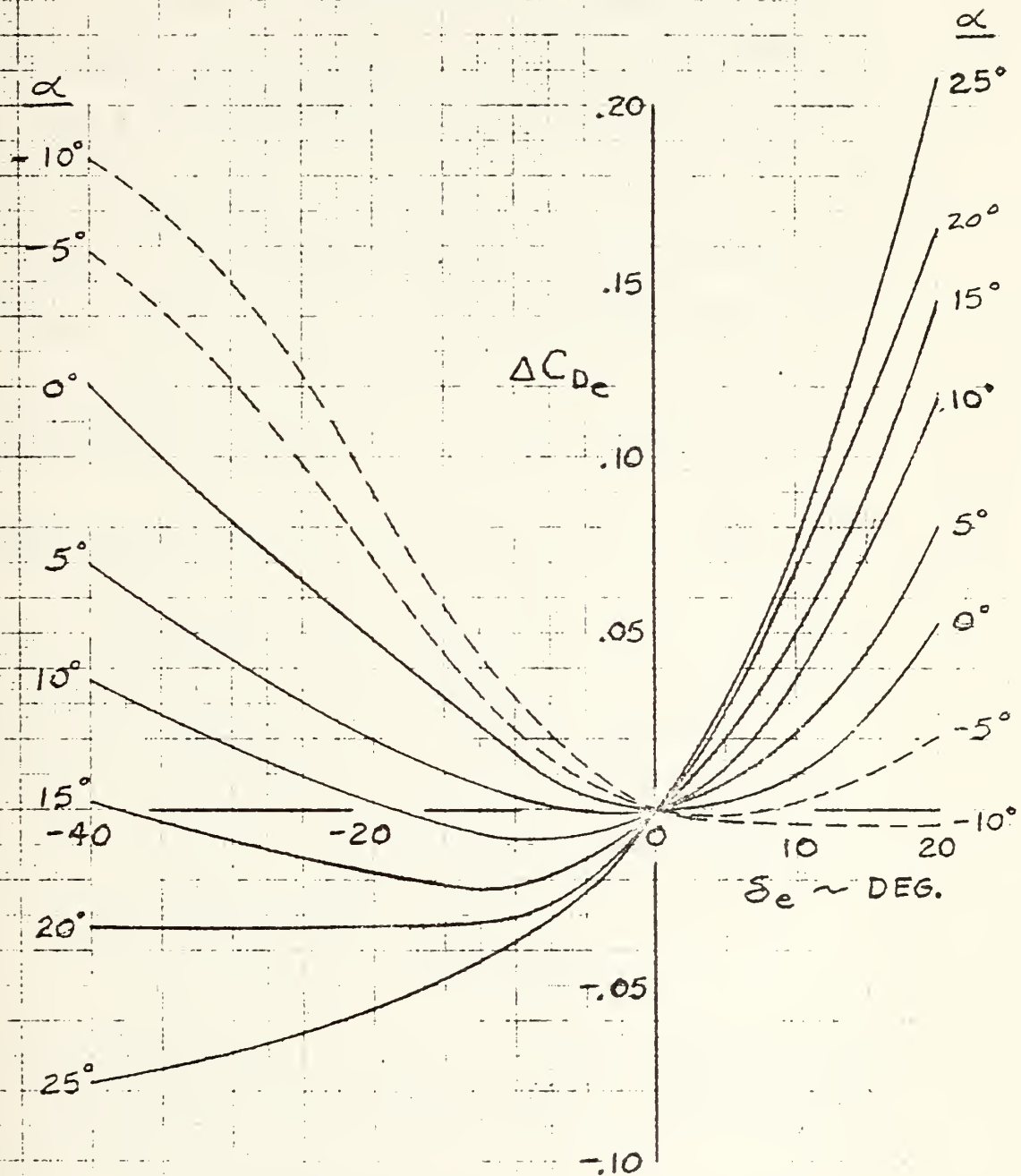
$\delta_e$	$C_{D\delta_e}$
-25°	-0.0018
-20	-0.0014
-15	-0.0012
-10	0.0024
-5	0.0050
0	0.0080

$\delta_e$	$C_{M\delta_e}$
-30°	-0.0010
-25	-0.0016
-20	-0.0026
-15	-0.0042
-10	-0.0058
0	-0.0067
20	-0.0089

Table 8-2



$M_\infty = 1.05$



$S_{REF} = 2690 \text{ FT}^2$

Fig 3.5-11. ELEVON EFFECTIVENESS DRAG INCREMENT ( $M_\infty = 1.05$ )

Figure 8-7





In cases where U was the independent variable, angle of attack was assumed to be  $10^\circ$ ; where angle of attack was the independent variable, U was 1016.9 fps (Mach = 1.05). The  $\delta_e$  derivatives were based upon an angle of attack of  $10^\circ$ .

The point in the design reentry trajectory where the Mach number is 1.05 occurs at approximately 62000 feet in altitude. Also, at this point, the load factor  $n_z = 1.09$ , and the air density  $\rho = 2.0325E-4$  slugs/ft<sup>3</sup>.

Other constants which are required for computations are:

$$\text{wing area} = S = 2690 \text{ ft}^2$$

$$\text{wing M.A.C.} = \bar{c} = 39.56 \text{ ft}$$

$$\text{moment of inertia} = I_y = 5.7830E+6 \text{ slug-ft}^2$$

$$\text{gravity} = g = 32.073 \text{ ft/sec}^2 \text{ (corrected for altitude and latitude)}$$

$$\text{pitch angle} = \Theta = 9.0 \text{ deg}$$

$$\text{mass} = m = 5839 \text{ slugs}$$

For the condition of Mach = 1.05 and angle of attack =  $10^\circ$ , the stability derivatives take on the following values:

$$X_u = \frac{\rho U S}{m} \left( -\frac{U}{2} C_{D_u} - C_D \right) = -0.04410$$



$$X_w = \frac{\rho U S}{2m} (C_L - C_{D\alpha}) = 0.02849$$

$$X_g = X_w = \emptyset$$

$$X_{\delta e} = -\frac{\rho U^2 S}{2m} C_{D\delta e} = -0.44219$$

$$Z_u = \frac{\rho U S}{m} \left(-\frac{U}{2} C_{Lu} - C_L\right) = -0.09845$$

$$Z_w = \frac{\rho U S}{2m} (-C_{L\alpha} - C_D) = -0.01635$$

$$Z_g = Z_w = \emptyset$$

$$Z_{\delta e} = -\frac{\rho U^2 S}{2m} C_{L\delta e} = -0.78489$$

$$M_u = \frac{\rho U S \bar{c}}{I_y} \left(\frac{U}{2} C_{Mu} + C_M\right) = -4.725 E-4$$

$$M_w = \frac{\rho U S \bar{c}}{2 I_y} C_{M\alpha} = -1.042 E-5$$

$$M_g = \frac{\rho U S \bar{c}^2}{4 I_y} C_{Mg} = -0.05583$$

$$M_{\dot{w}} = \frac{\rho S \bar{c}^2}{4 I_y} C_{M\dot{\alpha}} = -4.223 E-5$$

$$M_{\delta e} = \frac{\rho U^2 S \bar{c}}{2 I_y} C_{M\delta e} = -0.01479$$



Entering these values into the plant matrix (see page 54) yields

$$[A] = \begin{bmatrix} -0.04410 & 0.02849 & 0.0 & -32.073 \\ -0.09845 & -0.01635 & 1016.9 & 0.0 \\ -4.683E-4 & -9.730E-6 & -0.09877 & 0.0 \\ 0.0 & 0.0 & 1.0 & 0.0 \end{bmatrix}$$

$$\{B\} = \begin{Bmatrix} -0.44219 \\ -0.78489 \\ -0.01476 \\ 0.0 \end{Bmatrix}$$

Entering BASMAT with  $[A]$  yields the results shown in Figure 8-8. Using the GRAPH program developed in Chapter VI (see page 71), the time response to an initial condition of  $w_0 = 10$  fps was plotted. The results are shown in Figure 8-9. The vehicle is clearly unstable in the open-loop configuration.

A look at the eigenvalues printed out in Figure 8-8 showed that the phugoid had disappeared, being replaced by two real roots, one of which was positive. Although the negative (stable) root was larger, the instability became dominant very quickly.

The eigenvalues were not widely separated, having



\*\*\*\*\*

THE A MATRIX

```

-4.1099999E-02      2.8489999E-02      0.0000000E+00      -5.2072999E  01
-9.8449945E-02     -1.0349997E-02      1.0101999E  03      0.0
-4.6829996E-04     -9.7299999E-06      -9.8799999E-02      0.0
  0.0                0.0                1.0000000E+00      0.0
  
```

THE DETERMINANT OF THE MATRIX

-2.1435006E-04

THE INVERSE OF THE MATRIX

```

-1.3113022E-06      1.4544937E  00      -2.8497419E  03      -1.7181243E  05
 1.5258789E-05     -6.9998999E  01      1.4090144E  04      7.2541188E  04
 2.5283664E-10      9.3122257E-11     -1.7601593E-07      9.9999993E-01
-3.1178858E-02     -0.5995971E-02     1.6338553E  04      6.0039674E  01
  
```

\*\*\*\*\*

THE MATRIX COEFFICIENTS OF THE HUFFALO OF THE RESOLVED MATRIX

THE MATRIX COEFFICIENT OF S\*\*5

```

1.0000000E  00      0.0000000E  00      0.0000000E  00      0.0000000E  00
 0.0000000E  00      1.0000000E  00      0.0000000E  00      0.0000000E  00
 0.0000000E  00      0.0000000E  00      1.0000000E  00      0.0000000E  00
 0.0000000E  00      0.0000000E  00      0.0000000E  00      1.0000000E  00
  
```

Figure 8-8





THE MATRIX COEFFICIENT OF S\*\*2

1.1511915E-01	2.845990E-02	0.0	-3.267290E-01
-9.8445945E-02	1.598055E-01	1.01E-09E-03	0.0
-4.682990E-04	-9.729999E-01	5.766000E-02	0.0
0.0	0.0	1.000000E-01	1.5121996E-01

THE MATRIX COEFFICIENT OF S\*\*1

1.1509518E-02	4.5130520E-03	-5.3015720E-04	-3.131417E-00
-4.550361E-01	4.0594414E-03	4.1791510E-01	3.1575442E-00
-1.0967794E-04	-1.3741709E-05	3.4709179E-02	1.510782E-02
-4.6629996E-04	-9.729999E-01	5.766000E-02	1.9145584E-02

THE MATRIX COEFFICIENT OF S\*\*0

0.0	5.1207013E-04	-5.245120E-04	-3.0913830E-01
1.4901101E-08	-1.5819780E-02	5.1579705E-00	1.5515618E-01
7.9100756E-13	2.7264841E-12	-2.5215104E-11	2.1406683E-04
-0.6937764E-00	-1.3741709E-05	3.4709179E-02	1.5317601E-02

\*\*\*\*\*

THE CHARACTERISTIC POLYNOMIAL - IN ASCENDING POWERS OF S

-2.1415308E-04	-7.0238113E-04	1.045591E-01	1.5691960E-01	1.000000E-01
----------------	----------------	--------------	---------------	--------------

\*\*\*\*\*

THE EIGENVALUES OF THE A MATRIX  
REAL PART                      IMAGINARY PART

0.3461827E-02	0.0
-0.5664649E-02	-1.4255620E-01
-0.5604648E-02	1.4255620E-01
-1.0205231E-01	0.0

Figure 8-8 (continued)



\*\*\*\*\*

THE ELEMENTS OF THE STATE TRANSITION MATRIX

THE MATRIX COEFFICIENT OF EXP(-0.56113E-02)T

2.9041117E-01      9.2157105E-02      -5.6733201E-01      -1.1135905E-02  
 -5.1610166E-06      -1.6167375E-01      1.0091791E-03      1.9566219E-03  
 -6.7340702E-04      -1.5024759E-04      1.5770512E-01      1.6155420E-01  
 -5.6666531E-03      -1.7965300E-03      1.0054701E-00      2.1760131E-00

THE MATRIX COEFFICIENT OF EXP(-0.810405E-02)T\*OS( 1.425703E-01)T

4.4712102E-01      -1.1317804E-02      4.5250740E-01      2.8353973E-01  
 1.7389830E-01      -1.1615091E-01      0.5015479E-02      1.8565322E-03  
 -5.1808224E-04      4.7726633E-04      0.5603100E-01      -5.1322830E-01  
 1.6661658E-02      -1.3867556E-03      1.4353400E-01      2.0004153E-00

THE MATRIX COEFFICIENT OF EXP(-0.106400E-02)T\*OP( 1.025303E-01)T

-5.4532409E-02      8.2133114E-02      1.1001740E-02      -8.0481900E-01  
 1.3415012E-00      2.8958374E-00      4.7473477E-03      -3.0004505E-03  
 -2.5261822E-03      1.4124014E-05      -3.3033321E-01      -1.1469591E-01  
 5.5760868E-03      2.0799231E-03      4.5117924E-00      -2.0009725E-00

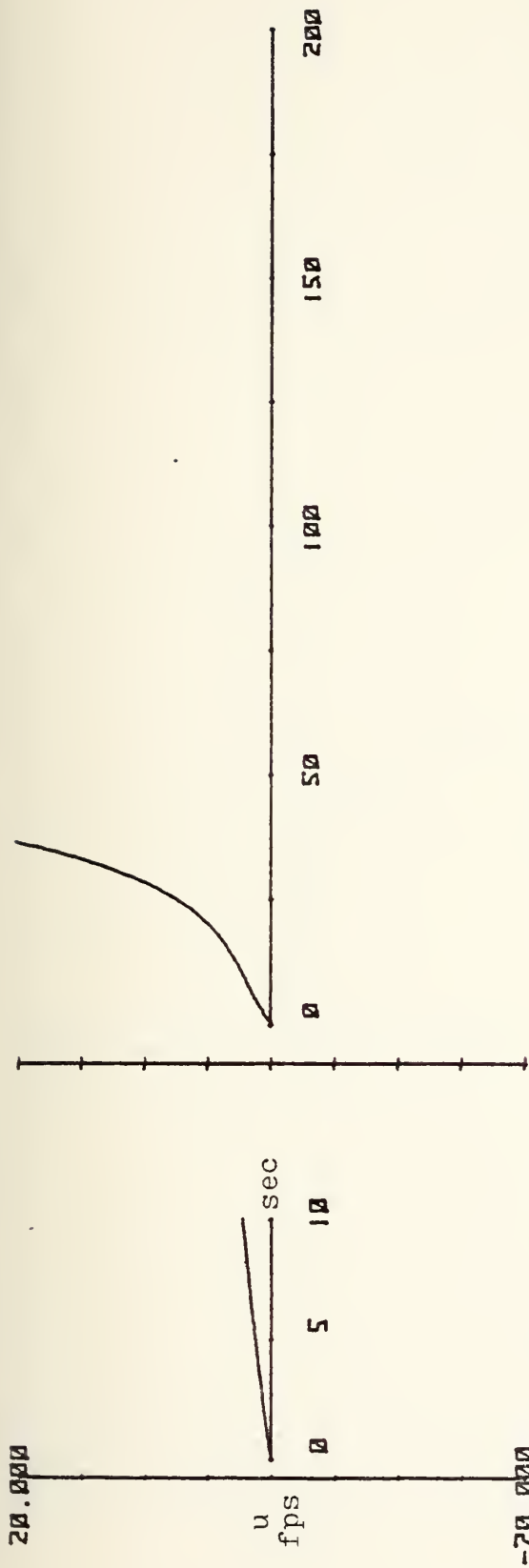
THE MATRIX COEFFICIENT OF EXP(-1.03023E-01)T

2.0246972E-01      -8.6059034E-02      5.1909470E-01      0.2005000E-01  
 -1.2208820E-01      3.7603045E-00      -2.591224E-03      -3.814552E-03  
 1.0615524E-03      -3.205700E-04      2.0001600E-01      5.310760E-01  
 -1.8341210E-02      5.1056071E-03      -2.0001600E-01      -3.2316371E-00

CP

Figure 8-8 (continued)





short period

phugoid

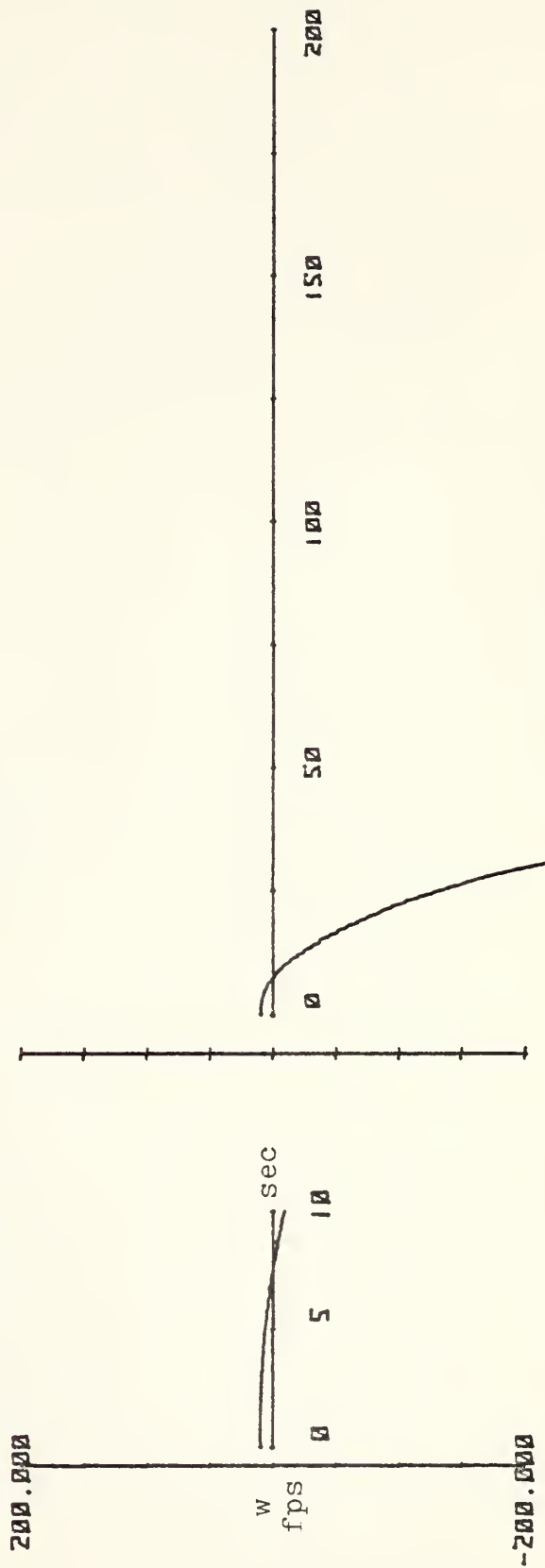
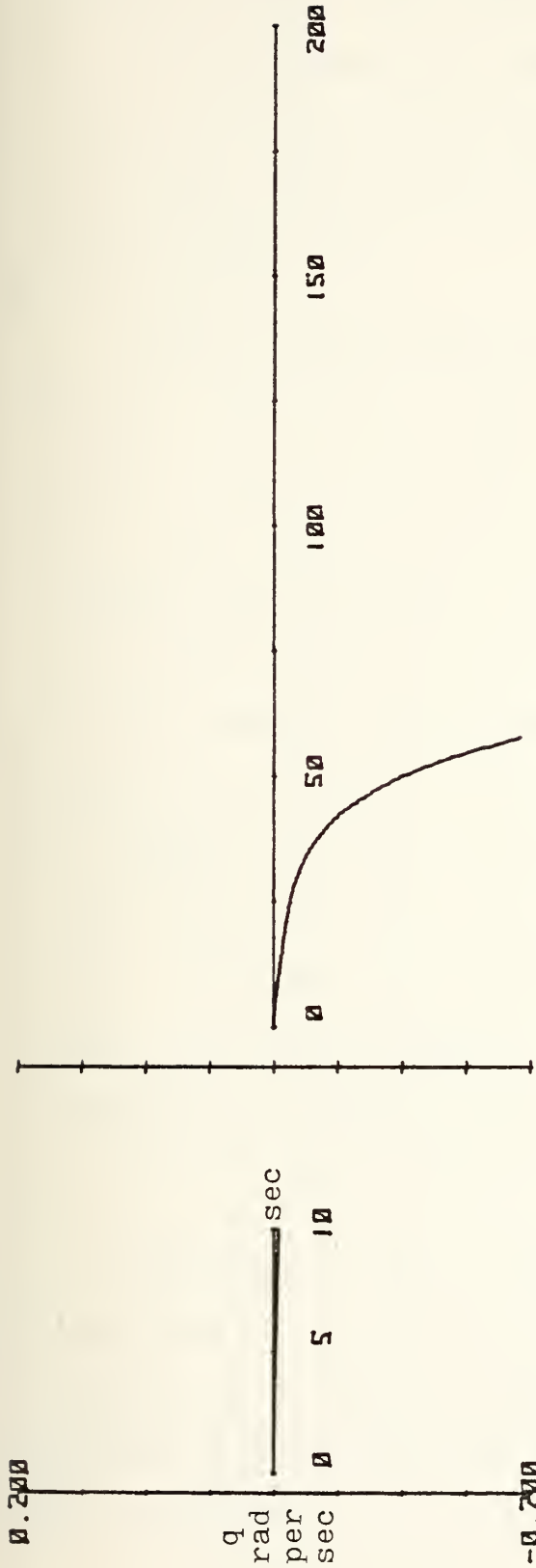


Figure 8-9





phugoid

short period

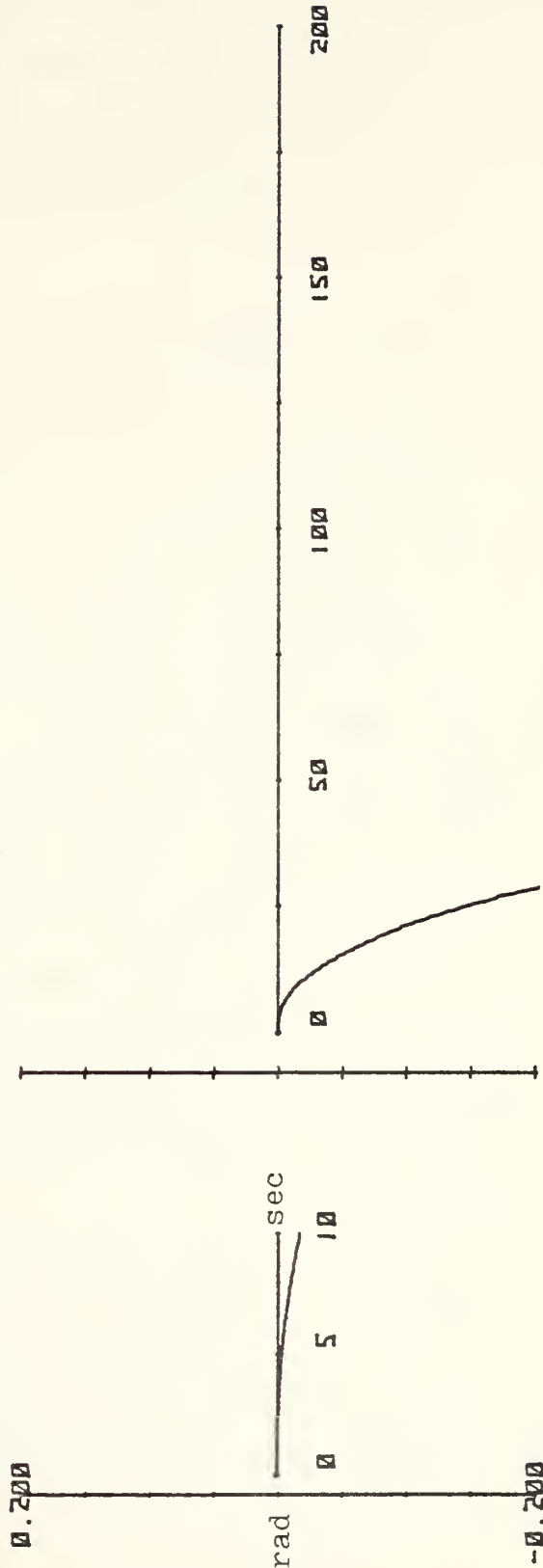


Figure 8-9 (continued)





periods of 75.1, 61.2, and 39.7 seconds, respectively, so the short period was effectively missing as well. Although its theoretical damping ratio was 0.4337, it was completely suppressed by the instability of the positive real root.

It was obvious that some form of feedback network would be necessary so that the stability of the vehicle would be more in line with that of conventional aircraft. And, since the orbiter was designed to fly at the very extremes of atmospheric conditions, the system would necessarily depend upon many parameters, among them dynamic pressure, Mach number, true airspeed, load factor (which is a function of  $C_L$ ), pitch angle and rate, angle of attack, and elevon deflection angle. Other factors could have been used, e.g., vertical velocity, descent angle, to name a few, but the ones chosen appeared to be those most easily obtainable and from which other necessary information could be computed. The end result of the engineering design is shown in Figure 8-10.

In order to solve the equations of motion as they were modified by the various gains, feedbacks, lead-lag elements, and limits, the Continuous System Modeling Program (version III), as incorporated on the IBM360, was utilized.



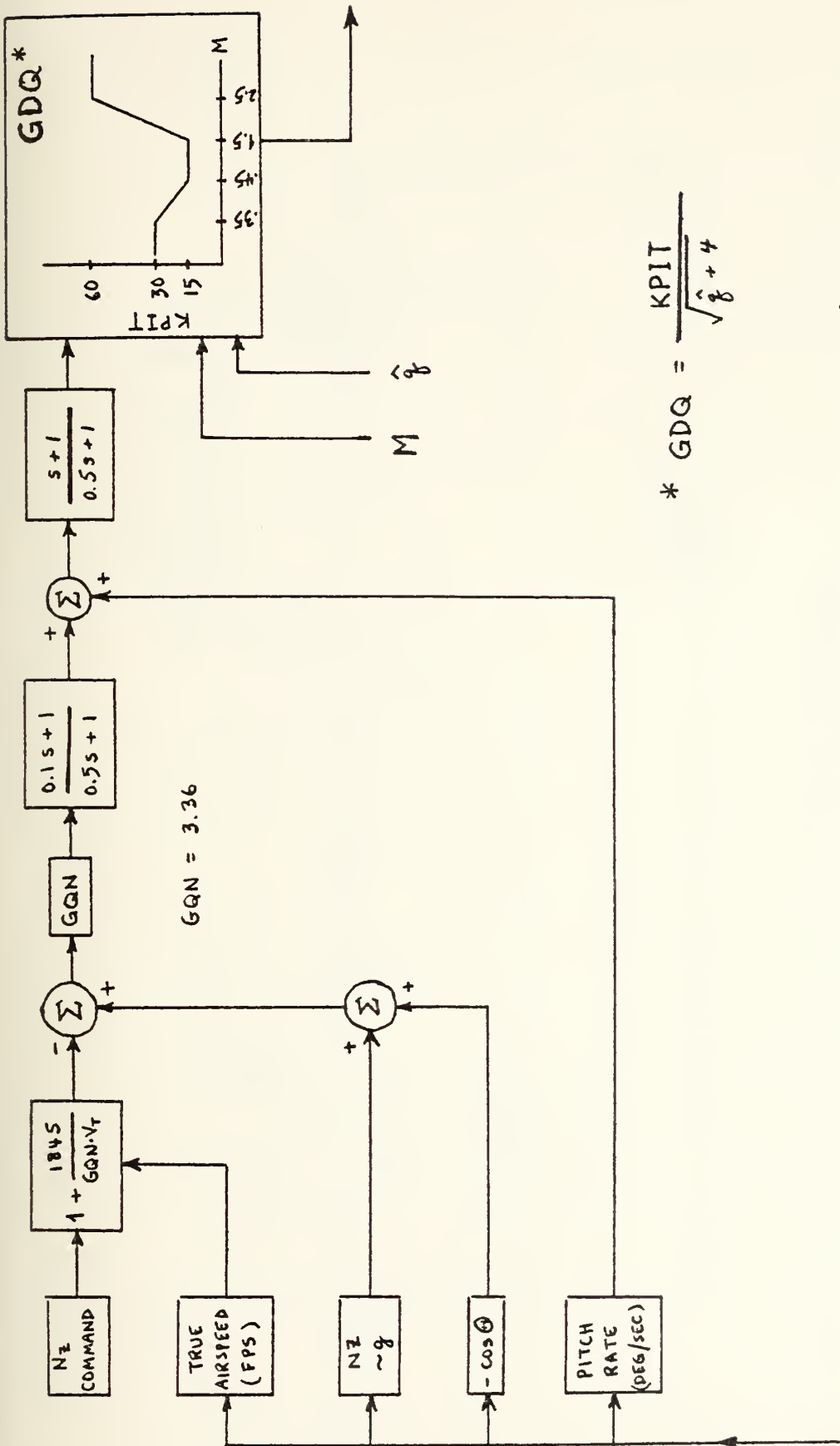


Figure 8-10



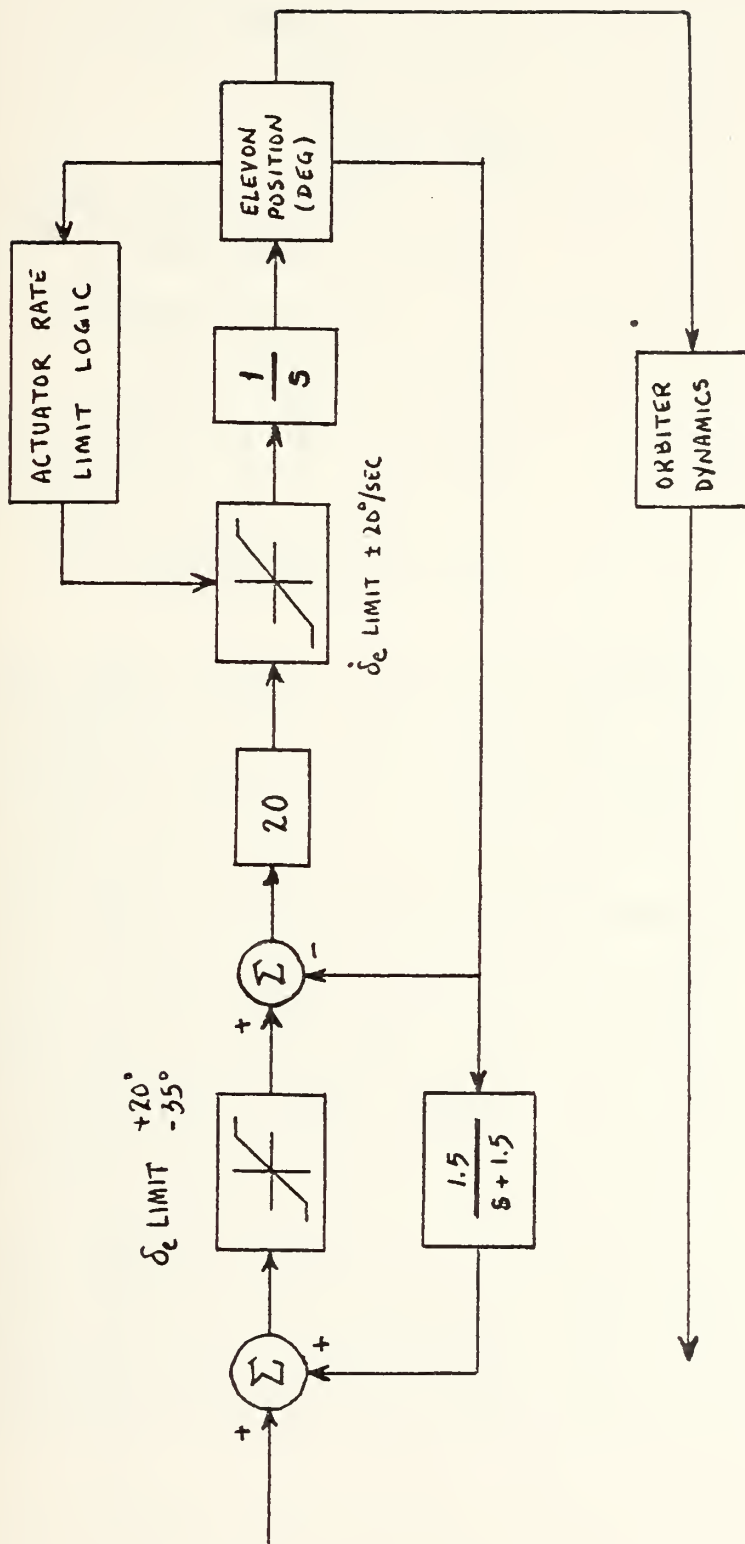


Figure 8-10 (continued)



The system variables were assigned names as follows:

$N_z$  command = GCMD

true airspeed = U1

$N_z \sim g$  = NZ

Ⓜ = THETA1

horizontal velocity  
perturbation = X1

vertical velocity  
perturbation = X2

pitch rate perturbation = X3

pitch angle perturbation = X4

elevon deflection  
perturbation = X8

The input signal to the first lead-lag element was called X5IN and its output called X5. The input to the second lead-lag element was called X6IN and its output X6.

The signal entering the  $\delta_e$  LIMIT was called X8PRE1 and the limited signal X8PRE2; the signal entering the  $\dot{\delta}_e$  LIMIT was called X8PRE3 and its output called X8DOT; the integration of X8DOT was X8. The signal X8 was fed back through a lag element whose output was labeled X7.

The CSMP III program is divided into three segments, INITIAL, DYNAMIC, and TERMINAL. The INITIAL part is for defining parameters whose value will not change for the





duration of the program. The DYNAMIC segment contains the equations of motion and other computations. The TERMINAL section (optional) contains any final operations which are desired. For this analysis, the following terms were assumed constant:

$$\text{gravity} = \text{GRVTY} = 32.073 \text{ ft/sec}^2$$

$$X_q = Z_q = 0.0$$

$$\text{density} = \text{RHO} = 2.0325\text{E-}4 \text{ slug/ft}^3$$

$$C_{M\dot{\alpha}} = \text{CMADOT} = -2.0$$

The initial values of two parameters were listed:

$$\text{pitch angle} = \text{THETA} = 0.1571 \text{ rad}$$

$$\text{true airspeed} = U_0 = 1016.9 \text{ fps}$$

The other constants listed in the program (see Figure 8-11) are dimensional parameters or mass properties of the orbiter. AREA refers to wetted wing area; ISUBY ( $I_y$ ) is the mass moment of inertia about the pitch axis; CHORD is the reference wing chord length; MASS is the mass of the vehicle with the payload out.

The FUNCTION statements enable the program to find a dependent variable knowing the value of the independent variable, much like reading a graph. The interpolation between the points listed in the statement may be linear or quadratic. Should an independent variable value fall



INITIAL

```

NOSORT
CONSTANT
  GRVTY = 32.073, X0 = 0.0, Z0 = 0.0, THETA = 0.0
  U0 = 10.16, PHO = 2.0325E-4, AREA = 2.690, ...
  CHORO = 39.56, MASS = 5839, ISUBY = 5.7B3JF+6, ...
  CMADOT = -2.0, PI = 3.14159

FUNCTION F1 = (-.5236,-.9573),(-.4363,-.3917),(-.3491,-.149),(.3491,....
  (-.2618,-.2406),(-.1745,-.3323),(.0,-.3039),(.3491,....
  5099)
FUNCTION F2 = (-.4363,-.1731),(-.3491,-.3802),(-.2618,-.0688),....
  (-.1745,-.0573),(-.0873,-.9229),(.0,-.0802),(.0873,....
  1375),(-.1745,-.2855),(.3491,-.4584)
FUNCTION F3 = (-.3491,-.3266),(-.3054,-.4125),(-.2618,-.4354),....
  (-.1745,-.4927),(.0,-.6188),(.3491,-.8136)
FUNCTION F4 = (-.3491,-.3917),(-.3054,-.4125),(.3491,-.3917),....
  (-.0873,-.0573),(-.1309,-.1065),(-.60,-.108),(-.200,-.122),....
  (-.0873,-.2317),(-.1309,-.2865),(-.1745,-.3025),(-.2182,....
  2865),(-.2618,-.2865),(-.0873,-.0180),(-.1745,-.0247),(-.2618,-.0367),....
  3491,-.0528)
FUNCTION F5 = (-.0873,-.0573),(-.1309,-.1065),(-.1745,-.2317),....
  (-.2618,-.2865),(-.0873,-.0180),(-.1745,-.0247),(-.2618,-.0367),....
  1162,(-.1745,-.2865),(-.1309,-.2317),(-.1745,-.0538),(-.2182,-.0661),....
  2618,-.0256),(-.1309,-.0397),(-.1745,-.0538),(-.2182,-.0661),....
  0873,-.0256),(-.1309,-.0397),(-.1745,-.0538),(-.2182,-.0661),....
  0873,-.0256),(-.1309,-.0397),(-.1745,-.0538),(-.2182,-.0661),....
  3491,-.0528)
FUNCTION F6 = (-.0873,-.0573),(-.1309,-.1065),(-.1745,-.2317),....
  (-.2618,-.2865),(-.0873,-.0180),(-.1745,-.0247),(-.2618,-.0367),....
  1113,-.2182,-.0661),(-.1309,-.0397),(-.1745,-.0538),(-.2182,-.0661),....
  162,-.2182,-.0661),(-.1309,-.0397),(-.1745,-.0538),(-.2182,-.0661),....
  0873,-.0397),(-.1309,-.0518),(-.1745,-.0330),....
  1309,-.0518),(-.1745,-.0275),(-.2182,-.0206),....
  2618,-.0275),(-.1745,-.130),(-.1920,-.100),(-.2094,-.100)
DYNAMIC
SORT
  UI = U0 + XI
  THETA = THETA + X4
  QHAT = 0.5*RHO*UI**2
  GQ = 15.0/SCRT(OHAT+4.0)
  AOA = X2/UI + 0.2316
  GMDE = AFGEN(F1,X8)
  MOE = RHO*UI**2*AREA*CHORD*CMDF/(2*ISUBY)
  XDDE = AFGEN(F2,X8)
  XDE = -RHO*UI**2*AREA*CDDE/(2*MASS)
  CLDE = AFGEN(F3,X8)
  ZDE = -RHO*UI**2*AREA*CLDE/(2*MASS)
  GCMD = AFGEN(F4,TIME)
  ZW = RHO*UI*AREA*(-CLA-COI)/(2.0*MASS)
  CLA = AFGEN(F5,AOA)
  CD = AFGEN(F6,AOA)

```

Figure 8-11



```

CL = AFGEN(F8,ADA)
XW = RHO*UI*AREA*(CL-COA)/I2.0*MASS)
CDA = AFGEN(F9,ADA)
XU = RHO*UI*AREA*(UI*COU/2.0-CO)/MASS
CDU = AFGEN(F10,UI)
MU = RHO*UI*AREA*CHORD*(UI*CMU/2.0*CMU/I SURY)
CMU = AFGEN(F11,UI)
CM = AFGEN(F12,ADA)
MW = RHO*UI*AREA*CHORD*CMU/(2.0*(SURY)
CMA = AFGEN(F13,ADA)
MQ = RHO*UI*AREA*CHORD**2*CMQ/(4.0*(SURY)
CMQ = AFGEN(F14,ADA)
MWDJT = RHO*AREA*CHORD**2*CHADDT/(4.0*(SURY)

X8PRE1 = G00*X6 + X7
X8PRE2 = LIMIT(-.6100, .3471, X8PRE1)
X8PRE3 = J-.3491*(X8PRE2 - X9)
X8DGT = LIMIT(-.3491, .3491, X8PRE3)

X1DUT = XU*X1 + XW*X2 + X0*X3 - GRVY*X4 + XDE*XH
X2DUT = ZU*X1 + ZW*X2 + (ZU*UI)*X3 + ZDE*XH
X3DUT = (MU*ZU*MWDJT)*X1 + (MU*ZU*MWDJT)*X2 + (MU*MWDJT*(UI*(ZU)))*X3 ...
X4DUT = X3
X7DUT = 1.5*(X8 - X7)

X5IN = 3.36*(NZ1 - COS(THETA1) - GCMQ*(1.0+549.-(UI)))
X6IN = X5 + X3

METHOD STIFF
X1 = INTGRL(J, X1DUT)
X2 = INTGRL(0.0, X2DUT)
X3 = INTGRL(0.0, X3DUT)
X4 = INTGRL(J, X4DUT)
X5 = (FDLAG(1.0, 0.5, X5IN)
X6 = (FDLAG(1.0, 0.5, X6IN)
X7 = INTGRL(0.0, X7DUT)
X8 = INTGRL(-0.048, X8DCT)
H = INTGRL(6233, X2)

NZ1 = CL*WHAT*AREA/(MASS*GRVY)

N3SRT = ANA*180./PI
ANADEG = X3*180./PI
X3DEG = X4*180./PI
X8DEG = X8*180./PI
X8DDEG = X8DUT*180./PI
THETA2 = THETA1*100./PI
W = X2 + 11.74

TIMER FINISH = 10.0, OUTDEL = 0.125
PRTPLT ANADEG
PRTPLT ANGLE OF ATTACK (DEGREES)
PRTPLT UI
PRTPLT HORIZONTAL VELOCITY RESPONSE (FPS)
PRTPLT W

```

Figure 8-11 (continued)



```

LABEL VERTICAL VELOCITY RESPONSE (FPS)
PRTP T X3DFG
LABEL PITCH RATE RESPONSE (DEG/SEC)
PRTP T THEAD
LABEL PITCH ANGLE RESPONSE (DEGREES)
PRTP T X8DEG
LABEL ELEVON DEFLECTION (DEGREES)
PRTP T X8DDDFG
LABEL ELEVON DEFLECTION RATE (DEGREES/SEC)
PRTP T NZ1
LABEL LOAD FACTOR (HZ)
PRTP T QHAT
LABEL DYNAMIC PRESSURE
PRTP T G00
LABEL GAIN G00
PRTP T H
LABEL ALTITUDE
PRTP T CIA
LABEL LEFT COEFF WRT ACA
PRTP T CLU
LABEL LEFT COEFF WRT VELOCITY
PRTP T CLDE
LABEL LEFT COEFF WRT ELEVON DEFLECTION
PRTP T CDA
LABEL DRAG COEFF WRT ACA
PRTP T CDU
LABEL DRAG COEFF WRT VELOCITY
PRTP T CDDE
LABEL DRAG COEFF WRT ELEVON DEFLECTION
PRTP T CMA
LABEL PITCHING MOMENT COEFF WRT ACA
PRTP T CMU
LABEL PITCHING MOMENT COEFF WRT VELOCITY
PRTP T CMO
LABEL PITCHING MOMENT COEFF WRT PITCH RATE
PRTP T CMDE
LABEL PITCHING MOMENT COEFF WRT ELEVON DEFLECTION
END
STOP

```

```

OUTPUT VARIABLE SEQUENCE
UT C00
X1DOT XI ZU
CMU CM MWCOT
X3DOT X3 X4
Z1J29 X5 X5IN Z1J12 Z1J13
X8PRE2 X8PRE3 X8DOT X8
THEAD W
AQA CD
CLU ZU
MU MWCOT
X4DOT X4
X5IN Z1J12 Z1J13
X8DOT X8
AOA DEG X30FG
CL ZW
CLA ZW
CMA MW
QHAT NZ1
Z1J12 Z1J13
AOA DEG X30FG
COA
CLDE
CMU THETA
GCMO
GDD X7
X4D5G X4D5G
X2DOT X2
CMDE X5IN
X6 X6
X8PRE1 X8PRE1
X8DDDFG X8DDDFG

```

Figure 8-11 (continued)





outside the range of points listed, the program will extrapolate a value based on the slope of the function at the nearest point listed.

The FUNCTION statements are entered with an AFGEN command (for linear interpolation). Since linear interpolation was used in this analysis, it was necessary to insure that the dependent variable varied linearly between the points chosen. The functions were

- F1: CMDE =  $C_{M\delta_e}$
- F2: CDDE =  $C_{D\delta_e}$
- F3: CLDE =  $C_{L\delta_e}$
- F4: GCMD =  $n_z$  command
- F5: CLA =  $C_{L\alpha}$
- F6: CD =  $C_D$
- F7: CLU =  $C_{L_u}$
- F8: CL =  $C_L$
- F9: CDA =  $C_{D\alpha}$
- F10: CDU =  $C_{D_u}$
- F11: CMU =  $C_{M_u}$
- F12: CM =  $C_M$
- F13: CMA =  $C_{M\alpha}$
- F14: CMQ =  $C_{M_q}$



These coefficients were in turn used to compute the stability derivatives. As the values of the independent variables changed, so did the dependent variables and so also did the stability derivatives. In this manner, the stability derivatives were modified due to changing flight conditions, and thus an important facet of the model was maintained. The stability derivatives were then used to write the equations of motion (the X1DOT through X4DOT equations).

The modeling of the system was completed by writing four other equations as the block diagram signified. X5 and X6 were written simply as lead-lag (LEDLAG) functions of X5IN and X6IN, respectively, where the parameters listed were the coefficients of s in the numerator and denominator.

The term X7 was found by writing the lag compensation from which it came as a differential equation. Since output divided by input equals the transfer function,

$$\frac{X7}{X8} = \frac{1.5}{s + 1.5}$$

$$(X7)s + 1.5(X7) = 1.5(X8)$$

Taking the inverse Laplace transform,



$$\dot{X7} = 1.5(X8) - 1.5(X7)$$

$$\text{and } X7 = \int \dot{X7}$$

Writing this in the CSMP III language,

$$X7 = \text{INTGRL}(0.0, X7\text{DOT})$$

where the 0.0 referred to the initial condition.

The equation to find X8 was somewhat more complex. The signal was first the sum of  $\text{GDQ} * X6 + X7 = X8\text{PRE1}$ ; this was then limited to  $-35/+20^\circ$ , compared to X8, and the difference multiplied by 20 (here, in radians). After limiting this signal to  $-20/+20^\circ$  per second, it was integrated to find X8.

The eight equations were solved simultaneously using the STIFF method of integration, and, after converting some of the parameters into degrees, the results were printed.

It may be seen from the block diagram that the forcing function is the command load factor, GCMD. This value, plotted as FUNCTION F4, was available from the Aero-dynamic Design Data Book and was programmed accordingly.



The value of CMADOT was not available from the above publication. To arrive at the value of -2.0, several aircraft were studied, considering wing planform, aircraft size, airspeed, and altitude. The larger aircraft (C-47 and DC-8) had values of -10 and -6.8, respectively, the DC-8 figure being at Mach 0.88 and 33000 feet. The A-4D, having a delta planform, had a  $C_{M_x}$  of -2.1 at 15000 feet and -1.4 at 35000 feet. Considering the size of the orbiter and its altitude for this study, the value of -2.0 was deemed appropriate.

Several equations to compute the load factor on the vehicle were considered. The one chosen was derived from the lift equation:

$$n_z = \frac{L}{W} \quad \text{where } L = C_L \hat{q} S$$

$$\begin{aligned} \text{so, } n_z &= C_L \hat{q} S / mg \\ &= C_L * \hat{q} * \text{AREA} / (\text{MASS} * \text{GRVITY}) \end{aligned}$$

This equation was chosen as it was most independent of the equations of motion and would therefore amplify to a less extent any errors due to integration round-off or to other sources during the solution of the simultaneous equations.





The results are shown in Figure 8-12 (short period) and Figure 8-13 (phugoid). Inasmuch as both modes were evidently stable, the steady state magnitudes were extremely high. Several causes must be considered.

One, the equations of motion were written as perturbed motions. This was necessary in order to justify their linearization. The parameter values were treated as perturbations throughout the program, being added to the large scale motion where necessary for computation (as in the case of THETA1 and U1) and for output plots. Their initial conditions were collectively zero. The initial conditions for the other parameters, X5 through X7, were not zero, however, and a method for incorporating (or even deriving) their initial value was not available. The initial condition for X8 was available from the Data Book and was so used. It is not known if the lack of initial conditions for these parameters caused the large excursions in the response; it is doubtful that this was the case because the steady state values should still have been reasonable; they were not.

Two, the simulation was begun at some point other than  $t=0$  in the trajectory. That is, the vehicle had







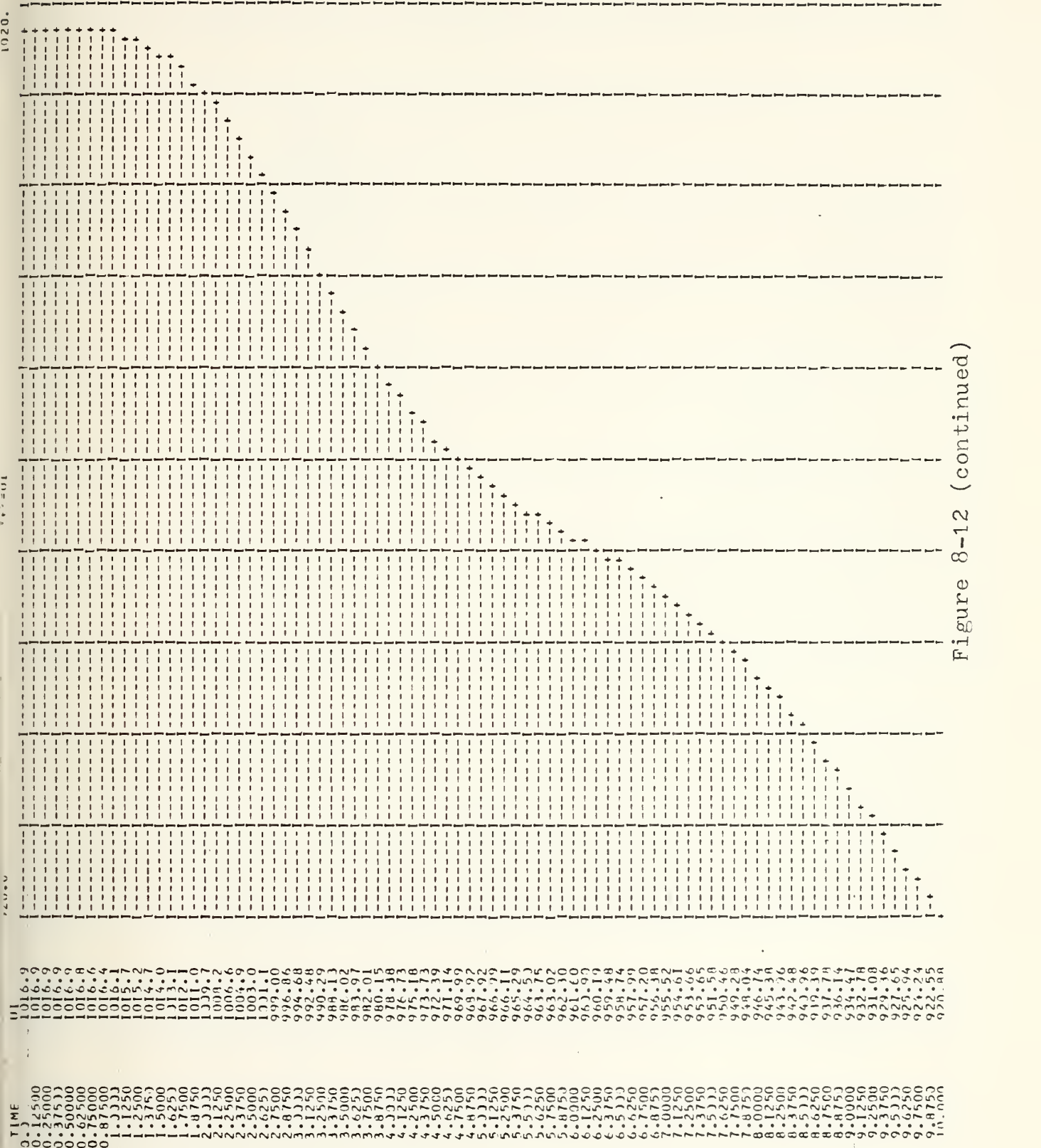
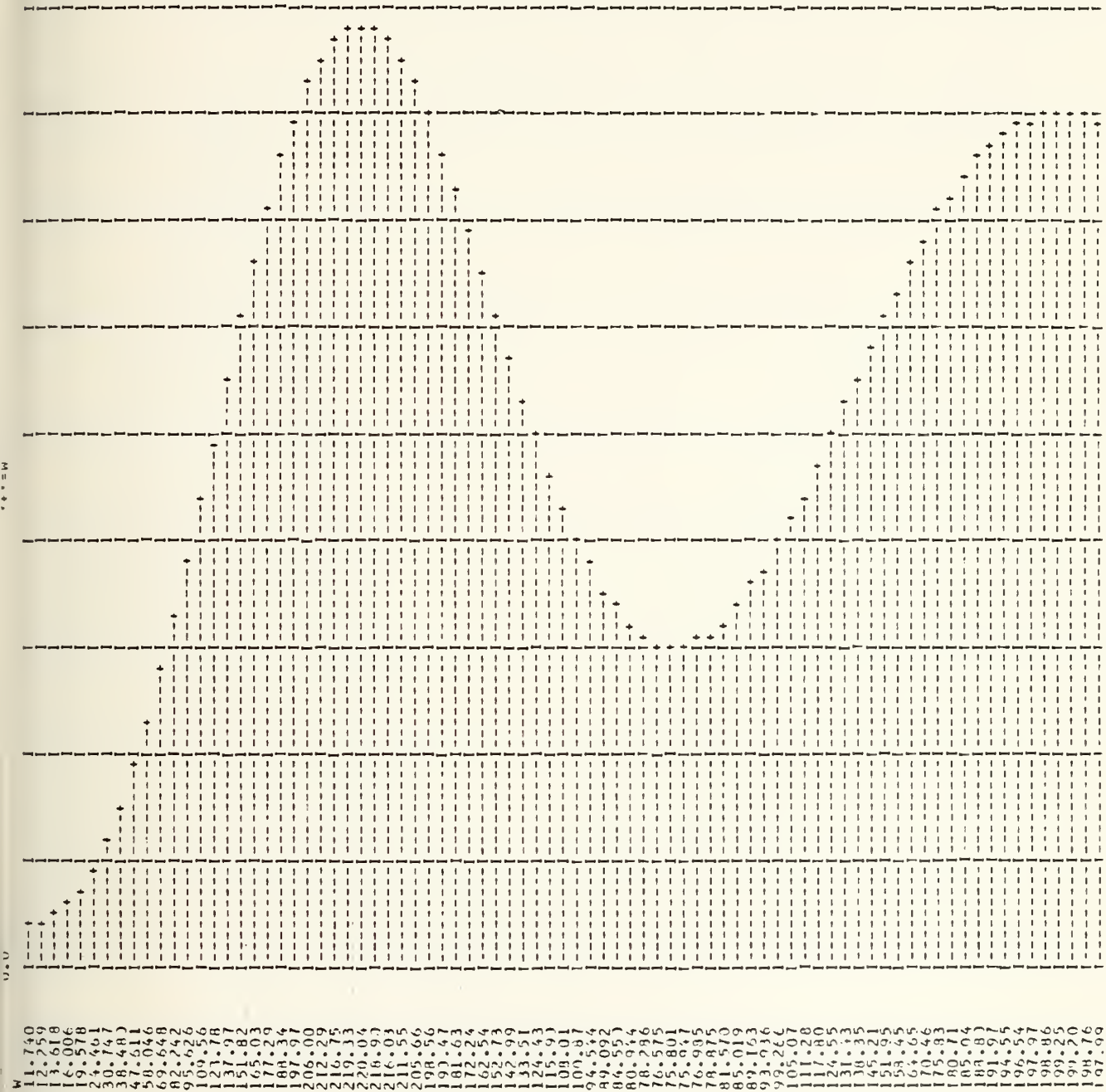


Figure 8-12 (continued)





TIME  
 0.0  
 0.1  
 0.2  
 0.3  
 0.4  
 0.5  
 0.6  
 0.7  
 0.8  
 0.9  
 1.0  
 1.1  
 1.2  
 1.3  
 1.4  
 1.5  
 1.6  
 1.7  
 1.8  
 1.9  
 2.0  
 2.1  
 2.2  
 2.3  
 2.4  
 2.5  
 2.6  
 2.7  
 2.8  
 2.9  
 3.0  
 3.1  
 3.2  
 3.3  
 3.4  
 3.5  
 3.6  
 3.7  
 3.8  
 3.9  
 4.0  
 4.1  
 4.2  
 4.3  
 4.4  
 4.5  
 4.6  
 4.7  
 4.8  
 4.9  
 5.0  
 5.1  
 5.2  
 5.3  
 5.4  
 5.5  
 5.6  
 5.7  
 5.8  
 5.9  
 6.0  
 6.1  
 6.2  
 6.3  
 6.4  
 6.5  
 6.6  
 6.7  
 6.8  
 6.9  
 7.0  
 7.1  
 7.2  
 7.3  
 7.4  
 7.5  
 7.6  
 7.7  
 7.8  
 7.9  
 8.0  
 8.1  
 8.2  
 8.3  
 8.4  
 8.5  
 8.6  
 8.7  
 8.8  
 8.9  
 9.0  
 9.1  
 9.2  
 9.3  
 9.4  
 9.5  
 9.6  
 9.7  
 9.8  
 9.9  
 10.0

W  
 0.0  
 0.1  
 0.2  
 0.3  
 0.4  
 0.5  
 0.6  
 0.7  
 0.8  
 0.9  
 1.0  
 1.1  
 1.2  
 1.3  
 1.4  
 1.5  
 1.6  
 1.7  
 1.8  
 1.9  
 2.0  
 2.1  
 2.2  
 2.3  
 2.4  
 2.5  
 2.6  
 2.7  
 2.8  
 2.9  
 3.0  
 3.1  
 3.2  
 3.3  
 3.4  
 3.5  
 3.6  
 3.7  
 3.8  
 3.9  
 4.0  
 4.1  
 4.2  
 4.3  
 4.4  
 4.5  
 4.6  
 4.7  
 4.8  
 4.9  
 5.0  
 5.1  
 5.2  
 5.3  
 5.4  
 5.5  
 5.6  
 5.7  
 5.8  
 5.9  
 6.0  
 6.1  
 6.2  
 6.3  
 6.4  
 6.5  
 6.6  
 6.7  
 6.8  
 6.9  
 7.0  
 7.1  
 7.2  
 7.3  
 7.4  
 7.5  
 7.6  
 7.7  
 7.8  
 7.9  
 8.0  
 8.1  
 8.2  
 8.3  
 8.4  
 8.5  
 8.6  
 8.7  
 8.8  
 8.9  
 9.0  
 9.1  
 9.2  
 9.3  
 9.4  
 9.5  
 9.6  
 9.7  
 9.8  
 9.9  
 10.0

Figure 8-12 (continued)





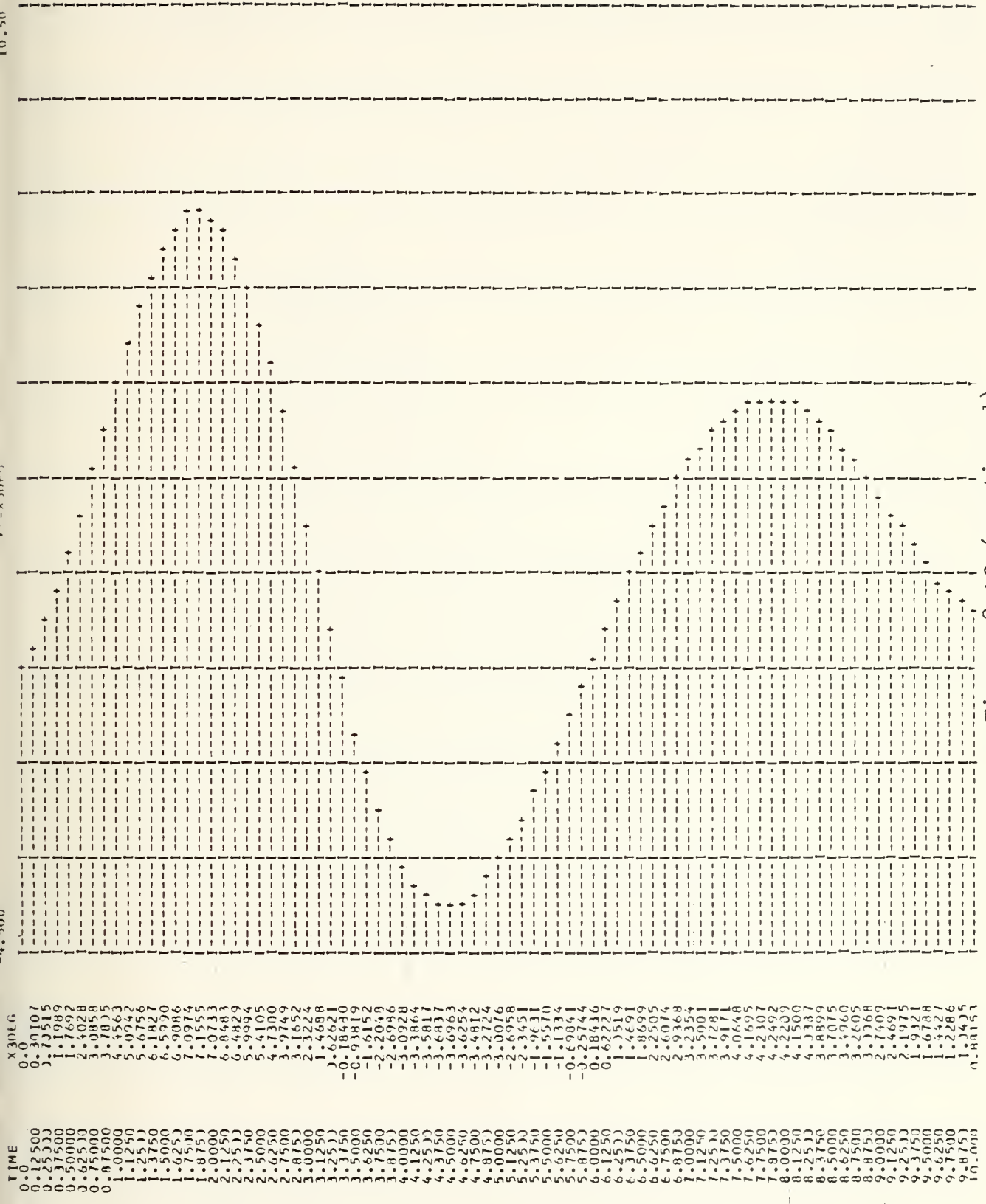


Figure 8-12 (continued)



TIME  
0.07500  
0.15000  
0.37500  
0.50000  
0.62500  
0.75000  
0.87500  
1.00000  
1.12500  
1.25000  
1.37500  
1.50000  
1.62500  
1.75000  
1.87500  
2.00000  
2.12500  
2.25000  
2.37500  
2.50000  
2.62500  
2.75000  
2.87500  
3.00000  
3.12500  
3.25000  
3.37500  
3.50000  
3.62500  
3.75000  
3.87500  
4.00000  
4.12500  
4.25000  
4.37500  
4.50000  
4.62500  
4.75000  
4.87500  
5.00000  
5.12500  
5.25000  
5.37500  
5.50000  
5.62500  
5.75000  
5.87500  
6.00000  
6.12500  
6.25000  
6.37500  
6.50000  
6.62500  
6.75000  
6.87500  
7.00000  
7.12500  
7.25000  
7.37500  
7.50000  
7.62500  
7.75000  
7.87500  
8.00000  
8.12500  
8.25000  
8.37500  
8.50000  
8.62500  
8.75000  
8.87500  
9.00000  
9.12500  
9.25000  
9.37500  
9.50000  
9.62500  
9.75000  
9.87500  
10.00000

THE TAD  
9.012  
9.018  
9.024  
9.030  
9.036  
9.042  
9.048  
9.054  
9.060  
9.066  
9.072  
9.078  
9.084  
9.090  
9.096  
9.102  
9.108  
9.114  
9.120  
9.126  
9.132  
9.138  
9.144  
9.150  
9.156  
9.162  
9.168  
9.174  
9.180  
9.186  
9.192  
9.198  
9.204  
9.210  
9.216  
9.222  
9.228  
9.234  
9.240  
9.246  
9.252  
9.258  
9.264  
9.270  
9.276  
9.282  
9.288  
9.294  
9.300  
9.306  
9.312  
9.318  
9.324  
9.330  
9.336  
9.342  
9.348  
9.354  
9.360  
9.366  
9.372  
9.378  
9.384  
9.390  
9.396  
9.402  
9.408  
9.414  
9.420  
9.426  
9.432  
9.438  
9.444  
9.450  
9.456  
9.462  
9.468  
9.474  
9.480  
9.486  
9.492  
9.498  
9.504  
9.510  
9.516  
9.522  
9.528  
9.534  
9.540  
9.546  
9.552  
9.558  
9.564  
9.570  
9.576  
9.582  
9.588  
9.594  
9.600  
9.606  
9.612  
9.618  
9.624  
9.630  
9.636  
9.642  
9.648  
9.654  
9.660  
9.666  
9.672  
9.678  
9.684  
9.690  
9.696  
9.702  
9.708  
9.714  
9.720  
9.726  
9.732  
9.738  
9.744  
9.750  
9.756  
9.762  
9.768  
9.774  
9.780  
9.786  
9.792  
9.798  
9.804  
9.810  
9.816  
9.822  
9.828  
9.834  
9.840  
9.846  
9.852  
9.858  
9.864  
9.870  
9.876  
9.882  
9.888  
9.894  
9.900  
9.906  
9.912  
9.918  
9.924  
9.930  
9.936  
9.942  
9.948  
9.954  
9.960  
9.966  
9.972  
9.978  
9.984  
9.990  
9.996  
10.000

29.00

\*\*\* = THE TAD

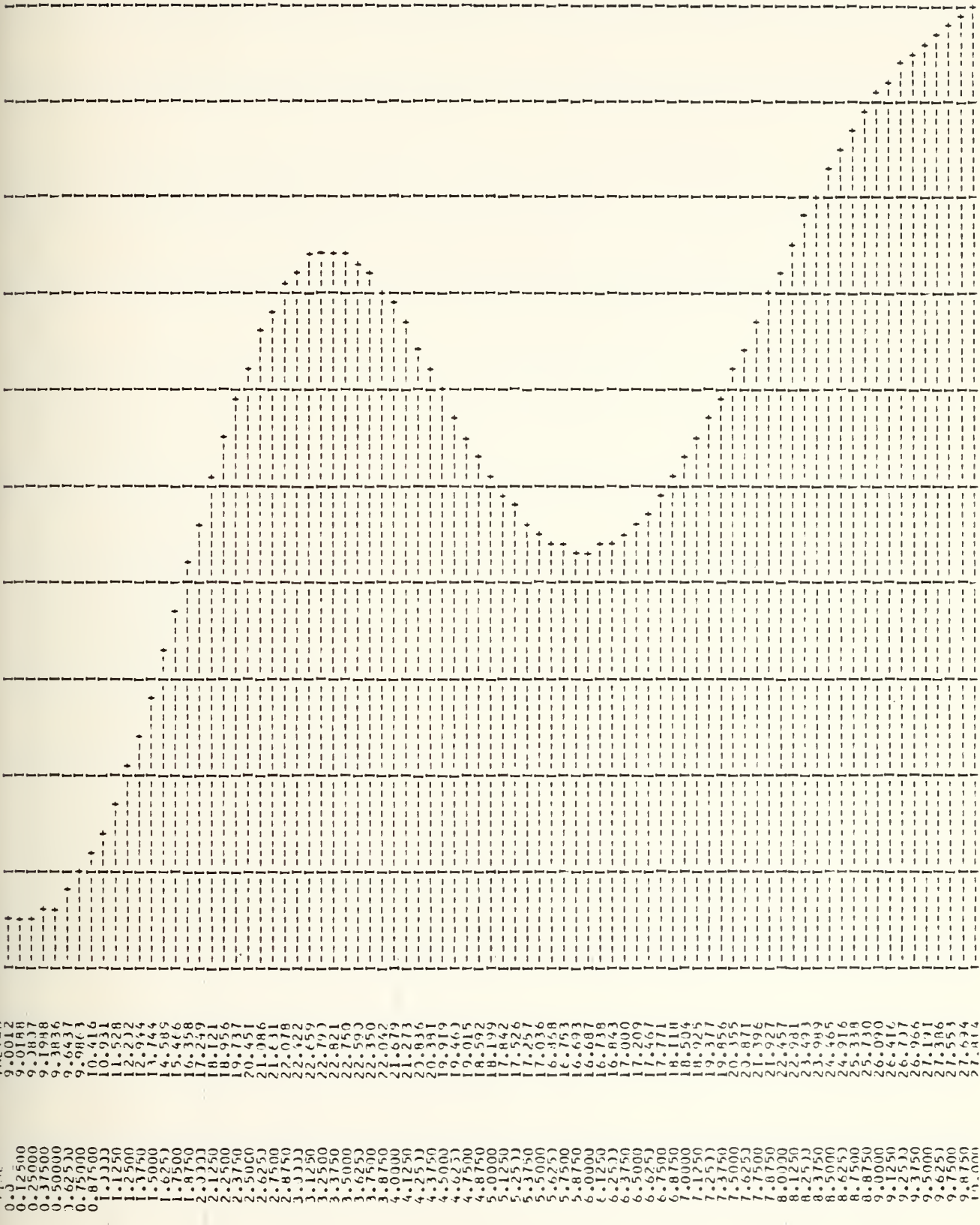


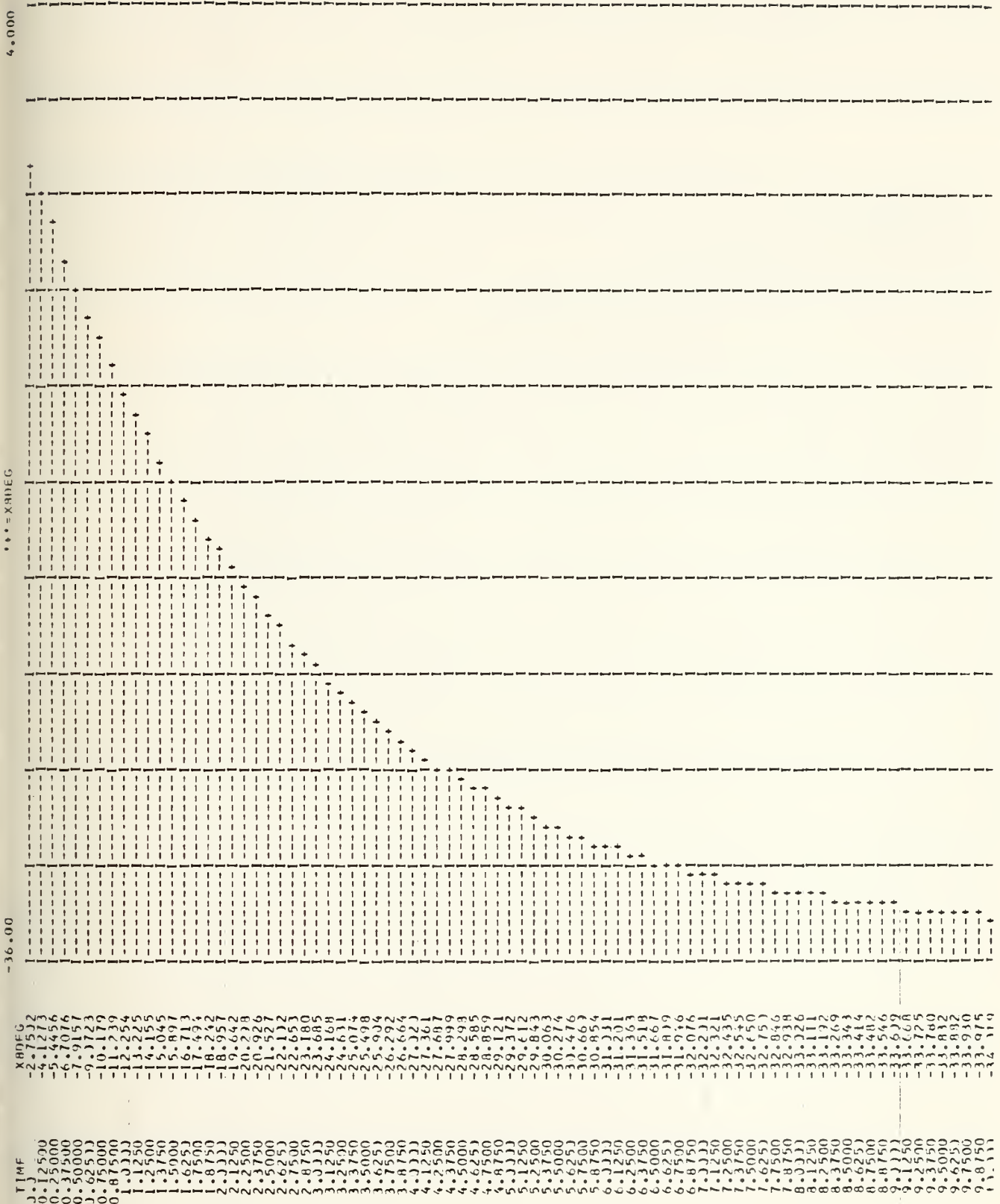
Figure 8-12 (continued)



4.000

\* \* \* = X RDEG

-36.00



TIME  
 X RDEG  
 2.7532  
 4.1273  
 5.4456  
 6.7016  
 7.9151  
 9.1723  
 10.479  
 11.739  
 13.045  
 14.355  
 15.691  
 17.013  
 18.344  
 19.697  
 21.042  
 22.396  
 23.750  
 25.104  
 26.453  
 27.805  
 29.158  
 30.514  
 31.871  
 33.229  
 34.588  
 35.947  
 37.307  
 38.667  
 40.028  
 41.390  
 42.753  
 44.117  
 45.486  
 46.856  
 48.227  
 49.599  
 50.972  
 52.346  
 53.715  
 55.085  
 56.456  
 57.828  
 59.201  
 60.575  
 61.950  
 63.326  
 64.703  
 66.081  
 67.460  
 68.840  
 70.221  
 71.603  
 72.986  
 74.370  
 75.755  
 77.141  
 78.528  
 79.916  
 81.305  
 82.695  
 84.086  
 85.478  
 86.871  
 88.265  
 89.660  
 91.056  
 92.453  
 93.851  
 95.250  
 96.650  
 98.051  
 99.453  
 100.856  
 102.260  
 103.665  
 105.071  
 106.478  
 107.886  
 109.295  
 110.705  
 112.116  
 113.528  
 114.941  
 116.355  
 117.770  
 119.186  
 120.603  
 122.021  
 123.440  
 124.860  
 126.281  
 127.703  
 129.126  
 130.550  
 131.975  
 133.401  
 134.828  
 136.256  
 137.685  
 139.115  
 140.546  
 141.978  
 143.411  
 144.845  
 146.280  
 147.716  
 149.153  
 150.591  
 152.030  
 153.470  
 154.911  
 156.353  
 157.796  
 159.240  
 160.685  
 162.131  
 163.578  
 165.026  
 166.475  
 167.925  
 169.376  
 170.828  
 172.281  
 173.735  
 175.190  
 176.646  
 178.103  
 179.561  
 181.020  
 182.480  
 183.941  
 185.403  
 186.866  
 188.330  
 189.795  
 191.261  
 192.728  
 194.196  
 195.665  
 197.135  
 198.606  
 200.078  
 201.551  
 203.025  
 204.500  
 205.976  
 207.453  
 208.931  
 210.410  
 211.890  
 213.371  
 214.853  
 216.336  
 217.820  
 219.305  
 220.791  
 222.278  
 223.766  
 225.255  
 226.745  
 228.236  
 229.728  
 231.221  
 232.715  
 234.210  
 235.706  
 237.203  
 238.701  
 240.200  
 241.700  
 243.201  
 244.703  
 246.206  
 247.710  
 249.215  
 250.721  
 252.228  
 253.736  
 255.245  
 256.755  
 258.266  
 259.778  
 261.291  
 262.805  
 264.320  
 265.836  
 267.353  
 268.871  
 270.390  
 271.910  
 273.431  
 274.953  
 276.476  
 278.000  
 279.525  
 281.051  
 282.578  
 284.106  
 285.635  
 287.165  
 288.696  
 290.228  
 291.761  
 293.295  
 294.830  
 296.366  
 297.903  
 299.441  
 300.980  
 302.520  
 304.061  
 305.603  
 307.146  
 308.690  
 310.235  
 311.781  
 313.328  
 314.876  
 316.425  
 317.975  
 319.526  
 321.078  
 322.631  
 324.185  
 325.740  
 327.296  
 328.853  
 330.411  
 331.970  
 333.530  
 335.091  
 336.653  
 338.216  
 339.780  
 341.345  
 342.911  
 344.478  
 346.046  
 347.615  
 349.185  
 350.756  
 352.328  
 353.901  
 355.475  
 357.050  
 358.626  
 360.203  
 361.787  
 363.372  
 364.958  
 366.545  
 368.133  
 369.722  
 371.312  
 372.903  
 374.495  
 376.088  
 377.682  
 379.277  
 380.873  
 382.470  
 384.068  
 385.667  
 387.267  
 388.868  
 390.470  
 392.073  
 393.677  
 395.282  
 396.888  
 398.495  
 400.103  
 401.712  
 403.322  
 404.933  
 406.545  
 408.158  
 409.772  
 411.387  
 413.003  
 414.620  
 416.238  
 417.857  
 419.477  
 421.098  
 422.720  
 424.343  
 425.967  
 427.592  
 429.218  
 430.845  
 432.473  
 434.102  
 435.732  
 437.363  
 438.995  
 440.628  
 442.262  
 443.897  
 445.533  
 447.170  
 448.808  
 450.447  
 452.087  
 453.728  
 455.370  
 457.013  
 458.657  
 460.302  
 461.948  
 463.595  
 465.243  
 466.892  
 468.542  
 470.193  
 471.845  
 473.498  
 475.152  
 476.807  
 478.463  
 480.120  
 481.778  
 483.437  
 485.097  
 486.758  
 488.420  
 490.083  
 491.747  
 493.412  
 495.078  
 496.745  
 498.413  
 500.082  
 501.752  
 503.423  
 505.095  
 506.768  
 508.442  
 510.117  
 511.793  
 513.470  
 515.148  
 516.827  
 518.507  
 520.188  
 521.870  
 523.553  
 525.237  
 526.922  
 528.608  
 530.295  
 531.983  
 533.672  
 535.362  
 537.053  
 538.745  
 540.438  
 542.132  
 543.827  
 545.523  
 547.220  
 548.918  
 550.617  
 552.317  
 554.018  
 555.720  
 557.423  
 559.127  
 560.832  
 562.538  
 564.245  
 565.953  
 567.662  
 569.372  
 571.083  
 572.795  
 574.508  
 576.222  
 577.937  
 579.653  
 581.370  
 583.088  
 584.807  
 586.527  
 588.248  
 590.070  
 591.793  
 593.517  
 595.242  
 596.968  
 598.695  
 600.423  
 602.152  
 603.882  
 605.613  
 607.345  
 609.078  
 610.812  
 612.547  
 614.283  
 616.020  
 617.758  
 619.497  
 621.237  
 622.978  
 624.720  
 626.463  
 628.207  
 629.952  
 631.698  
 633.445  
 635.193  
 636.942  
 638.692  
 640.443  
 642.195  
 643.948  
 645.702  
 647.457  
 649.213  
 650.970  
 652.728  
 654.487  
 656.247  
 658.008  
 659.770  
 661.533  
 663.297  
 665.062  
 666.828  
 668.595  
 670.363  
 672.132  
 673.902  
 675.673  
 677.445  
 679.218  
 680.992  
 682.767  
 684.543  
 686.320  
 688.098  
 689.877  
 691.657  
 693.438  
 695.220  
 697.003  
 698.787  
 700.572  
 702.358  
 704.145  
 705.933  
 707.722  
 709.512  
 711.303  
 713.095  
 714.888  
 716.682  
 718.477  
 720.273  
 722.070  
 723.868  
 725.667  
 727.467  
 729.268  
 731.070  
 732.873  
 734.677  
 736.482  
 738.288  
 740.095  
 741.903  
 743.712  
 745.522  
 747.333  
 749.145  
 750.958  
 752.772  
 754.587  
 756.403  
 758.220  
 760.038  
 761.857  
 763.677  
 765.498  
 767.320  
 769.143  
 770.967  
 772.792  
 774.618  
 776.445  
 778.273  
 780.102  
 781.932  
 783.763  
 785.595  
 787.428  
 789.262  
 791.097  
 792.933  
 794.770  
 796.608  
 798.447  
 800.287  
 802.128  
 803.970  
 805.813  
 807.657  
 809.502  
 811.348  
 813.195  
 815.043  
 816.892  
 818.742  
 820.593  
 822.445  
 824.298  
 826.152  
 828.007  
 829.863  
 831.720  
 833.578  
 835.437  
 837.297  
 839.158  
 841.020  
 842.883  
 844.747  
 846.612  
 848.478  
 850.345  
 852.213  
 854.082  
 855.952  
 857.823  
 859.695  
 861.568  
 863.442  
 865.317  
 867.193  
 869.070  
 870.948  
 872.827  
 874.707  
 876.588  
 878.470  
 880.353  
 882.237  
 884.122  
 886.008  
 887.895  
 889.783  
 891.672  
 893.562  
 895.453  
 897.345  
 899.238  
 901.132  
 903.027  
 904.923  
 906.820  
 908.718  
 910.617  
 912.517  
 914.418  
 916.320  
 918.223  
 920.127  
 922.032  
 923.938  
 925.845  
 927.753  
 929.662  
 931.572  
 933.483  
 935.395  
 937.308  
 939.222  
 941.137  
 943.053  
 944.970  
 946.888  
 948.807  
 950.727  
 952.648  
 954.570  
 956.493  
 958.417  
 960.342  
 962.268  
 964.195  
 966.123  
 968.052  
 970.082  
 972.013  
 973.945  
 975.878  
 977.812  
 979.747  
 981.683  
 983.620  
 985.558  
 987.497  
 989.437  
 991.378  
 993.320  
 995.263  
 997.207  
 999.152  
 1001.098  
 1003.045  
 1004.993  
 1006.942  
 1008.892  
 1010.843  
 1012.795  
 1014.748  
 1016.702  
 1018.657  
 1020.613  
 1022.570  
 1024.528  
 1026.487  
 1028.447  
 1030.408  
 1032.370  
 1034.333  
 1036.297  
 1038.262  
 1040.228  
 1042.195  
 1044.163  
 1046.132  
 1048.102  
 1050.073  
 1052.045  
 1054.018  
 1055.992  
 1057.967  
 1059.943  
 1061.920  
 1063.898  
 1065.877  
 1067.857  
 1069.838  
 1071.820  
 1073.803  
 1075.787  
 1077.772  
 1079.758  
 1081.745  
 1083.733  
 1085.722  
 1087.712  
 1089.703  
 1091.695  
 1093.688  
 1095.682  
 1097.677  
 1099.673  
 1101.670  
 1103.668  
 1105.667  
 1107.667  
 1109.668  
 1111.670  
 1113.673  
 1115.677  
 1117.682  
 1119.688  
 1121.695  
 1123.702  
 1125.710  
 1127.719  
 1129.729  
 1131.740  
 1133.752  
 1135.765  
 1137.779  
 1139.794  
 1141.810  
 1143.827  
 1145.845  
 1147.864  
 1149.884  
 1151.905  
 1153.927  
 1155.950  
 1157.974  
 1159.999  
 1162.025  
 1164.052  
 1166.080  
 1168.109  
 1170.139  
 1172.170  
 1174.202  
 1176.235  
 1178.269  
 1180.304  
 1182.340  
 1184.377  
 1186.415  
 1188.454  
 1190.494  
 1192.535  
 1194.577  
 1196.620  
 1198.664  
 1200.709  
 1202.755  
 1204.802  
 1206.850  
 1208.899  
 1210.950  
 1212.992  
 1215.035  
 1217.079  
 1219.125  
 1221.172  
 1223.220  
 1225.269  
 1227.319  
 1229.370  
 1231.422  
 1233.475  
 1235.529  
 1237.584  
 1239.640  
 1241.697  
 1243.755  
 1245.814  
 1247.874  
 1249.935  
 1251.997  
 1254.060  
 1256.125  
 1258.191  
 1260.258  
 1262.326  
 1264.395  
 1266.465  
 1268.536  
 1270.608  
 1272.681  
 1274.755  
 1276.830  
 1278.906  
 1280.983  
 1283.061  
 1285.140  
 1287.220  
 1289.301  
 1291.383  
 1293.466  
 1295.550  
 1297.635  
 1299.721  
 1301.808  
 1303.896  
 1305.985  
 1308.075  
 1310.166  
 1312.258  
 1314.351  
 1316.445  
 1318.540  
 1320.636  
 1322.733  
 1324.831  
 1326.930  
 1329.030  
 1331.131  
 1333.233  
 1335.336  
 1337.440  
 1339.545  
 1341.651  
 1343.758  
 1345.866  
 1347.975  
 1350.085  
 1352.196  
 1354.308  
 1356.421  
 1358.535  
 1360.650  
 1362.766  
 1364.883  
 1367.001  
 1369.120  
 1371.240  
 1373.361  
 1375.483  
 1377.606  
 1379.730  
 1381.855  
 1383.981  
 1386.108  
 1388.236  
 1390.365  
 1392.495  
 1394.626  
 1396.758  
 1398.891  
 1401.025  
 1403.160  
 1405.296  
 1407.433  
 1409.571  
 1411.710  
 1413.850  
 1415.991  
 1418.133  
 1420.276  
 1422.420  
 1424.565  
 1426.711  
 1428.858  
 1431.006  
 1433.155  
 1435.305  
 1437.456  
 1439.608  
 1441.761  
 1443.915  
 1446.070  
 1448.226  
 1450.383  
 1452.541  
 1454.700  
 1456.860  
 1459.021  
 1461.183  
 1463.346  
 1465.510  
 1467.675  
 1469.841  
 1472.008  
 1474.176  
 1476.345  
 1478.515  
 1480.686  
 1482.858  
 1485.031  
 1487.205  
 1489.380  
 1491.556  
 1493.733  
 1495.911  
 1498.090  
 1500.270  
 1502.451  
 1504.633  
 1506.816  
 1509.000  
 1511.185  
 1513.371  
 1515.558  
 1517.746  
 1519.935  
 1522.125  
 1524.316  
 1526.508  
 1528.701  
 1530.895  
 1533.090  
 1535.286  
 1537.483  
 1539.681  
 1541.880  
 1544.080  
 1546.281  
 1548.483  
 1550.686  
 1552.890  
 1555.095  
 1557.301  
 1559.508  
 1561.716  
 1563.925  
 1566.135  
 1568.346  
 1570.558  
 1572.771  
 1574.985  
 1577.200  
 1579.416  
 1581.633  
 1583.851  
 1586.070  
 1588.290  
 1590.511  
 1592.733  
 1594.956  
 1597.180  
 1599.405  
 1601.631  
 1603.858  
 1606.086  
 1608.315  
 1610.545  
 1612.776  
 1615.008  
 1617.241  
 1619.475  
 1621.710  
 1623.946  
 1626.183  
 1628.421  
 1630.660  
 1632.900  
 1635.141  
 1637.383  
 1639.626  
 1641.870  
 1644.115  
 1646.361  
 1648.608  
 1650.856  
 1653.105  
 1655.355  
 1657.606  
 1659.858  
 1662.111  
 1664.365  
 1666.620  
 1668.876  
 1671.133  
 1673.391  
 1675.650  
 1677.910  
 1680.171  
 1682.433  
 1684.696  
 1686.960  
 1689.225  
 1691.491  
 1693.758  
 1696.026  
 1698.295  
 1700.565  
 1702.836  
 1705.108  
 1707.381  
 1709.655  
 1711.930  
 1714.206  
 1716.483  
 1718.761  
 1721.040  
 1723.320  
 1725.601  
 1727.883  
 1730.166  
 1732.450  
 1734.735  
 1737.021  
 1739.308  
 1741.596  
 1743.885  
 1746.175  
 1748.466  
 1750.758  
 1753.051  
 1755.345  
 1757.640  
 1759.936  
 1762.233  
 1764.531  
 1766.830  
 1769.130  
 1771.431  
 1773.733  
 1776.036  
 1778.340  
 1780.645  
 1782.951  
 1785.258  
 1787.566  
 1789.875  
 1792.185  
 1794.496  
 1796.808  
 179



3.000

\*\*\*XRDPEG

-12.00

TIME	XRDPEG
0.02500	-1.47229
0.03750	-1.04318
0.05000	-0.45521
0.06250	-0.66555
0.07500	-7.94133
0.08750	-7.60222
0.10000	-7.27726
0.11250	-6.96694
0.12500	-6.39446
0.13750	-6.11220
0.15000	-5.45122
0.16250	-5.36212
0.17500	-5.13331
0.18750	-4.91339
0.20000	-4.70322
0.21250	-4.31110
0.22500	-4.31269
0.23750	-3.95270
0.25000	-3.78205
0.26250	-3.62559
0.27500	-3.31779
0.28750	-3.11763
0.30000	-3.0406
0.31250	-2.9108
0.32500	-2.7895
0.33750	-2.6672
0.35000	-2.5532
0.36250	-2.4446
0.37500	-2.3402
0.38750	-2.2405
0.40000	-2.1447
0.41250	-2.0531
0.42500	-1.9654
0.43750	-1.8815
0.45000	-1.8012
0.46250	-1.7243
0.47500	-1.6502
0.48750	-1.5787
0.50000	-1.5127
0.51250	-1.4441
0.52500	-1.3803
0.53750	-1.3201
0.55000	-1.2642
0.56250	-1.2123
0.57500	-1.1645
0.58750	-1.1210
0.60000	-1.0819
0.61250	-1.0460
0.62500	-1.0140
0.63750	-0.9840
0.65000	-0.9578
0.66250	-0.9311
0.67500	-0.9061
0.68750	-0.8812
0.70000	-0.8578
0.71250	-0.8349
0.72500	-0.8112
0.73750	-0.7882
0.75000	-0.7652
0.76250	-0.7422
0.77500	-0.7192
0.78750	-0.6962
0.80000	-0.6732
0.81250	-0.6502
0.82500	-0.6272
0.83750	-0.6042
0.85000	-0.5812
0.86250	-0.5582
0.87500	-0.5352
0.88750	-0.5122
0.90000	-0.4892
0.91250	-0.4662
0.92500	-0.4432
0.93750	-0.4202
0.95000	-0.3972
0.96250	-0.3742
0.97500	-0.3512
0.98750	-0.3282
1.00000	-0.3052

Figure 8-12 (continued)





2.000

0.000

0.000

NZL  
 1.0567  
 1.0599  
 1.0649  
 1.0715  
 1.0795  
 1.1114  
 1.1383  
 1.1712  
 1.2100  
 2.2544  
 3.3032  
 4.3562  
 5.4122  
 6.4702  
 7.5289  
 8.5870  
 9.6432  
 10.6956  
 11.7441  
 12.7865  
 13.8224  
 14.8509  
 15.8717  
 16.8844  
 17.8890  
 18.8856  
 19.8744  
 20.8551  
 21.8287  
 22.7955  
 23.7566  
 24.7149  
 25.6714  
 26.6270  
 27.5826  
 28.5389  
 29.4962  
 30.4546  
 31.4143  
 32.3764  
 33.3409  
 34.3076  
 35.2766  
 36.2478  
 37.2212  
 38.1968  
 39.1745  
 40.1543  
 41.1361  
 42.1199  
 43.1055  
 44.0929  
 45.0819  
 46.0724  
 47.0644  
 48.0578  
 49.0525  
 50.0484  
 51.0453  
 52.0431  
 53.0418  
 54.0413  
 55.0415  
 56.0423  
 57.0436  
 58.0454  
 59.0477  
 60.0504  
 61.0535  
 62.0570  
 63.0608  
 64.0649  
 65.0693  
 66.0739  
 67.0786  
 68.0834  
 69.0882  
 70.0930  
 71.0977  
 72.1023  
 73.1068  
 74.1112  
 75.1154  
 76.1194  
 77.1232  
 78.1267  
 79.1300  
 80.1330  
 81.1357  
 82.1381  
 83.1401  
 84.1417  
 85.1429  
 86.1437  
 87.1441  
 88.1441  
 89.1437  
 90.1429  
 91.1417  
 92.1401  
 93.1381  
 94.1357  
 95.1330  
 96.1300  
 97.1267  
 98.1232  
 99.1194  
 100.1154

TIME  
 0.0  
 0.12500  
 0.25000  
 0.37500  
 0.50000  
 0.62500  
 0.75000  
 0.87500  
 1.00000  
 1.12500  
 1.25000  
 1.37500  
 1.50000  
 1.62500  
 1.75000  
 1.87500  
 2.00000  
 2.12500  
 2.25000  
 2.37500  
 2.50000  
 2.62500  
 2.75000  
 2.87500  
 3.00000  
 3.12500  
 3.25000  
 3.37500  
 3.50000  
 3.62500  
 3.75000  
 3.87500  
 4.00000  
 4.12500  
 4.25000  
 4.37500  
 4.50000  
 4.62500  
 4.75000  
 4.87500  
 5.00000  
 5.12500  
 5.25000  
 5.37500  
 5.50000  
 5.62500  
 5.75000  
 5.87500  
 6.00000  
 6.12500  
 6.25000  
 6.37500  
 6.50000  
 6.62500  
 6.75000  
 6.87500  
 7.00000  
 7.12500  
 7.25000  
 7.37500  
 7.50000  
 7.62500  
 7.75000  
 7.87500  
 8.00000  
 8.12500  
 8.25000  
 8.37500  
 8.50000  
 8.62500  
 8.75000  
 8.87500  
 9.00000  
 9.12500  
 9.25000  
 9.37500  
 9.50000  
 9.62500  
 9.75000  
 9.87500  
 10.00000

Figure 8-12 (continued)



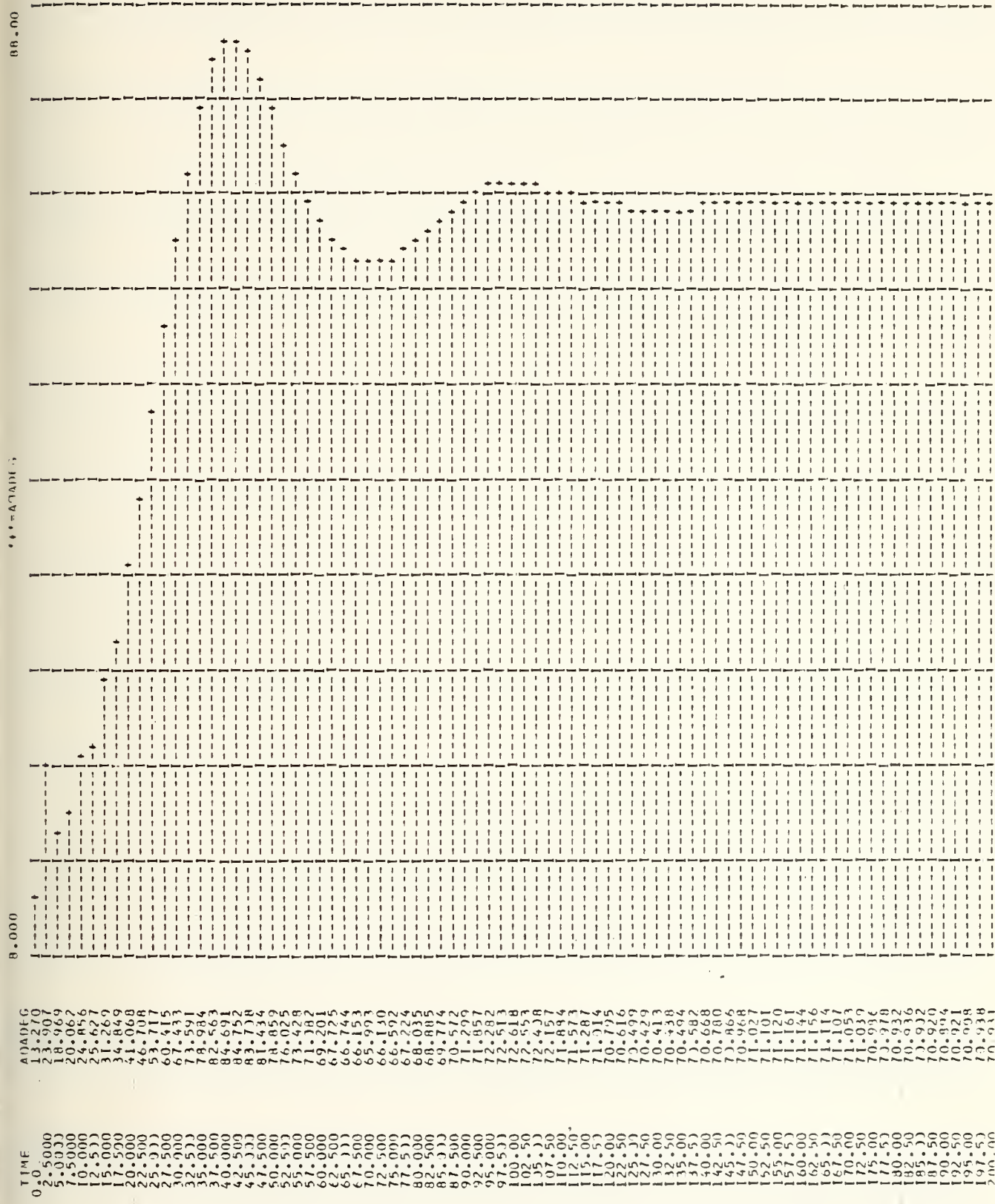


Figure 8-13



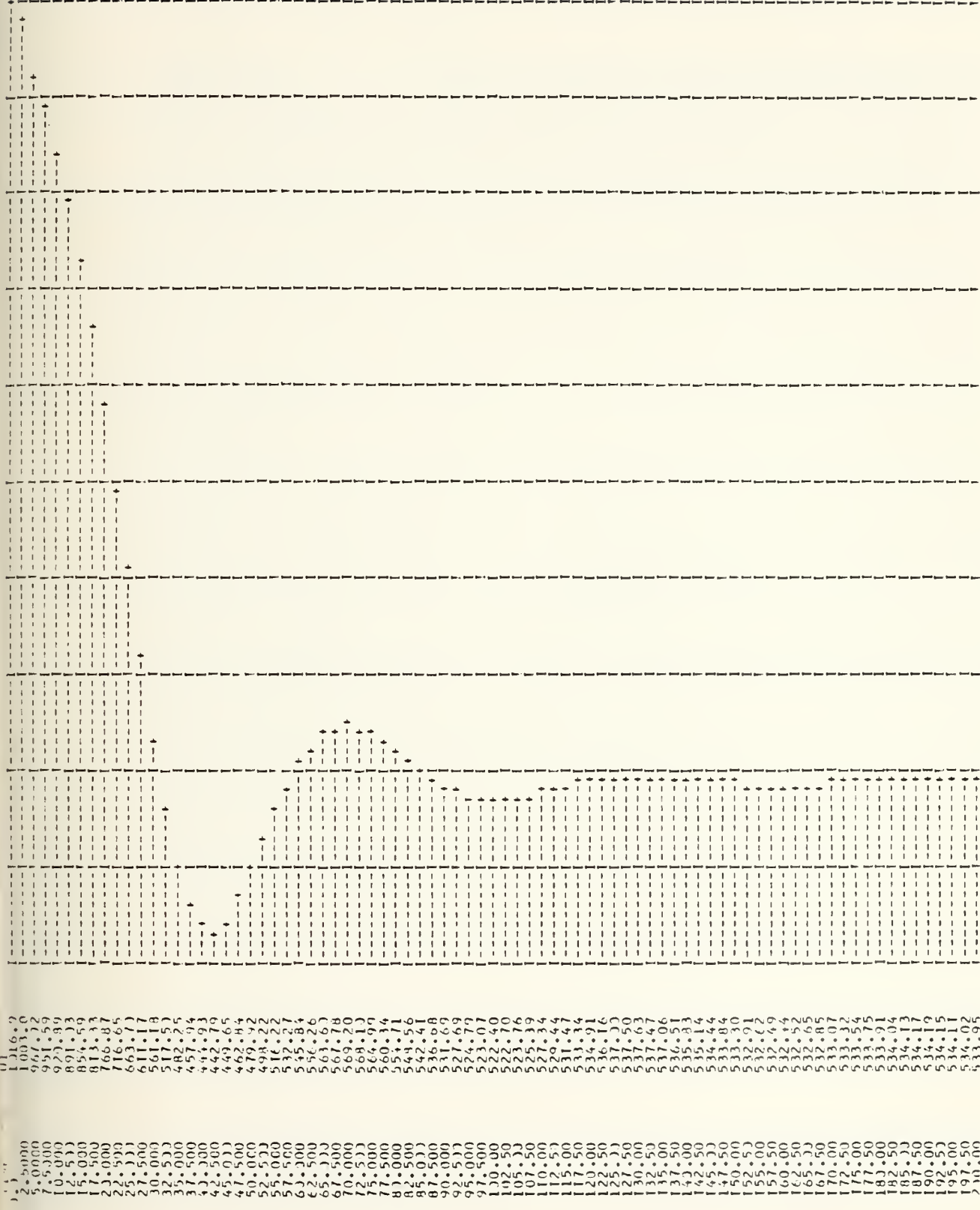


Figure 8-13 (continued)



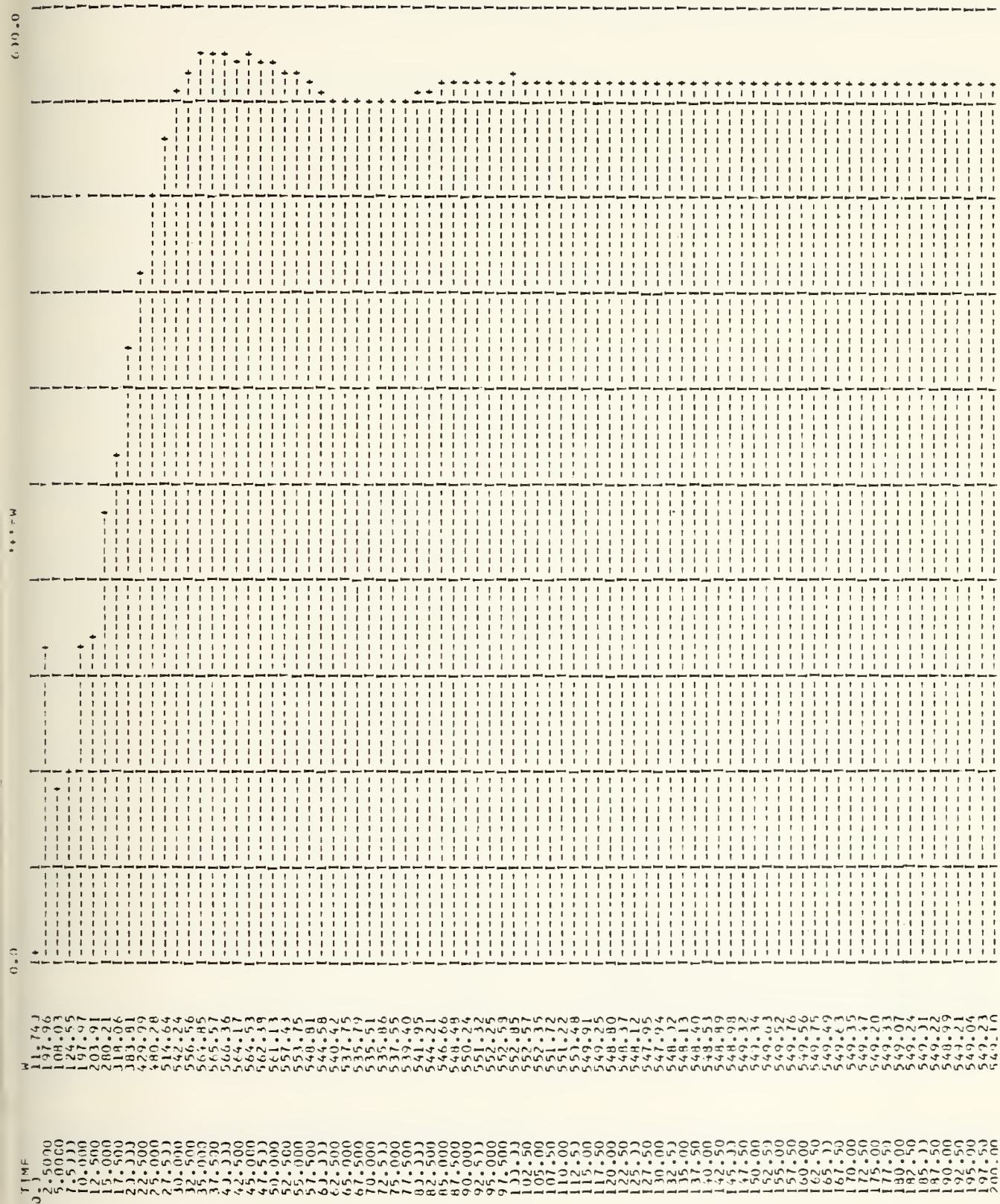


Figure 8-13 (continued)









100.0

0.0

0.0

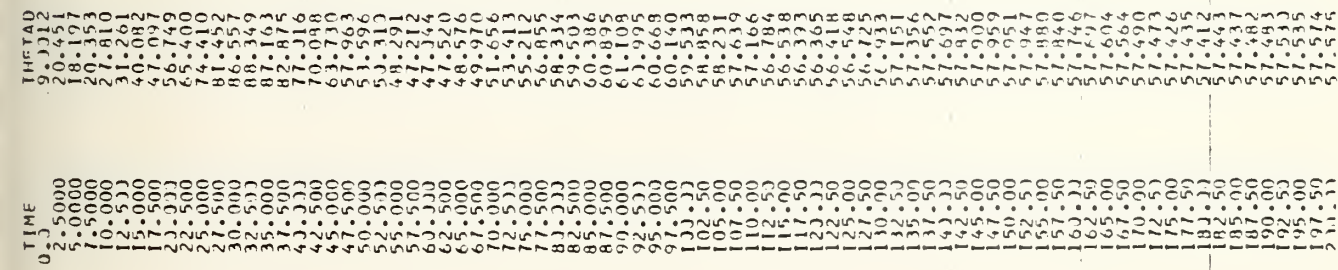


Figure 8-13 (continued)



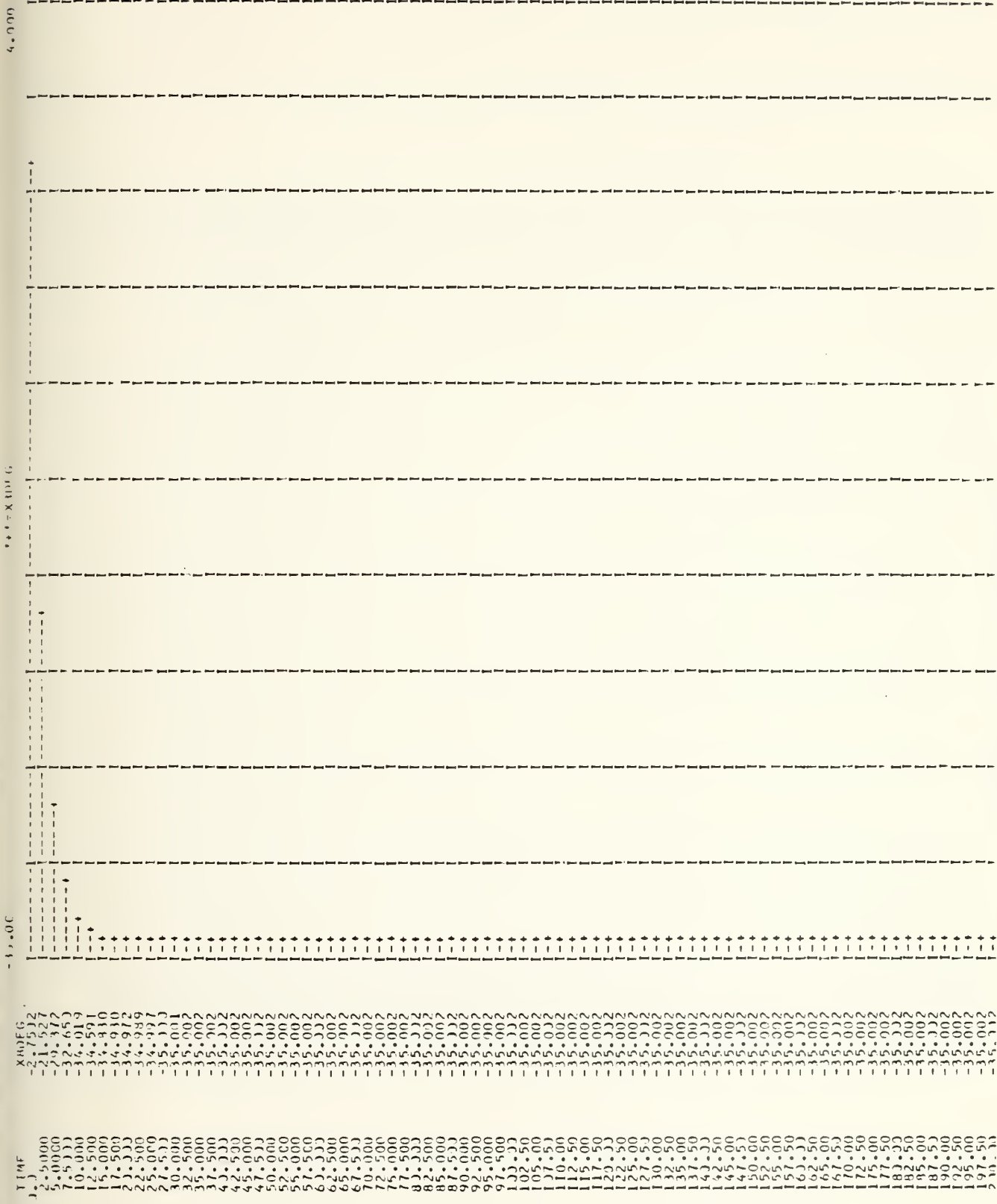


Figure 8-13 (continued)



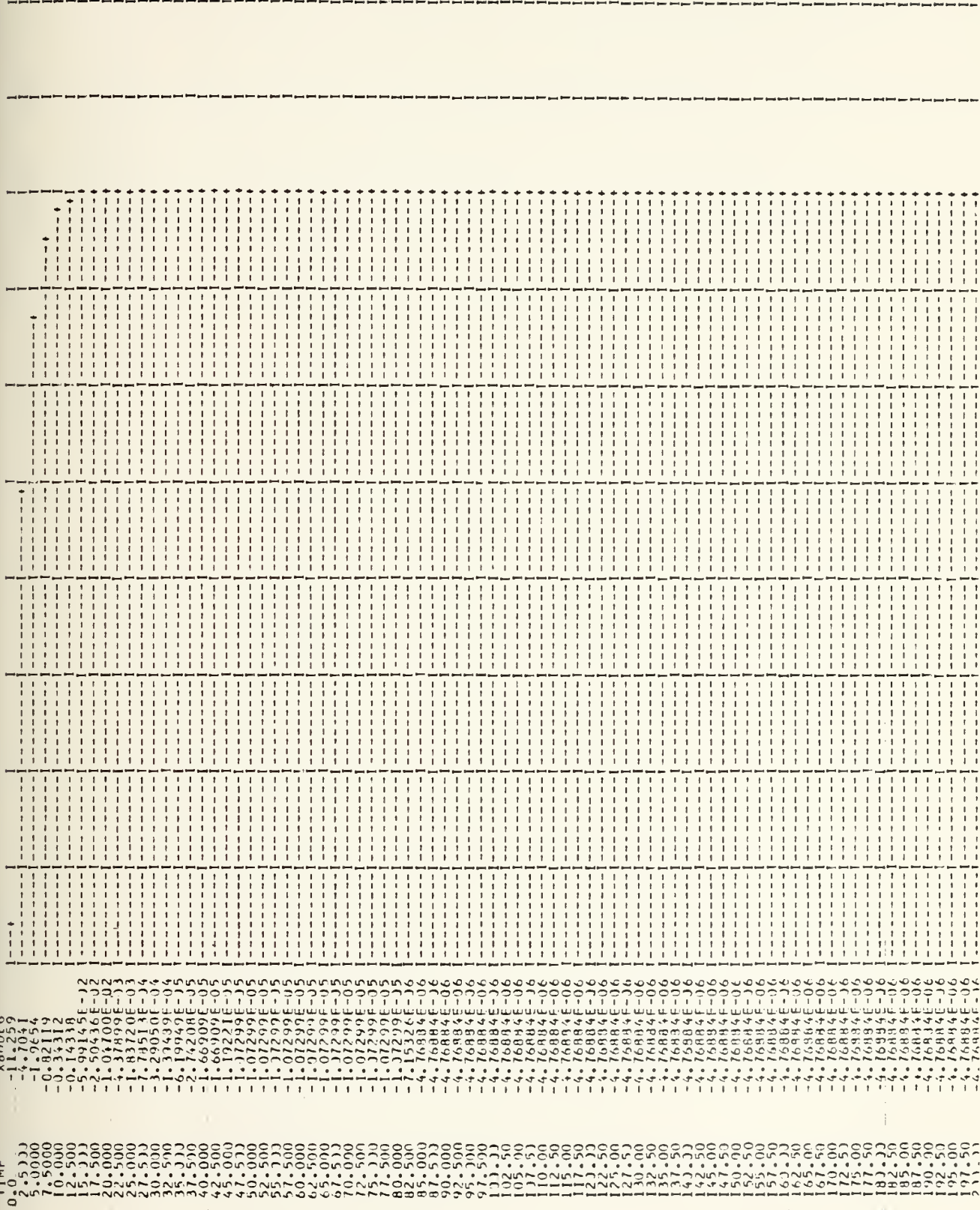


Figure 8-13 (continued)





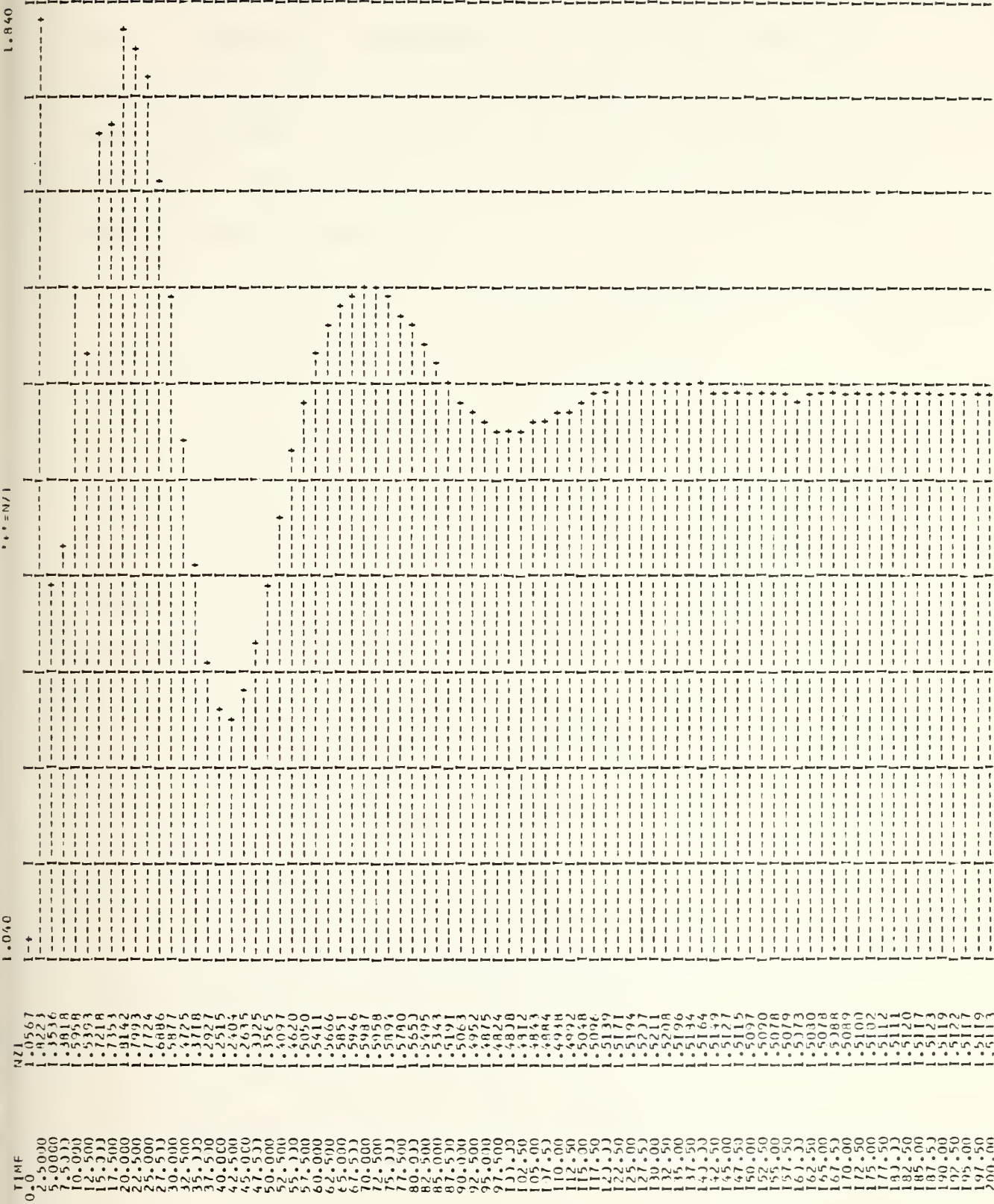


Figure 8-13 (continued)





already entered the atmosphere, was flying aerodynamically, being commanded, responding, etc., in short, was in a dynamic environment when this program started. Unless the parameters existing at  $t_0$  for this simulation can be precisely ascertained, it is doubtful that meaningful results can be expected.

To this end, angle of attack corresponding to the commanded load factor at  $t_0$  was calculated:

$$n_z = 1.09 = C_L(\frac{1}{2}\rho V^2)S/mg$$

Solving for  $C_L$  yielded 0.722. Since the angle of attack at 1.0 "g" was  $10^\circ$  with a  $C_L$  of 0.544, the angle of attack at 1.09 "g" was found to be  $10^\circ(0.722/0.544)$  or  $13.27^\circ$  (0.2316 rad).

An initial pitch rate would affect the X2 coefficient in the X1DOT equation and the X1 coefficient in the X2DOT equation, so it was computed using  $n_z = Q_0U_0/g + 1.0$  and found to be 0.0344 rad/sec.

Both of these modifications were made to the program with negligible effect on the results.

To analyze the results as they stand:

The angle of attack first exceeded the limits of the



FUNCTION statements (requiring interpolation of the force coefficients well outside the linear range of the functions) at approximately 2 seconds, oscillated in and out of the range, and left the range for good at approximately 10 seconds. All stability derivatives dependent upon angle of attack must be considered suspect after this time. The angle of attack was computed by dividing the vertical velocity perturbation by the horizontal velocity and adding this to the initial angle of attack.

The vertical velocity response (positive is downward) reached an extremely high value very quickly, and if applied to altitude, would have the orbiter impacting the ground before the simulation period was half over. Such a rate of descent would also cause a rapid change in air density, which was originally assumed constant, leading to very different values of those stability derivatives proportional to  $\rho$ . The assumption of a constant  $\rho$  should be valid for the three minute duration of the simulation.

The pitch rate magnitudes are not unusual, perhaps a bit high, but the steady state pitch angle is much too high. The steady state values of  $58^\circ$  pitch angle and  $71^\circ$  angle of attack indicate a glide angle of  $13^\circ$ , also much too high.



The elevon deflection, going to the trailing edge up limit in just over ten seconds, indicated that the vehicle sensed an insufficient nose up pitching moment with a GCMD of 1.09 and was trying vainly to create that moment. The result of the full trailing up deflection was instead a stalling angle of attack and a high rate of descent.

The actual load factor experienced by the vehicle in the simulation was only slightly higher than expected; the large elevon deflection was undoubtedly the cause of the initial rapid rise in this parameter. However, since the program computed  $n_z$  as a function of  $\rho$ , the steady state value was meaningless.

Taking the above observations into consideration, the program appeared to be consistent. Many possible reasons for the magnitude discrepancies were examined, but no changes in the program made more than a modicum of change in the results. It appeared that the error was basic in nature and not related to the model as presented or to the CSMP program. The most likely cause is, as was mentioned earlier, the fact that the simulation is not commencing at  $t=0$ .





## BIBLIOGRAPHY

- National Aeronautics and Space Administration Technical Memorandum TM X-2804, Supersonic Aerodynamic Characteristics of the North American Rockwell ATP Shuttle Orbiter, by G. M. Ware, B. Spencer, Jr., and R. H. Fournier, August 1973
- National Aeronautics and Space Administration Technical Memorandum TM X-2786, Subsonic Aerodynamic Characteristics of a Space Shuttle Orbiter, by J. C. Ellison, July 1973
- Greensite, A. L., Elements of Modern Control Theory, Spartan Books, 1970
- Space Division, North American Rockwell, Aerodynamic Design Data Book, v. 1, SD 72-SH-0060-1I
- Melsa, J. L. and Jones, S. K., Computer Programs for Computational Assistance, 2d ed., McGraw-Hill Book Company, 1973
- Arden, B. W. and Astill, K. N., Numerical Algorithms, Origins, and Applications, Addison-Wesley Publishing Company, 1970
- Organick, E. I. and Meissner, L. P., Fortran IV, Addison-Wesley Publishing Company, 2d ed., 1974
- Ogata, K., Modern Control Engineering, Prentice-Hall, Inc., 1970
- McRuer, D., Ashkenas, I., and Graham, D., Aircraft Dynamics and Automatic Control, Princeton University Press, 1973
- Dommasch, D. O., Sherby, S. S., and Connolly, T. F., Airplane Aerodynamics, 4th ed., Pitman Publishing Corp., 1967
- Melsa, J. L. and Schultz, D. G., Linear Control Systems, McGraw-Hill Book Co., 1969



Etkin, B., Dynamics of Flight, John Wiley & Sons, Inc.,  
1959

DiStefano, J. J., III, Stubberud, A. R., and Williams,  
I. J., Feedback and Control Systems, McGraw-Hill Book  
Co., 1967

Standard Mathematical Tables, 22d ed., CRC Press, 1974

Fullerton, C. G., LTCOL, USAF, "Space Shuttle Orbiter  
Approach and Landing Test Program," The Society of  
Experimental Test Pilots, 1975 Report



## INITIAL DISTRIBUTION LIST

	No. Copies
1. Defense Documentation Center Cameron Station Alexandria, Virginia 22314	2
2. Library, Code 0142 Naval Postgraduate School Monterey, California 93940	2
3. Department Chairman, Code 67 Department of Aeronautics Naval Postgraduate School Monterey, California 93940	1
4. Professor D. J. Collins Department of Aeronautics Naval Postgraduate School Monterey, California 93940	1
5. LCDR C. J. Pierce, USN Code 50 Naval Air Development Center Warminster, Pennsylvania 18974	1









19 JUN 70

269950

Thesis

169950

P533

Pierce

c.1

A mathematical model  
for the longitudinal  
control system of the  
space shuttle orbiter.

19 JUN 70

Thesis

169950

P533

Pierce

c.1

A mathematical model  
for the longitudinal  
control system of the  
space shuttle orbiter.



A mathematical model for the longitudina



3 2768 001 92396 4

DUDLEY KNOX LIBRARY